School of Civil & Mechanical Engineering

Modelling Study of Stress Displacement Theories for Retaining Walls under Seismic Excitation

Su Yang

This **thesis is presented for the Degree of**

Master of Philosophy (Civil Engineering)

of

Curtin University

June 2014

To the best of my knowledge and belief this thesis contains no material previously published by any other person except where due acknowledgement has been made. This thesis contains no material which has been accepted for the award of any other degree or diploma in any university

Signature: *Su Yang*

Table of Contents

Abstract

Two models of diaphragm retaining walls with struts retaining normally consolidated homogeneous dry sand under seismic excitations were simulated using PLAXIS and ABAQUS respectively. The produced results for seismic wall response, including displacement, lateral earth pressure and free field responses, are critically evaluated against analytical solutions related with stress displacement relationships: strain increment ratio dependent lateral earth pressure theory, free field theory and subgrade modulus method. Simple methods were established to utilize software's output for the determination of essential parameters such as critical state wall displacement, elastic / plastic subgrade modulus etc. The results were also compared with traditional method and showed good agreement. PLAXIS produced wall lateral pressure that agrees well with that from strain increment ratio lateral earth pressure theory and the stress – displacement relationship proposed by Zhang et al. (1998). ABAQUS produced similar but somewhat greater lateral pressure compared to analytical solutions and PLAXIS and the reason is studied and explained based the concept of "spring displacement". Both softwares and analytical solutions produced very similar free field displacement. "Spring displacement" produced by PLAXIS and ABAQUS were evaluated and it explained well the variance of local lateral earth pressures between modelling outputs and theoretical results. New research direction was proposed to incorporate freefield displacement into seismic stress displacement relationship for a better and more comprehensive future analytical solution of seismic retaining walls.

Two papers were produced from this thesis for publication:

1. Review of Studies on Retaining Wall's Behavior on Dynamic / Seismic Condition (in International Journal of Engineering Research and Applications)

2. Modelling Evaluation of Seismic Retaining Wall Theories Based on the Displacement-Stress Relationship and Free Field Response (in construction)

Full Manuscripts of the first paper above is attached in Appendix A, and a draft of paper 2 is attached in Appendix B.

Chapter 1. Introduction

The structure of this chapter is listed below:

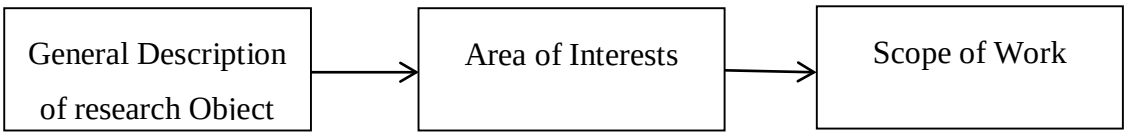

1.1. General Description of Object

A retaining wall system normally consists of a retaining wall and retained soil. There are various applications of retaining system in basement wall, bridge abutments, highway walls etc. The mechanism of a retaining wall is to prevent the retained soil from failure or excessive displacement, in other words, both stability and serviceability status should be satisfied. For retaining walls under static cases, there are many researches and solutions for the lateral earth pressure such as the two classical solutions: Rankine's theory and Coulomb's theory. For retaining walls under dynamic/seismic excitations, changes for the lateral pressure and wall displacements are evident based on real earthquake studies.

Similar to many geotechnical studies, there are three main categories of research methods for retaining walls: analytical solutions, experimental studies and numerical simulation. Different researches were conducted due to different soils, wall structures, dynamic and structural conditions etc. However, there is a lack of analytical solutions that interpret real soil wall behaviour while most current methods have insufficiencies. As a result, lateral earth pressure generated by retained backfill on the wall and relevant soil / wall deformations are interested and more investigation in this area is required.

1.2. Areas of Interests

Compared to research for static behaviour of retaining walls, the dynamic/seismic behaviour of the wall is more ambiguous and is normally solved with pseudo-static acceleration to represent seismic excitation. There are many analytical solutions trying to solve the seismic lateral earth pressure using concepts such as limit equilibrium of failure block, elasticity/plasticity of soil under certain displacement etc., but these theories are still only applicable for a certain range of problems such as a rigid wall with normal displacement modes, or have generalized the stress-displacement behaviour by rough estimation of "spring stiffness" such as subgrade

modulus method. Currently, there are few research that directly and accurately address the soil's stress strain behaviour right behind the wall and most current methods are either limited at predicting accurate pressure distribution under certain conditions, especially for working state, or too tedious to be applied. One of the fundamental reasons are that most current methods are not based on interpretation of real soil and wall behaviour, while the only few that satisfies this are just partially relevant and the results are not sufficiently justified. As a result, strain increment ratio lateral earth pressure theory (Zhang et al. 1998) and free field dependent subgrade modulus method (Rowland et al. 1999) have been concerned by the author since the former one is built on stress strain relationship of soil, although transferred from static case. And the later one was established on the relationship of free field displacement on lateral earth pressure.

In addition, there is always a need for a convenient, accurate and interpretative analytical solution for seismic retaining wall responses under various conditions such as non-rigid wall, plastic response, working state response etc. And thus, it is meaningful to firstly evaluate the above mentioned two theories that are related with stress displacement behaviour of the retaining wall, based on which we could figure out a direction for future research effort for the establishment of seismic stress strain relationship for retaining walls and finally a systematic analytical solution based on it. Else, commercial numerical soft-wares like ABAQUS and PLAXIS both have seismic functions, but their performances are yet to be assessed based on stress increment ratio theory and freefield theories for retaining walls under seismic excitation. On the other hand, numerical soft-wares could be a tool to conduct back analysis of certain parameters that could only be determined by rough approximation before.

1.3. Scope of Work

As a result, this paper utilizes ABAQUS and PLAXIS to build a seismic retaining wall model to:

1. Investigate the performance of theoretical solutions of strain increment ratio lateral earth pressure for seismic cases, plus subgrade modulus method based on free field theory.

2. Compare PLAXIS and ABAQUS's results at interpreting the stress displacement behaviour and free field responses
3. Use the numerical output from the software to obtain parameters for theories and compare with empirical approaches.
4. Investigate the influence of the combined displacement between wall and free field on local lateral earth pressure

The aim of this study is:

1. Provide meaningful findings for seismic stress displacement behaviour of retaining walls and shed light on future research in this area
2. Validate softwares applicability in terms of producing reasonable seismic stress and displacement
3. Lay the foundation for a comprehensive and interpretative analytical solution built on real soil and wall behaviour for seismic response of retaining wall under comprehensive conditions.

Chapter 2. Literature Review

This literature review is an extension for the author and supervisors' literature study during the research degree and a published paper regarding significant current research outcome for analytical, experimental and numerical studies on the matter of dynamic/seismic retaining wall response(Yang et al. 2013). The permission from the journal for the use of this paper is attached in Appendix B. In addition, literatures regarding the stress displacement behaviour of retaining system were further extended; also, meaningful existing static stress strain relationship and relevant retaining wall methods were introduced. The basic structure of this review is listed below:

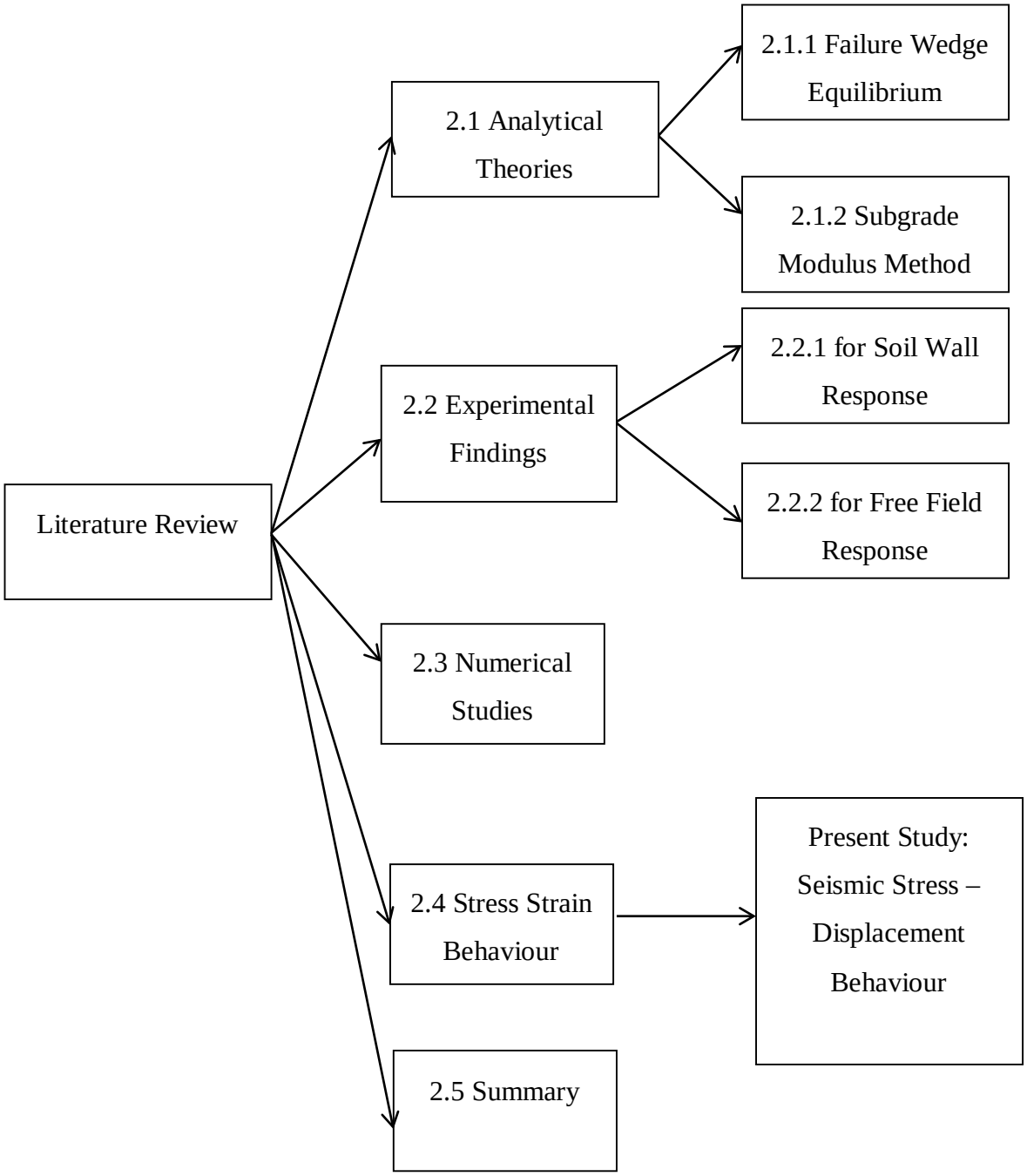

2.1. Analytical Theories

There two main categories of analytical approaches for the dynamic lateral earth pressure of retaining walls. Firstly, a soil wedge is taken out from the soil behind the wall, and the equilibrium of this soil wedge takes into account inertia force, soil weight, friction angle etc. to solve for lateral earth pressure. This type of method usually applies to limit states: passive or active, and they are called failure wedge equilibrium theories. Secondly, the soil is simulated as elastic or plastic elements with subgrade modulus, and so the pressure generated could be solved by knowing the displacement of element and the subgrade modulus. These two categories of methods will be introduced below separately.

2.1.1. Failure Wedge Equilibrium

In this section, significant outcome of analytical solutions based on the equilibrium of failure wedge are discussed.

After the famous Kanto earthquake in 1923, Mononobe and Okabe conducted a series of shaking table tests (using old facilities of the time) that leads into a famous analytical method called Mononoke and Okabe method (abbreviated as MO method in this script). This method assumes a failure wedge is formed along a planner failure plane in active or passive states. Equilibrium equations could then be made by combining Coulomb's wedge theory with quasi–static inertial force. The method directly solve for passive and active coefficient of lateral earth pressure, for which a triangular pressure distribution is assumed along the wall depth, in other words, the calculated Ka and Kp are assumed constant along the wall depth.(Yang et al. 2013)

Although MO method has been a major analytical solution for seismic retaining walls, it is also evident that some points are inherently neglected by it (Seed and Whitman 1970, Nadim and Whitman 1983):

1. Dry, cohesionless, isotropic, homogenous and elastic backfill material with a constant internal friction angle and negligible deformation.
2. The wall deflects sufficiently to exert full strength along the failure plane. This means no wall rigidity is considered.
3. The soil wedge is rigid and so subjects to uniform acceleration throughout the body.
4. The failure plane is planner and the soil deformation is neglected.

5. End effects are neglected by assuming a wall that is sufficiently long.

What's more, the MO method is a pseudo-static approach in which the time effect of dynamic force and the dynamic amplification effect are neglected. However, the MO method as an extension of Coulomb's wedge theory is a widely used traditional method for solving seismic retaining wall matters. It is widely used as the basic theory for new research and retaining wall design standards, such as Euro code 8 and Australian Standard 4678.(Yang et al. 2013)

Based on the MO method, Seed and Whiteman (1970) investigated the influence of various factors on the responses of retaining walls. These factors are angle of friction, slope of backfill, dry / wet condition, horizontal acceleration, source of load (seismic or blast) and soil-wall friction, which were studied to establish a relationship with coefficient of lateral earth pressure. The results from MO method are also compared with various experimental results at that time. Remarkably, they have worked out a simplified adaption of the MO method that is widely used in practice. On the other hand, Seed and Whiteman (1970) proposed a height of 0.6H (H is wall height) above the wall bottom as the location for the resultant force.(Yang et al. 2013)

Referring to serviceability issues, Nadim and Whiteman (1983) summarized the relevant analytical solutions and did relevant numerical evaluations for wall displacement. In that study, they mentioned that Richards and Elem (1976) worked out a solution (R-E model) for calculating the required horizontal acceleration for a specified horizontal displacement based on sliding block model. The limiting acceleration level corresponds to wall displacement when soil wedge slides along the failure plane. This acceleration level could then be applied into MO method if the lateral earth pressure in this state is required. Considering the negligence of vertical acceleration in Richards and Elem's method, Zarrabi (1979) improved this method by taking into account vertical acceleration: this normally renders a slightly lower displacement value than the R-E model. Later on, Wong (1982) worked out a displacement solution based on results from Zarrabi (1979)'s method under many real earthquake records. Based on these previous studies, Nadim and Whiteman (1983) also did a numerical study regarding the influence of realistic acceleration distribution and amplification of motion on wall displacement. The evaluation of numerical results by Nadim and Whiteman (1983) had lead into a design procedure using displacement-based methods. These methods are categorized into limit

equilibrium method in this paper since, for all of them, the MO method is used for pressure calculations by knowing the displacement. However, the numerical model used is limited for its rigid boundaries and relatively simple acceleration record is used.

Similar to sliding block methods mentioned above, Zeng and Steedman (2000) established a method for rotational displacement of seismic retaining walls. A new notion of threshold acceleration was introduced and the wall starts to rotate once it is exceeded and stops when it reduces to zero. Centrifuge tests data has proved the procedure. (Yang et al. 2013)

When soil is subject to ground seismic acceleration, shear wave is propagating through the soil as well as a changing acceleration with time. This phenomenon is not taken into account in pseudo-static approaches mentioned above, since MO method assumes a constant uniform acceleration for the whole soil body and neglects dynamic amplification factor. To consider time effect on dynamic/seismic retaining walls, Steedman and Zeng (1990) investigated the influence of phase on dynamic increment of lateral earth pressure. Dynamic amplification is found to incur significant influence on lateral earth pressure, which is supported by results from centrifuge experiment. This study considered shear wave velocity, non-uniform shear modulus and dynamic amplification factor on the pressure distribution. In addition, it can be derived that, for low frequency dynamic excitation, when dynamic amplification is not significant, pseudo – static condition is well satisfied (Steedman and Zeng 1990). (Yang et al. 2013)

Anderson et al. (2008) produced a chart method for the application of the MO method for cohesive soils. Similar to MO method, the chart method is also insufficient in cases like non-homogeneous soils and complex back-slope geometry. (Yang et al. 2013)

Choudhury and Nimbalkar (Choudhury and Nimbalkar 2007), (Choudhury and Nimbalkar 2005, Basha and Babu 2010) established a pseudo - dynamic method for lateral earth pressure and wall displacement in a passive case. In addition to Steedman and Zeng's original pseudo-dynamic methods mentioned above, they studied and incorporated vertical acceleration, inertia effect between wall and soil plus comprehensive relevant factors, but the equations seem lengthy and so hamper

practical use. Basha and Babu(2010) also did a similar pseudo – dynamic research for the case of failure plane as a curved rupture surface, which is believed to be more realistic. (Yang et al. 2013)

The MO method and it's variants are based on limit state wedge theories: it only applies when a wedge behind the wall is triggered, mostly a failure wedge. So it is normally used for active and passive state analysis, and working state when "intermediate wedge" is introduced. Although many new solutions have been produced to overcome the inherent assumptions of the MO method, most new solutions seem tedious and so hamper their practical uses. The same goes to the method used for wall displacement calculation. In addition, the location of the resultant force for the MO method is arguable, as well as the stress distribution, especially when the rigidity of the wall exceeds a certain level (this will also be covered in the experimental study section). However, many experimental and numerical findings pointed that the MO method and many of its variants do not take into account displacement modes and rigidity of the wall. While the solutions like Zhang et al. (1998) for various deformation medes are based on a rigidly deforming wall, the application of strain dependent lateral pressure calculations are difficult for non-rigidly deformed walls or walls that has uncertain deformation modes. For details of strain increment ratio related lateral earth pressure theory, view section 2.4.

2.1.2. Subgrade Modulus Method

As an alternative to equilibrium wedge method, the sub-grade modulus method use a subgrade modulus to describe soil and wall response, while the soil-wall interaction is modelled by elements like springs or beams with a stiffness modulus (e.g bulk constant) to relate displacement and generated pressure on wall. Basically, these solutions model the soil as elastic, visco-elastic or plastic material. The significant developments of subgrade modulus methods are introduced below.

To more properly address the seismic pressure on rigid walls, Wood developed a linear elastic theory to calculate the dynamic soil pressures on rigid walls under relatively idealized conditions such as modelling the soil as massless springs with linear elastic response(Wood 1973, Wood 1975). This study address rigid wall, for which MO method is not sufficient, and initially found the influence of wall

displacement on lateral force on the wall. Scott produced a method that simulated the retained soil as shear beams made of visco-elastic material and free at its upper surface and connect the beams to the walls (Scott 1973). Similar to Wood's method, only a linear elastic condition with constant soil stiffness is used in this method. To amend these methods, horizontal bars with mass has been applied(Veletsos and Younan 1997). However, still, soil wall interaction is modelled by springs with constant stiffness. For most sub-grade modulus method, numerical tool such as MATLAB are needed to carry out the mathematical works, so some similar studies are conducted using numerical tools, which is discussed later.(Yang et al. 2013)

With sub-grade modulus method, it is also possible to establish a method based on stress-strain (or force-constant) behaviour of the retaining system. Since either springs or visco-elastic beams are actually a form of stress – strain relationship. And it has become useful if a convenient way is obtained for the relevant displacement value under seismic excitations. Considering this "free-field theories" has gained particular attention since it interprets the soil displacement under seismic influences. Academically, free field refers to a field where the dynamic response of the soil is unrestrained by boundary conditions (Rowland et al. 1999).Thus free field response normally occurs at a soil section at certain distance away from obstructions such as a retaining wall. Combining free field response and wall displacement, a good platform for carrying out sub-grade modulus analysis of lateral earth pressure could be produced as below.(Yang et al. 2013)

Fishman firstly proposed a simplified pseudo-static equation for free field displacement under an active condition. Both a constant shear modulus (G) and a linearly varying (with depth) shear modulus are used (Fishman et al. 1995). In addition, the plastic deformation of free field for dry granular soil are studied by Huang using the theory of plastic flow (Huang 1996). From Huang's study, a solution is produced to calculate the free-field displacement under plastic conditions by factoring the elastic shear modulus with a factor f(kh). It is important to know the premises of these theories: the soil is elastic – perfectly plastic with Mohr – Coulomb failure criterion and the dynamic force is assumed as pseudo – static (Huang 1996).(Yang et al. 2013)

Based on the analytical solutions for freefield response, Rowland Richards et al. (1999) present a simple kinematic and pseudo – static approach to evaluate the

distribution of dynamic lateral pressure (Rowland et al. 1999).The soil between the free field and the wall is modelled by a series of springs, while the wall pressure is calculated by at rest stress and stresses caused by deformation of soil “springs” (as shown in Equation. 14). Both elastic and plastic responses could be addressed. This method could be applied to calculate both limit state and working state wall responses if relevant wall displacements are known. And generalized solutions could be produced by knowing the wall displacement mode. For unknown wall displacement modes, this theory provides a way once the wall displacement or the free field displacement could be obtained through other approaches such as experiment or numerical modelling. In this case, the determination of “spring” modulus K for soil displacement becomes crucial (as shown in Equation 14). In Rowland Richards et al.’s work, Ks is estimated through empirical values but an accurate identification of Ks for specific cases is more useful and computational back-analysis would be a good choice.(Yang et al. 2013)

Rowland et al. (1999)’s freefield dependent Sub-grade modulus method has following limitations. Firstly, most of these methods are based on zero vertical acceleration and pseudo-static excitations, these do not produce accurate real life free field behaviour. So the obtained displacement should be a rough estimation and may incur large local deviation from true results. Secondly, the subgrade modulus (spring constant) is crucial for these methods. However, as mentioned above, the derivation of a correct K is difficult or complex, and the simplified empirical input of constituting parameters such as shear modulus is inevitable at triggering inaccurate results. (Yang et al. 2013)

For the sub-grade modulus method, the formulation of a free- field response is idealized on assumptions such as zero vertical acceleration, pseudo-static etc.: so it does not represent the real free field behaviour. And, except in some laboratory studies, only rigid non-deflecting walls are considered by current analytical sub-grade modulus methods (Veletsos and Younan 1997). Also, the adoption of a shear modulus is difficult, since G actually varies with confining pressures, strain level and stress history. What’s more, the concept of using a fixed K to represent the displacement – force relationship for soil is against the nonlinear nature of most soils, not to mention the dynamic/seismic influence on K is due to be sufficiently investigated, since at least the damping effect would influence the wall pressure.

2.2. Experimental Findings

At present, the most effective tool for experimental study of earthquake engineering is combination shaking table. Combined with centrifuge, a shaking table test is believed to be able to provide reliable results in relevant engineering behaviours. A shaking table model is often equipped with measuring tools such as strain gauge, pressure transducers and accelerometers, while a variety of retaining walls could be made such as cantilever wall, gravity wall, diaphragm wall etc. The experimental results usually provide a good platform to evaluate both current and previous studies in interested engineering areas. The following paragraphs provide a literature review of significant shaking table experiment studies on retaining walls. These experimental studies have developed or justified some of the above mentioned theories, such as MO method etc. and provided details about the applicability and limitations of these theories. (Yang et al. 2013)

2.2.1. Experimental Findings Regarding Soil Wall Response

MO method is widely assessed by some experimental studies, and the wall flexibility, soil elasticity, pressure distribution, total force etc are usually the major concern. Firstly, Ortiz Scott and Lee (1983) carried out a series of shaking table tests on walls with different rigidity in centrifuge. Compared to MO method, they have obtained results that agree well to MO method in terms of resultant forces. However, the experimental results and MO method do not match well regarding the produced moment on the wall and the pressure distribution is found not linear along the depth. What's more, post-shaking residual values are found for all parameters, which has lead into greater values than initial values (Ortiz et al. 1983). Later on, a similar centrifuge shaking table test was carried out with various intensities by M.D. Bolton and Steedman (1982). Particularly, they used micro-concrete retaining walls that were rigidly bolted to the shaking table platform. The results agreed well with pseudo-static estimation of displacement and rotation mentioned above for non-rigid walls. It is also is justified that MO method and relevant displacement methods produced reasonable maximum displacement for walls that are sufficiently flexible. An evaluation was made regarding soil elasticity, wall flexibility and soil-wall interaction as well as their influence of the wall deflections. What's more, it has been

found that pressure will build up along permanent deformation after a certain amount of cycles (M.D.Bolton and Steedman 1982).(Yang et al. 2013)

A number of famous shaking table tests are done by Ishibashi and Fang (1987) on rigid retaining walls and cohesionless dry sand. Numerical analysis was also conducted to assist the results investigation. Various displacement modes including rotation about the top, rotation about the base, translation etc. were investigated respectively. The produced wall responses include total lateral force (thrust), point of force application and lateral earth pressure distribution. These results are believed to be reliable and have been used for verification of many relevant researches. It is derived that the wall displacement mode has significant influence on lateral earth pressure, and the related factors for soil arching, while significant influence is found for soil arching and high residual stress on pressure distribution and point of application of active force(Ishibashi and Fang 1987). In addition, inertial body force was found to increase significantly under high acceleration levels; in contrast, wall displacement dominate the pressure under lower acceleration level. Linear distribution is again found to be inaccurate regardless of displacement modes. Lastly, MO method is found to be more accurate in certain displacement modes compared to others. (Yang et al. 2013)

In Atik and Sitar(2010)'s centrifuge tests, the experiment results agree that the triangular distribution of lateral earth pressure is a reasonable assumption. They have also found that the dynamic inertia force and dynamic earth pressure are not in the same phase, and so the maximum earth pressure does not coincide with maximum moment(Al Atik and Sitar 2010). This is against the assumptions made by many theoretical studies such as MO method and Seed and Whiteman's simplified approach (Seed and Whitman 1970).(Yang et al. 2013)

The point of resultant lateral earth force under the cases of neutral and active static and dynamic stress is investigated by Sherif et al (1982). A critical evaluation is also made regarding the triggering wall displacement for active cases under both static and dynamic cases. They proposed that the critical state displacement increases with the height of the wall and decreases with a weaker soil strength. This experimental study has provided useful insights for future research in the area of displacement dependent lateral earth pressure (Sherif et al. 1982).(Yang et al. 2013)

2.2.2. Experimental Findings Regarding Free Field

Regarding seismic freefield investigations, a number of laboratory and computational modelling studies was conducted by Fishman et al (1995). In these experiments, the advantage of using a flexible end wall was utilized. Compared with numerical results, both rigid and flexible walls have gained wall pressure, shear stress and displacement profiles along the wall. One interesting finding is that, the wall deformation is almost the same with the freefield displacement for a perfectly flexible end wall. What's more, the pressure, shear stress and displacement of the wall also coincide with those of freefield. In these experiments, both small and large strain shear modulus are obtained through the methods which shed lights on similar experimental researches (Fishman et al 1995). (Yang et al. 2013)

2.3. Numerical Studies

Numerical methods and relevant computational tools are developing fast and have already become a crucial tool in engineering research, design and analysis. Recently, a combination of theoretical, numerical and experimental studies on engineering matters has been a dominant research trend. As a result, it is necessary to discuss some remarkable numerical research in the area of dynamic/seismic retaining wall response. While in this literature review, more advanced numerical techniques are selected to accompany the previous analytical and experimental findings.

The influence of wall rigidity and wall base flexibility on the response of retaining wall is firstly studied by Veletsos and Younan (1997). They built a model wall subjecting to horizontal ground shaking of both harmonic and real earthquake motions. The results showed that the generated wall pressure increases with reducing wall and wall base flexibility factors, so a fixed based flexible wall tend to trigger much greater horizontal wall pressure compared to walls with realistic flexibilities(Veletsos and Younan 1997). In addition, wall pressure distribution is affected by wall and wall base flexibility as well. The findings contradict the MO method, which assumes all walls yield sufficiently so that no extra pressure is triggered. This numerical study has proved the influence of wall and base rigidity on dynamic / seismic wall behavior, which are frequently neglected by analytical approaches such as widely used MO method. In addition, it was found that the wall and base flexibility also has influence on dynamic amplification factor (Veletsos and Younan 1997).(Yang et al. 2013)

The seismic behaviour of highway bridge abutment was studied by Al-Homoud and Whitman (1999), who developed a two dimensional finite element model using FLEX code, which is validated for this specific case. The constitutive model is selected as viscous cap and shear beams are utilized to model far-field ground motions. The soil model also considers hyesteretic similar damping by using viscoelastic behaviour, while obsorbing boundaries is used to cope with boundary conditions. When the results were compared with dynamic centrifuge experiemnt, good agreement was found (Al-Homoud and Whitman 1999). The outcome indicated that different displacement mode may occur for such retaining walls, while outward tilting, with certain permanent tilting after shake, is a dominant type for this rigid

retaining wall case. This finding also matches the bridge abutment behaviour in real cases (Al-Homoud and Whitman 1999). (Yang et al. 2013)

Commerical finite-element package ABAQUS was used by Psarropoulos, Klonaris and Gazetas (2005) to investigate some analytical solutions and their apllicabilities. Veletsos and Younan's elasticity method is used as a main tool and the soil model is visco-elastic. This study shed some light on the effect of rigidity on dynamic/seismic wall response and proved that MO method and Veletsos and Younan's elasticity method works well for flexible walls (Psarropoulos et al. 2005). What's more, this study also investigated soil inhomogeneity, wall flexural rigidity and translational flexibility of the wall's base, and the effects of these parameters to the wall response (Psarropoulos et al. 2005). (Yang et al. 2013)

Using numerical software FLAC, Green, Olgun and Cameron (2008) carried out a number of non-linear finite difference analysis to study cantilever walls. Elasto-plastic material response is used as constitutive model while Mohr-Coulom is adopted as the failure criterion. This study critically calibrated and validated the soil-wall system model and it justified that the MO method is sufficient for low acceleration level(Green et al. 2008). However, when the acceleration leve is high, discrepancies could be seen due to the influence of wall flexibility. In addition, a different critical load case is identified between soil failure and structural failure, which agrres well to experimental outcome by Atik and Sitar mentioned in previous section(Green et al. 2008).(Yang et al. 2013)

Other useful information regarding numerical studies in this area could be found in Pathmanathan's master's thesis (Pathmanathan 2006), which provides detailed discussion regarding some numerical approaches and meaningful comments are added.(Yang et al. 2013)

2.4. Stress Strain (or Displacement) Behaviour for Retaining Wall

From above literature studies, the author has found the local wall soil displacement behaviour is a main mechanism that is able to interpret the generated wall pressure. Since the wall flexibility affects the deformed shape and thus local displacement. Based on soil's stress strain behaviour, the displacement or strain for the soil behind the wall has inherent relation with the generated pressure. As a result, analytical solutions that are based on stress displacement or stress strain relationships have gained special concern in this study. The following lists significant studies in the field of stress – strain relationship and lateral earth pressure for retaining walls.

Stress strain behaviour, usually could also be converted into stress displacement behaviour, is able to interpret the real soil and structure response. The mechanism of soil behaviour for most geotechnical structures is stress and strain relationships. By correctly interpreting the stress strain behaviour, the wall behaviour under both static and seismic conditions, working state or limit state are able to be determined. And the current advancement in numerical tools, experimental facilities and real case inspections are able to provide useful information with regard to the wall displacement behaviour or to study the stress strain relationship for various soil conditions, such as Triaxial apparatus is able to obtain stress strain behaviour of sand or clay specimen under different strain rate or consolidation conditions. Thus, it is meaningful to investigate such behaviour for retaining system considering insufficiencies shown by current theoretical methods as mentioned above. There are several significant researches for stress strain behaviour of retaining system. Please note, in certain sense, elastic theories can also be classified as a stress displacement theory, in here, it means the behaviour for soil right behind the wall, and this will be related to the free field displacement under seismic cases.

Firstly, Bransby and Milligan (1975) utilised X–ray techniques and model tests to study the near wall soil deformations in dry sand, which leads into a simple analytical method for linking the deformations (strains) in the sand with deflections of the wall. The simplified soil deformation regions are termed the kinematic admissible soil strain field. The simplified equation (neglecting wall friction) is: $\delta\gamma = 2\delta\theta$.

Bolton and Powrie (1988) conducted series of centrifuge tests to gain a coherent view of the soil – structure interaction behaviour following the excavation of soil in front of a pre – constructed wall. The significance of this study is the validation of simplified kinematic admissible soil strain field proposed by Bransby & Milligan (1975). It intends to enable serviceability criterion for soil or wall displacements in simplified admissible strain fields, so the effective mobilized soil strain in the major zones of soil deformation can be deduced. It is proposed that in the aid of triaxial or plane strain test data, selection of a mobilized soil strength and thence an equilibrium analysis of the wall will be available.

Deriving from numerious triaxial tests results, Zhang et al. (1998) found a relationship between soil displacement and lateral earth pressure on normally consolidated dry sand. A solution was established relating the strain ratio to coefficient of lateral earth pressure K as shown in (3) and (4). This solution was further combined with formulas of Rankine and Coulomb theories to produce earth pressure solutions for retaining walls under any lateral deformation. When applied to real retaining wall, the strain ratio could be determined by knowing critical state (passive and active) displacement and current wall displacement as shown in Equations (7) and (8).

There is also a stress strain related retaining wall theories for seismic case, which is originated from theories from static stress strain relationships. Based on numerous stress strain relationship curves obtained from triaxial tests on normally consolidated sand, Zhang et al (1998) establish a relationship between the strain increment ratio and mobilised friction angle. In other words, this solution is another form of stress–strain relationship which can result in a mobilised friction angle. From this study, the pressure between passive and active states can be estimated. Zhang et al (1998) combined this method with sliding wedge equilibrium theories for calculating dynamic earth pressure on walls in working states between active and passive limit states. The solution has also been extended into the case of non-horizontal surface, non-vertical wall and with surface charges.

It follows with a solution for seismic earth pressure theory that combines the strain ratio dependent theory and pseudo-static wedge equilibrium theory by introducing the concept of “intermediate soil wedge” for any lateral deformation between active and passive state. Based on the “intermediate soil wedge” theory that relates wall

pressure to the strain increment ratio or mobilized frictional resistance, Zhang et al. (1998) developed a new theory by introducing a strain ratio factor into classical formulations of MO method. Besides, pressure component due to soil vibro-densification and surcharge pressure was taken into account for the final solution of seismic lateral pressure. This method relates the lateral pressure to the displacement, which provides an interpretation of the real soil behaviour behind retaining structures and, possibly, is able has lead into a solution that is based on true mechanism of soil behind the wall. The method places an emphasis on reliance of the seismic earth pressure on mode and level of wall displacement (Zhang et al. 1998) and could be simplified for normal displacement modes such as Translation, Rotate about Top, Rotate about Bottom etc for rigid walls. Distribution, resultant and point of application of the lateral seismic pressure are able to be predicted for any state between passive and active wall displacement by this method, which could be reduced to MO method at limits state by introducing Δ=Δ_a,$\Delta = \Delta_p$into equations (9) and (10).

However, the methods used to determinecertain essential parameters for the solution, such as Δ_a, $\Delta_p$are highly empirical and limited to certain types of soil. What's more, a very rough pragmatic charts are used to determine the strain ratio exponential factors$\beta_a$and β_b.

2.5. Summary

Current theoretical solutions for seismic response of retaining wall system are reviewed in line with relevant numerical and experimental researches. In general, retaining wall lateral earth pressure, displacement under seismic/dynamic excitations could be solved by both wedge equilibrium method and subgrade modulus method. However, both of them bear certain inefficiency or become unduly complex as theoretical solutions. The difficulty in accurately predicting seismic retaining wall response comes down: most current theories are not based on real stress strain behaviour of soil behind the wall and thus insufficient at predicting the behaviour under certain conditions such as a different wall or base flexibility, thus different wall displacement. As shown by mobilized strength method devised by Diakoumi and Powrie (2013), the interpretation of stress strain relationship for soil right behind the wall has lead into a one off solution for both stress and displacement for a non-

rigid diaphragm walls with nonlinear deformation along the depth. For seismic cases, the effect of seismic excitation on wall response should also be controlled by soil displacement considering free field theories and relevant analytical solutions. But this method, like other subgrade modulus methods, applies to rigid walls and has neglected the stress strain behaviour right behind the wall. In the contrast, strain increment ratio dependent method developed by Zhang et al. (1998) has produced a solution for seismic lateral earth pressure by taking into account various factors such as vibro densification and surcharge, but it is built on combination of relevant stress strain relationship from static case and Monoke and Okabe's failure wedge method, which assumes a failure plane and is based on wedge equilibrium. Although the notion of intermediate wedge is used for working state, the method has not taken into account the seismically produced free field displacement on the wall since intermediate wedge is not actually a failure plane that divides the soil body. In addition, both strain increment ratio method and subgrade modulus method has inherent difficulties at obtaining certain essential parameters.

To conclude, there is still a lack of analytical solutions that completely and directly interprete seismic stress displacement behaviour; also, the existing relevant theories like strain increment ratio theory and free field subgrade modulus theory are yet to be critically evaluated. Else, the empirical method for the determination of certain parameters are too rough and alternative method will be meaningful. The above mentioned points have lead into the present study, which utilized ABAQUS and PLAXIS to build a strutted diaphragm wall under strong seismic load excitations. The study intends to use the results from numerical softwares to critically investigate both free field dependent subgrade modulus method and strain increment ratio dependent lateral earth pressure theories. In the meanwhile, numerical output are utilized to produce a method for obtaining and validating certain parameters used in the analytical solutions. These procedures and relevant results are combined and analyzed further for better understanding of stress displacement relationship for retaining walls under seismic excitations. The ultimate goal that this study is to producea new analytical method that is based on real seismic stress displacement relationship and able to interprete more sufficiently the local wall and soil response for retaining walls under seismic excitations.

Chapter 3. Theoretical Background

The two theories investigated in this study are strain increment ratio lateral earth pressure theory and free field subgrade modulus method, due to their relevance regarding stress strain relationship or the influence of seismic displacement. In this Chapter, the equations and basic derivations of these theories are discussed. The general structure of this chapter is listed below:

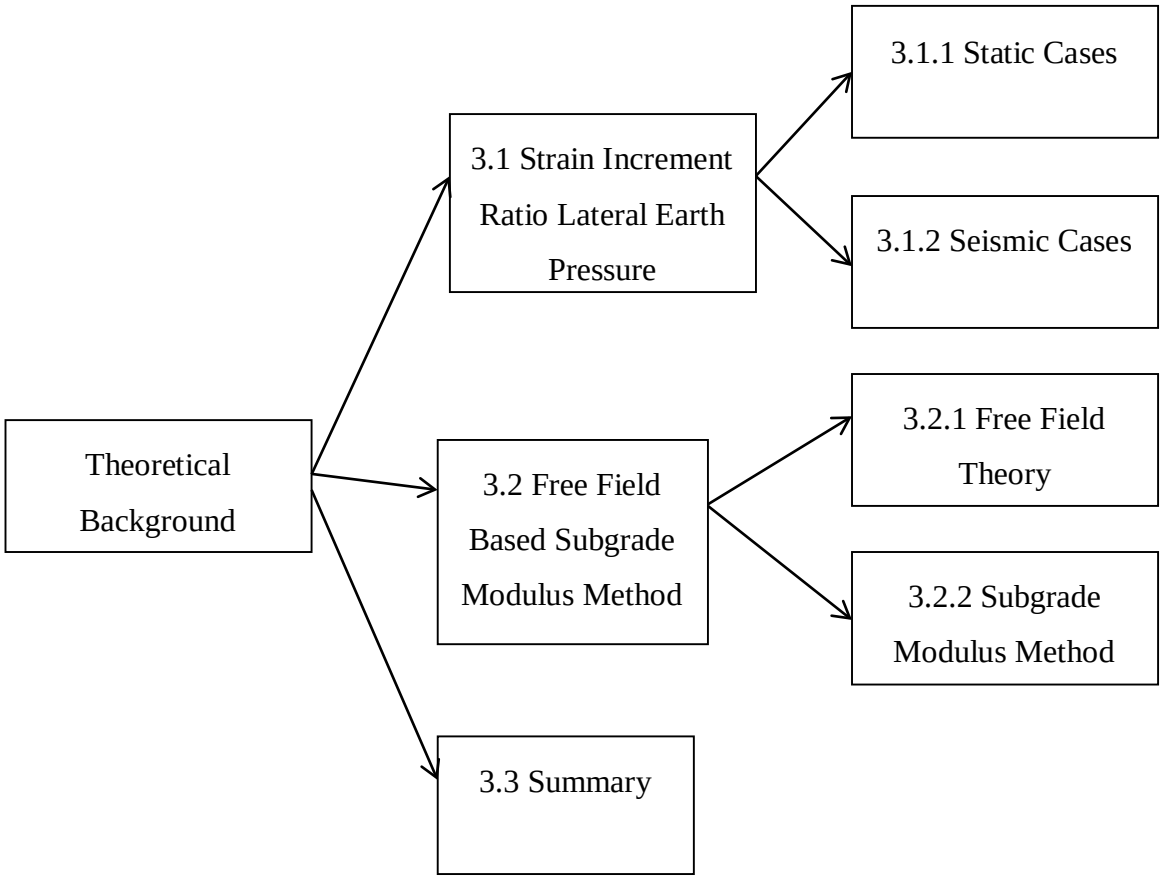

3.1. Strain Increment Ratio Dependent Lateral Earth Pressure Theory

3.1.1. Static Cases

All equations listed in this section is based on Zhang et al. (1998)'s works, except otherwise stated.

In Zhang et al. (1998)'s strain increment ratio dependent lateral earth pressure theory, as mentioned in literature review, consists an important factor of strain increment ratio R_ε. For a plane strain condition used in this PLAXIS model, R_ε could be written as:

$$R_\varepsilon = \begin{cases} \frac{\Delta\varepsilon_{xx}}{\Delta\varepsilon_{yy}} & (\text{or } K \leq 1) \\ \frac{\Delta\varepsilon_{yy}}{\Delta\varepsilon_{xx}} & (\text{for } K \geq 1) \end{cases} \quad (1)$$

$$R = \begin{cases} R_\varepsilon & (K \leq 1) \\ 2 - R_\varepsilon & (K \geq 1) \end{cases} \quad (2)$$

in which Δ, ε_{xx}, $\Delta\varepsilon_{yy}$ are lateral and axial strainincrementsthat could be read from PLAXIS Results after calculation. Since the strain conditions are originated from a state of rest, which corresponds to the phase 1 of PLAXIS Calculation, incremental strain values are adopted in theoretical verification accordingly.

Based on triaxial tests on stress-strain relationships, Zhang et al. (1998) produced a theory for the relationship between lateral earth pressure coefficient and strain increment ratio. Combining with Jaky's equation for Ko, which is the coefficient of lateral earth pressure at rest, the following equations are obtained:

$$K = \begin{cases} \frac{1-sin\phi'}{1-sin\phi' R_\varepsilon} (\text{for } K \leq 1) \\ \frac{1-sin\phi' R_\varepsilon}{1-sin\phi'} (\text{for } K \geq 1) \end{cases} \quad (3) \text{ or}$$

$$K = \begin{cases} \frac{1-sin\phi'}{1-sin\phi' R} (\text{for } -1.0 \leq R \leq 1.0) \\ 1 + \frac{sin\phi'(R-1)}{1-sin\phi'} (\text{for } 1.0 \leq R \leq 3.0) \end{cases} \quad (4)$$

The K≤1 condition represents two cases: 1. the horizontal movement is in active state. 2. The horizontal state is in passive state but the lateral strain increment is less than the vertical strain increment.

Based on sliding wedge model, Coulomb established a famous active and passive earth pressure on cohesionless soils. Integrating the strain ratio dependent lateral pressure theory into Coulomb's earth pressure theory, Zhang et al. (1998) established equations for coefficient of lateral earth pressure under any intermediate state between active and passive states. The following are these equations under conditions of zero surface pressure and vertical soil-foundation interface.

$$K=\frac{2COS^2(\phi')}{COS^2(\phi')(1+R)+COS(\delta_{mob})(1+R)\left[1+\sqrt{\frac{SIN(\phi'+\delta_{mob})SIN(\phi')}{COS(\delta_{mob})}}\right]^2},(-1.0\leq R\leq 1.0) \quad (5)$$

$$K=1+\frac{1}{2}(R-1)\left[\frac{cos^2\phi'}{COS(\delta_{mob})\left[1-\sqrt{\frac{SIN(\phi'+\delta_{mob})SIN\phi'}{COS(\delta_{mob})}}\right]^2}-1\right],(1.0\leq R\leq 3.0) \quad (6)$$

Alternatively, we could use wall displacement rather than wall strain, so R rather than $R_\varepsilon$provided by Zhang et al. (1998) to study intermediate earth pressure solutions:

$$R=\begin{cases}-\left(\frac{|\Delta|}{\Delta_a}\right)^{\beta_a} & (-\Delta_a\leq\Delta\leq 0)\\ -1 & (\Delta<-\Delta_a)\end{cases} \quad (7)$$

$$R=\begin{cases}3\left(\frac{\Delta}{\Delta_p}\right)^{\beta_p} & (0\leq\Delta\leq\Delta_p)\\ 3 & (\Delta>\Delta_p)\end{cases} \quad (8)$$

in which Δ is lateral displacement of wall, Δ_a and $\Delta_p$are lateral displacement for active and passive states respectively.

3.1.2. Seismic Cases

Using strain increment ratio dependent earth pressure theories, Zhang et al. (1998) produced solutions for earth pressure theories under any lateral displacement for retaining wall system subjecting to seismic excitations. The same theories for static case are used for R values such as listed in equations (1), (2), (7) and (8). By the case of no surface load and a vertical wall soil interface, the solution for coefficient of lateral earth pressure under pseudo-static case is

$$K=\frac{2COS^2(\phi\prime-\mathrm{i})}{COS^2(\phi\prime-\mathrm{i})(1+R)+\mathrm{COS(i)}*COS(\delta_{mob}+i)(1-R)\left[1+\sqrt{\frac{SIN(\phi\prime+\delta_{mob})SIN(\phi\prime-\mathrm{i})}{COS(\delta_{mob}+\mathrm{i})}}\right]^2},$$

(for-1.0≤R≤1.0)(9)

$$K = 1+\frac{1}{2}(R-1)\left[\frac{cos^2(\phi\prime-i)}{COS(i)*COS(\delta_{mob}+i)\left[1-\sqrt{\frac{SIN(\phi\prime+\delta_{mob})SIN(\phi\prime-i)}{COS(\delta_{mob}+i)}}\right]^2}-1\right],$$

(for1.0≤R≤3.0) (10)

in which i, angle of seismic coefficient, is calculated from tani= $k_h$for cases with zero vertical acceleration as adopted in present study.

Consequently, the earth pressure consists of four components: 1. Effective weight of soil 2. Inertial effects, 3. surcharge loads, and 4. the effect of soil vibro-densification (Zhang et al. 1998). While there is no surface load in this study, so component 3 is neglected. Component 4 is related with volumetric strain of compressibility. In PLAXIS results, volumetric strain could be read from Stress Point data, which is presented in Figure 4.19. So, the corresponding pressure caused by vibro-densification is represented as:

$$\gamma z K_{rh.o}= \gamma z\ \mathrm{Cr}\ \frac{\varepsilon_v}{1-\varepsilon_v}(11)$$

$\varepsilon_v$values are listed in a decreasing order in Figure 4.19, for these amount of ε_v, equation (11) leads into negligible amount of lateral pressure. So vibro-densification is also neglected for this study. As a result, the seismic lateral earth pressure solution has been:

$$Pz =\gamma z\ \mathrm{COS}(i)K+\gamma(H-z)(1-\ \mathrm{COS}i)K(12)$$

3.2. Free Field Theory Based Subgrade Modulus Method

3.2.1. Free Field Theory

All equations listed in this section is based on Richards et al. (1999)'s works, except otherwise stated.

In seismic analysis on geotechnical engineering, free field response represents the soil field where no influence is incurred from the wall, this normally applies to the response of the soil domain that is around 1.5 - 2.0H from the end wall (Fishman et al. 1995). Richards et al. (1999) worked out pseudo-static solutions for the calculation of free field displacement based on shear modulus that varies with depth. In this PLAXIS model, a constant G (shear modulus) is provided throughout the soil cluster. So Richards et al. (1999)'s equations can be changed into a constant G form as:

$$u_f = \frac{k_h r(z^2 - H^2)}{2G} \quad \text{(elastic response)} \quad (12)$$

$$u_f = \frac{k_h r(z^2 - H^2)}{2G_{sp}} \quad \text{(plastic response)} \quad (13)$$

in which u_f is free field displacement, H is the depth of the soil strata, k_h is coefficient of horizontal acceleration and G_{sp} is secant plastic shear modulus. Equations (12) and (13) are based on zero ground displacement, which means when z=H, the free field displacement is zero.

3.2.2. Subgrade Modulus Method

Rowland et al. (1999) produced a subgrade modulus method for predicting the seismic earth pressure on retaining wall. This method models the soil as springs with constants determined by:

$$\mathbf{K_s} = \mathbf{C_2} G/H \quad (13)$$

in which Ks is the subgrade modulus of the corresponding soil.

As a result, the seismic lateral earth pressure is represented as:

$$\sigma_w = \sigma_{xo} + Ks \times \boldsymbol{\Delta} u = \sigma_{xo} + C_2 G/H \times \boldsymbol{\Delta} u \quad (14)$$

in which σ_{xo} is the horizontal earth pressure at rest, G is the shear modulus of the soil. In this case study, G is constant for soil and mostly only elastic G is considered. σ_{xo} is calculated as $\sigma_{xo} = K_o \gamma z = (1-\sin\phi')\gamma z$ using Rankine's earth pressure theory. $\boldsymbol{\Delta} u$ is "spring displacement" which represents the displacement combining the wall and free field displacements.

3.3. Summary

Strain increment ratio dependent lateral earth pressure theory and free field subgrade modulus theory are listed in this chapter. Different forms of strain increment ratio R_ε are listed under active and passive state respectively. R_ε is transferred into R, which is determined by displacement. This transfers the experiments obtained stress strain relationship into stress displacement relationship. R could be determined by knowing critical state displacements, wall displacements and two exponential factors. Both static and seismic lateral earth pressure equations are listed. These two equations combined strain increment ratio theory and wedge equilibrium theories in both static and seismic cases.

For subgrade modulus method, free field equations based on certain assumptions are firstly introduced. It follows the equation for spring constant Ks and relevant lateral earth pressure solutions. The equations point out the importance of knowing shear modulus G and the combined displacement between wall and free field.

Chapter 4. PLAXIS Modelling and Results Study

In this chapter, PLAXIS modelling was used to investigate both seismic and static response of a strutted diaphragm wall. The used PLAXIS model was firstly introduced. It followed with a method that uses PLAXIS results to obtain analytical parameters, and comparison was made to traditional methods. The lateral earth pressure, displacement curves from PLAXIS results were produced and compared with results from strain increment ratio method. Free field displacement was produced from PLAXIS and the results were studied with a back analysis made to determine subgrade modulus. In this chapter, contents were organized as below:

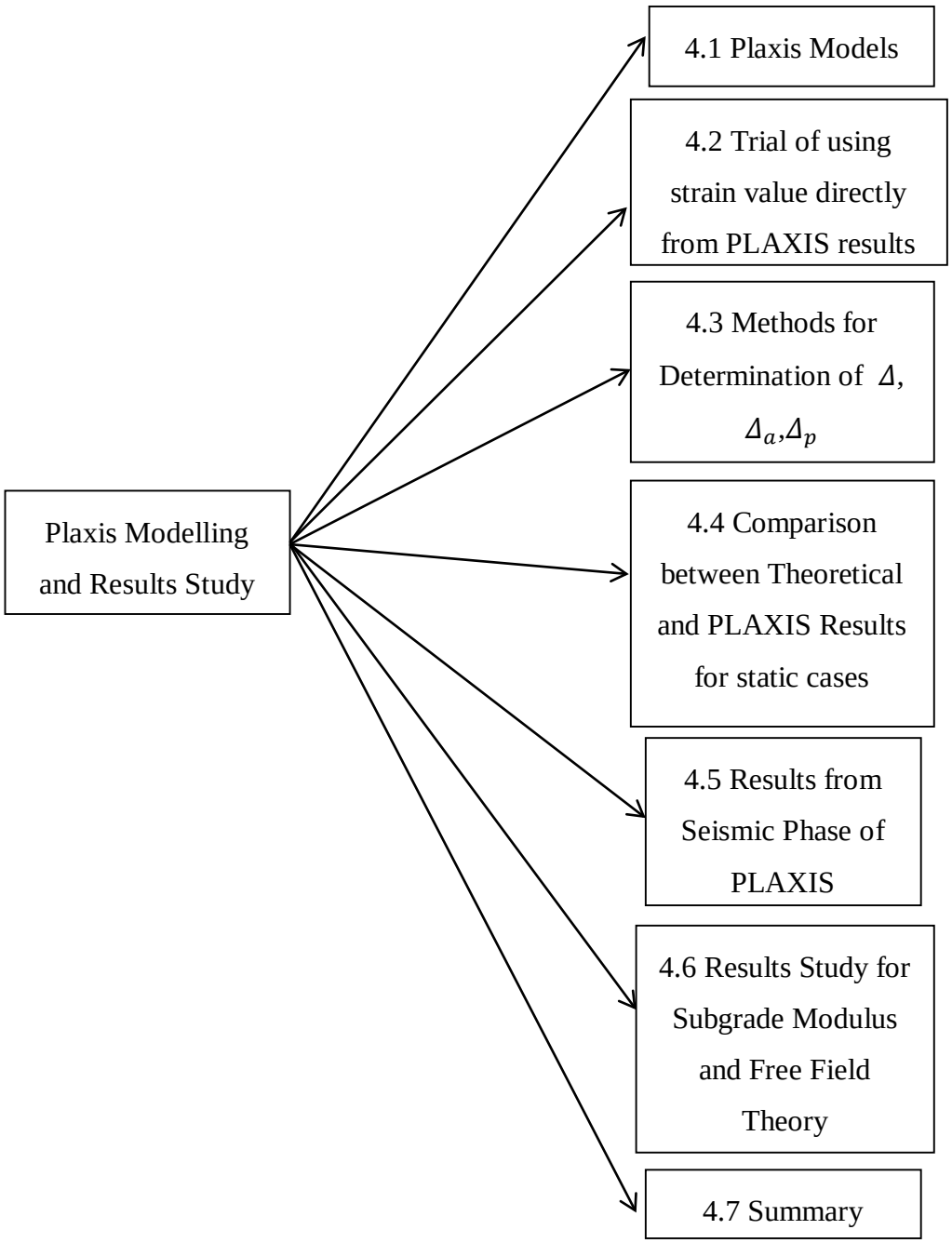

4.1. PLAXIS Models

PLAXIS 2D was used to build a strutted diaphragm wall as shown in Figure 4.1. The dynamic time integration approaches are typically explicit and implicit, while PLAXIS adopted implicit as the scheme. A dynamic time step of 100 is set.

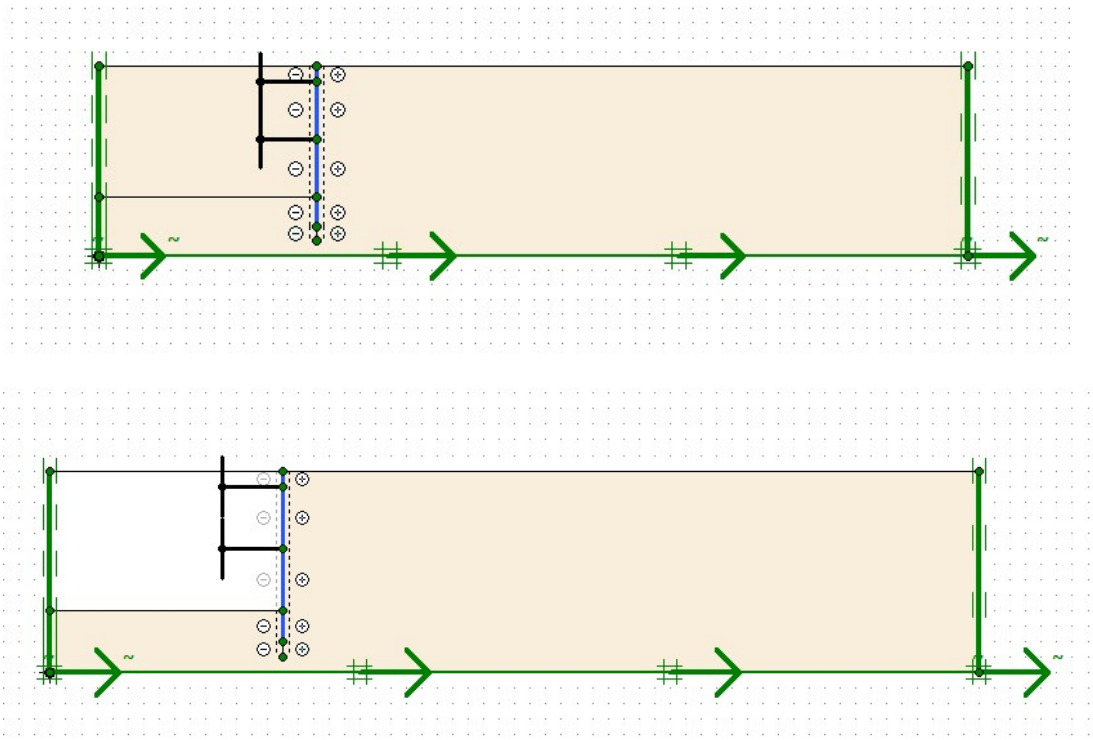

Figure 4.1: PLAXIS 2D model of diaphragm retaining wall under seismic excitation: Upper graph for before excavation; Lower graph for after excavation

4.1.1. Soil Properties

The soil body is 60 meters long and 13 meters high, with engineering properties shown in Table 4.1.

Table 4.1: The properties of soil

Soil type	***Material Model***	***Effective angle of friction ϕ' (o)***	***γsat (kN/m^3)***	***γunsat (kN/m^3)***	***Cohesion c_{ref} (kPa)***	***Poisson ratio v***	***Elasticity (kPa)***	***Initial void ratio e_0***
Sand	Mohr-Coulomb	30	20	17	0	0.3	17500	0.5

4.1.2. Wall Properties

Plate element is used to model the wall. The wall length is 11 meters and 9 meters of it are exposed to excavation as shown in Figure 4.1. The engineering properties of the wall are shown in Table 4.2.

Table 4.2: Diaphragm wall properties

Density (kg/m3)	***Elasticity (Pa)***	***Poisson ratio v***	***EI (N/m^2/m)***	***Length(m)***
378.774	5366726000	0.15	5e9	11

4.1.3. Strut Properties

Two struts are applied to support the wall at the location of 1 and 5 meters below the top of the wall respectively. Fixed end anchors are used to model the strut with properties shown in Table 4.3.

Table 4.3: Strut properties

Strut Siffness (kN)	***Strut Length(m)***	***Strut spacing (m)***
2e6	15	5

4.1.4. Boundary Conditions

Standard fixity provided in PLAXIS is used to model all boundaries plus dynamic absorbent boundaries to alleviate or eliminate wave reflections. The bottom line was applied with a dynamic prescribed displacement, upon which earthquake record will be applied at the seismic stage. The complete boundaries are also shown in Figure 4.1.

4.1.5. Interaction

In PLAXIS, the wall – soil interaction is simulated by interface element, which has an interface coefficient of $\boldsymbol{R_{inter}}$, defined as $\tan\boldsymbol{\delta_{mob}} = \boldsymbol{R_{inter}}\tan\boldsymbol{\phi}^{-}_{\boldsymbol{soil}}$, a default $\boldsymbol{R_{inter}}$ = 0.67 is applied in this study. $\boldsymbol{\delta_{mob}}$is the mobilized friction angle between wall and interface and is thus calculated as 21.2°.

4.1.6. Earthquake Excitations

PLAXIS is able to process the SMC file of real earthquake records of the ground acceleration/displacement values during certain earthquakes. In this study, SMC file for Offshore Maule Earthquake, downloaded from U.S. Geological Survey website, is applied to the bottom boundary in the seismic stage. The acceleration versus time graph of this earthquake is shown in Figure 4.2. The dynamic duration is set as 60 seconds.

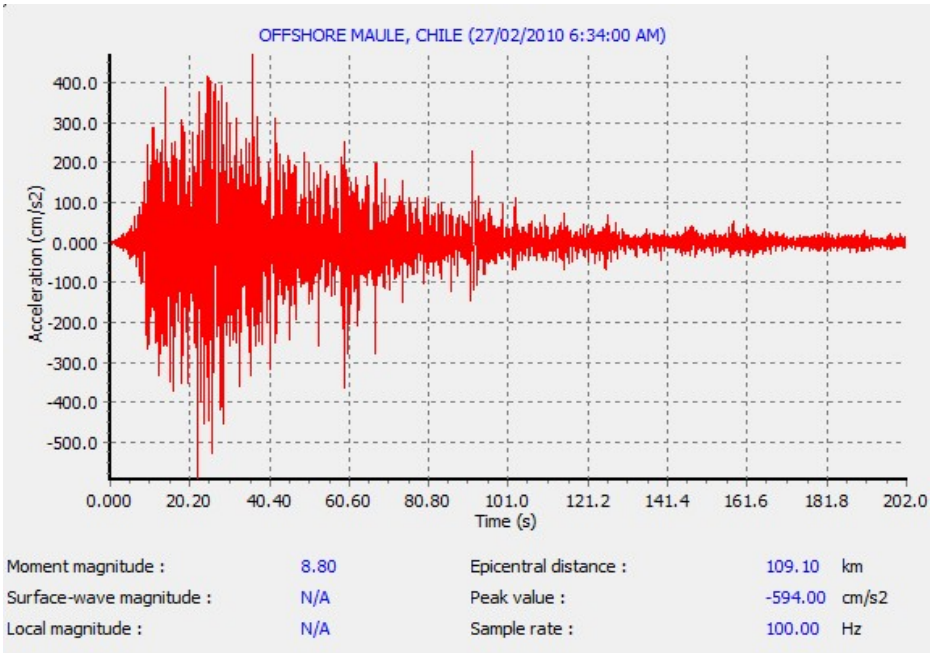

Figure 4.2: Acceleration versus Dynamic Time diagram for Offshore Maule earthquake (courtesy of the U.S. Geological Survey)

4.2. Trial of using strain value directly from PLAXIS results

PLAXIS is able to provide strain values for all stress points but not node points. Since Cartesian strain values are not available for nodes on interface and wall, a cross line is manually drawn as close as possible to the wall interface using “cross

section" tool provided by PLAXIS to select the stress points along the line (as shown in Figure 4.3). Both horizontal and vertical strains are readily available along this line to interpret the soil behaviour behind the wall. The PLAXIS results for lateral strain distribution and displacement distribution along A-A* is shown in Figure 4.4 and Figure 4.5.

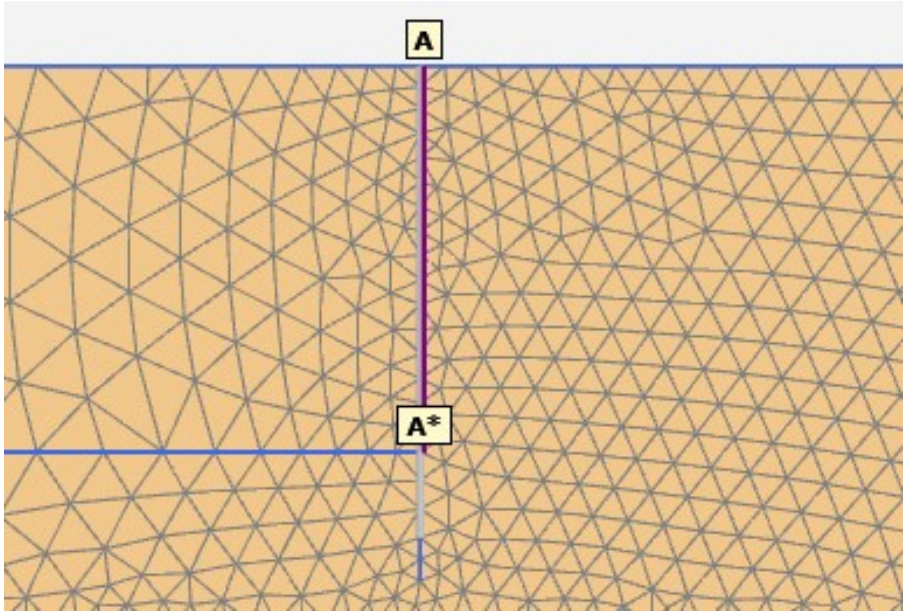

Figure 4.3: A cross line close to wall for Cartesian strain values in PLAXIS results

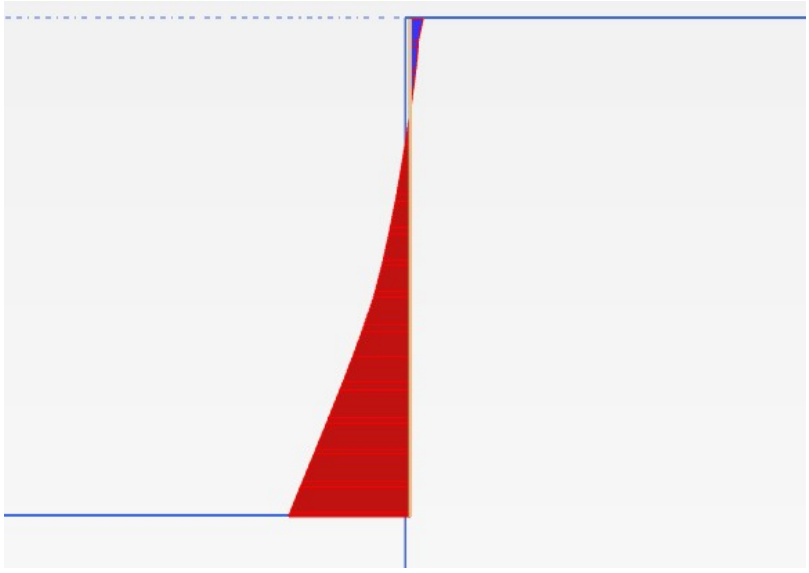

Figure 4.4: Horizontal displacement profile of line A-A

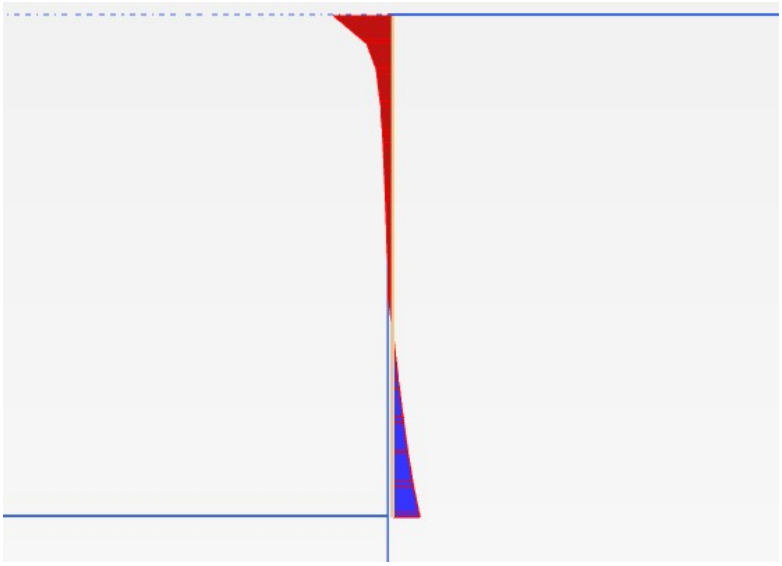

*Figure 4.5: Horizontal strain profile of line A-A**

Comparing two graphs, the obvious inconsistency is observed between horizontal strain profile and horizontal displacement profile, e.g. displacement and strain are in opposite directions at the top part. This contradicts the basis of above strain ratio dependent earth pressure theory that requires a negative strain for active displacement. This indicates the strain value obtained from PLAXIS is inconsistent with the relevant displacement for areas close to the wall. Thus, strain values orR_ε in equations (1) and (2) could not be used directly for verification of strain increment ratio lateral earth pressure theories. One possible reason for this might be that only stress points produced strain values, which are not recorded in nodes.

4.3. Methods for determination of Δ, Δ_a,Δ_p

There are a number of ways to determine relevant displacement parameters used in strain increment ratio equations. Zhang et al. (1998) listed typical modes of wall displacement and relevant solutions of Δ for each of those modes, but these only apply to rigid walls. In this study, Δ could be more easily obtained from PLAXIS results by reading the horizontal displacement of wall, which could be conveniently realized in PLAXIS output.

There are several methods to determine active and passive displacement factors Δ_a and Δ_p produced by different authors using both empirical and experimental methods, some of which are listed in Table 4.4.

Table 4.4: Selected estimation for active and passive state wall displacement to wall height H(Zhang et al. 1998)

Type of Soil	***Type of lateral movement***	***Critical state displacement***	
		$-\Delta_a$	Δ_p
Dense sand	Horizontal translation	0.001H	0.05H
	Rotation about base	0.001H	>0.1H
Silty sand	Horizontal translation	0.006H-0.008H	N/A
Slag		0.003H-0.005H	N/A
Dense sand (Dr=90%)	Horizontal translation	N/A	0.03H-0.04H
Quicklime slag	Rotation about base	0.009H-0.001H	>0.3H
Medium dense sand (Dr=68%)	Horizontal translation	0.004H	0.014H

However, these methods are mostly restricted to soil samples with certain relative density, displacement modes or soil type. For example, in present study, it is ambiguous to classify the sand we use in PLAXIS into any sand type of those methods. Not to mention these methods are originated on a rough estimation basis. Alternatively, PLAXIS results are able to provide useful information regarding active and passive displacements. The reason is that PLAXIS result is able to provide the status of stress point based on soil failure criterion selected for the material set, as well as the displacement information of a wall. In this case, it is dry homogeneous sand with Mohr-Coulomb failure criterion.

When Mohr-Coulomb mode is selected and diaphragm wall is used to retain dry sand, there is usually some soil behind the wall that is in failure, which could provide us information about the displacement to initiate this failure (Δ_a,Δ_p). The author chose

Mohr-Coulomb mode since strain increment ratio dependent lateral earth pressure theory is actually a combination of stress strain relationship and Mohr-Coulomb theories by Zhang et al. (1998). The procedures for obtaining Δ_a and Δ_p using PLAXIS are listed below:

1. Build a model that makes the retaining wall move towards passive/active direction. ForΔ_a, actively displacing wall is needed while for Δ_p, passively displacing wall is needed.The diaphragm wall model (see Figure 4.1) itself is usually actively displacing, while the passive case could be achieved by removing the strut for active case or applying a horizontal load on the wall to move it into passive failure, as shown in Figure 4.6.
2. Run the models and get the results. Check the results table and select "Cartesian Effective Stress", among those stress points marked "failure", find out the ones that locate close to the wall according to their coordinates shown in the table (see Figure 4.7). For example, in this model, since the wall is located at X coordinates of 15 meters, so the picked points could be those a little less or more than 15m considering a deformed shape of the wall. We can use "filter" in the toolbar to screen out all points based on the needs.
3. With reference to deformed mesh (see Figure 4.6) or displacement profile of wall or interface, estimate a point location at which the failure status is initiated, the displacement at this point could be used as critical state displacement. For example, stress point 3796(blue shaded in Figure 4.7) is the failure point that has lowest depth (excluding wall section below excavation). And based on Figure 4.6, stress point 3796should have the displacement that just initiate the "passive failure" since all points that has lower horizontal displacement is not at failure.
4. Select the wall to obtain displacement profile of the wall and thus a table containing values of horizontal displacement along the wall as shown in Figure 4.8. The horizontal displacement at around 11.67m deep could be picked asΔ_p as mentioned above. Although not the exact depth,$\Delta_p$can be roughly extrapolated as 117mm, the roughness at this value that would not affect much since $\Delta_p$it self is not a fixed value and keep varying from case to case even if soil and wall geometry are the same.

For verification, Δ_p/H= 117mm/9m=0.013

This is in reasonable agreement with the range of data provided in Table 4.4.

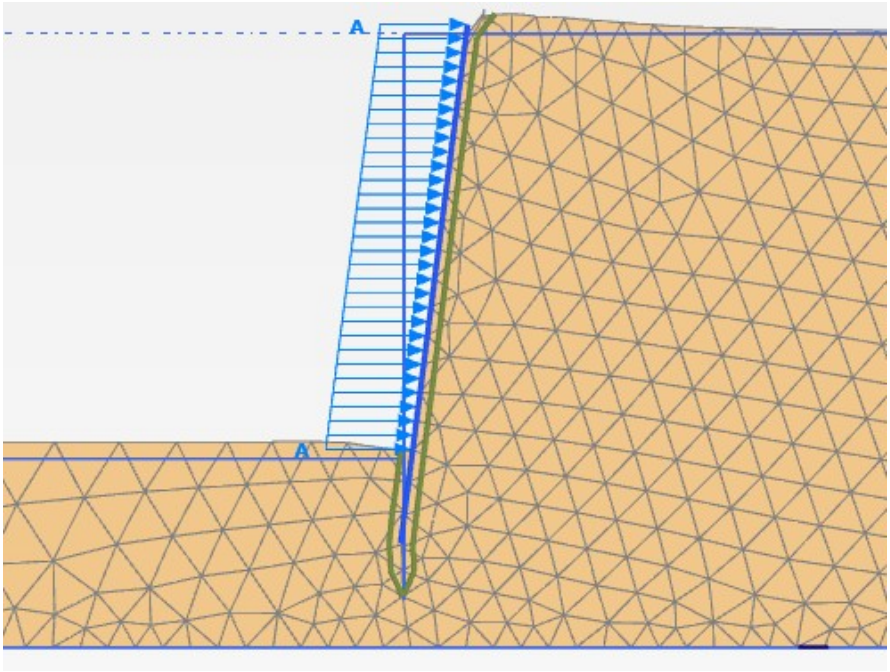

Figure 4.6: Schematic view of passively displacing wall

<Phase 2> (Step 36)

Soil element	Stress point	Local number	X [m]	Y [m]	σ'_{xx} [kN/m^2]	σ'_{yy} [kN/m^2]	σ'_{zz} [kN/m^2]	σ_{xy} [kN/m^2]	Status
Clus. 1 - El. 1475	4425	3	15.353	1.316	-37.645	-84.956	-38.481	-19.490	Failure
Clus. 1 - El. 1471	4411	1	15.268	1.780	-36.503	-83.350	-37.589	-18.685	Failure
Clus. 1 - El. 1290	3868	1	15.195	12.466	-46.959	-17.893	-19.534	7.187	Failure
Clus. 1 - El. 1269	3805	1	15.190	11.835	-111.765	-60.848	-51.953	34.843	Failure
Clus. 1 - El. 1383	4149	3	15.158	2.015	-22.877	-63.184	-27.418	-7.533	Failure
Clus. 1 - El. 1474	4420	1	15.155	1.524	-33.195	-72.529	-33.388	-17.658	Failure
Clus. 1 - El. 1336	4006	1	15.099	12.266	-45.763	-38.179	-25.289	20.640	Failure
Sand	4007	2	15.099	11.966	-88.706	-52.321	-42.459	30.201	Failure
Clus. 1 - El. 1364	4091	2	15.096	12.600	-29.439	-15.083	-13.415	8.507	Failure
Sand	4090	1	15.096	12.900	-5.824	-3.063	-2.681	1.741	Failure *
Clus. 1 - El. 1266	3796	1	15.091	11.670	-92.739	-57.052	-45.131	32.923	Failure
Clus. 1 - El. 1271	3813	3	15.091	2.161	-20.212	-60.135	-25.683	2.242	Failure
Clus. 1 - El. 1475	4423	1	15.088	1.392	-35.753	-76.927	-35.494	-19.228	Failure
Clus. 1 - El. 1471	4412	2	15.067	1.883	-27.578	-60.745	-28.116	-14.579	Failure
Sand	4413	3	15.067	1.633	-39.002	-67.355	-33.562	-22.495	Failure
Clus. 1 - El. 1473	4417	1	14.928	1.122	-37.065	-39.014	-24.553	-18.995	Failure
Clus. 1 - El. 1272	3816	3	14.907	2.419	-16.482	-36.902	-17.556	8.595	Failure
Clus. 1 - El. 1472	4415	2	14.907	1.891	-36.755	-29.878	-21.607	-16.299	Failure
Sand	4414	1	14.907	1.641	-25.425	-38.478	-20.825	-14.582	Failure
Clus. 1 - El. 1176	3528	3	14.905	3.889	-0.577	-1.317	-1.421	-0.296	Failure *
Sand	3527	2	14.905	3.556	-1.947	-5.841	-3.712	0.023	Failure *
Clus. 1 - El. 1082	3246	3	14.879	3.217	-3.716	-11.051	-5.855	0.425	Failure
Sand	3245	2	14.879	2.884	-6.282	-18.040	-8.770	1.553	Failure
Clus. 1 - El. 1086	3258	3	14.784	3.439	-3.426	-10.091	-5.447	0.562	Failure
Clus. 1 - El. 1085	3254	2	14.735	2.512	-15.533	-25.086	-13.713	8.961	Failure

Figure 4.7: Table view of passive collapse case – under "Effective Cartesian Stress" selection

<Phase 2> (Step 36)

Structural element	Node	Local number	X [m]	Y [m]	u_x [10^{-3} m]	u_y [10^{-3} m]	|u| [10^{-3} m]
Plate 1-1	862	3	15.000	13.000	134.483	19.473	135.885
(diaphram wall)	861	2	15.000	12.700	130.601	19.473	132.044
	860	1	15.000	12.400	126.717	19.473	128.204
Plate 1-2	860	3	15.000	12.400	126.717	19.473	128.204
(diaphram wall)	858	2	15.000	12.100	122.833	19.473	124.367
	859	1	15.000	11.800	118.948	19.473	120.532
Plate 1-3	859	3	15.000	11.800	118.948	19.473	120.532
(diaphram wall)	857	2	15.000	11.500	115.065	19.472	116.701
	856	1	15.000	11.200	111.183	19.472	112.875
Plate 1-4	856	3	15.000	11.200	111.183	19.472	112.875
(diaphram wall)	855	2	15.000	10.900	107.303	19.471	109.055
	854	1	15.000	10.600	103.425	19.470	105.242
Plate 1-5	854	3	15.000	10.600	103.425	19.470	105.242
(diaphram wall)	801	2	15.000	10.300	99.550	19.469	101.436
	800	1	15.000	10.000	95.678	19.468	97.639
Plate 1-6	800	3	15.000	10.000	95.678	19.468	97.639
(diaphram wall)	793	2	15.000	9.700	91.809	19.467	93.850
Plate 1-7	792	3	15.000	9.400	87.942	19.465	90.071
Plate 1-6	792	1	15.000	9.400	87.942	19.465	90.071
Plate 1-7	773	2	15.000	9.100	84.078	19.464	86.301
(diaphram wall)	772	1	15.000	8.800	80.216	19.462	82.543
Plate 1-8	772	3	15.000	8.800	80.216	19.462	82.543
(diaphram wall)	771	2	15.000	8.500	76.356	19.461	78.797
Plate 1-9	770	3	15.000	8.200	72.498	19.459	75.064
Plate 1-8	770	1	15.000	8.200	72.498	19.459	75.064

Figure 4.8: Results table of wall displacement for passive collapse model

In the same way, $\mathbf{\Delta_a}$of this sand material.is able to be obtained using a model (with exactly the same soil material set) that moves towards active state. Please note, the active mode should be any one that is able to provide the depth that distinguishes failure and elastic status, sometimes, even a collapsed model works. The lowest depth along the wall that subjects to soil active failure is read from Figure 4.10 as 9.814m (shaded in blue). The wall displacement value is shown in Figure 4.11, and it is estimated 19mm as the horizontal displacement at which the soil reaches active state, so $\mathbf{\Delta_a}$=19mm. For verification:

Δ_a/H= 19mm/9m=0.00211

which also agrees well with the range of values of other estimation methods based on ratio of active state displacement to wall height as shown in Table 4.4.

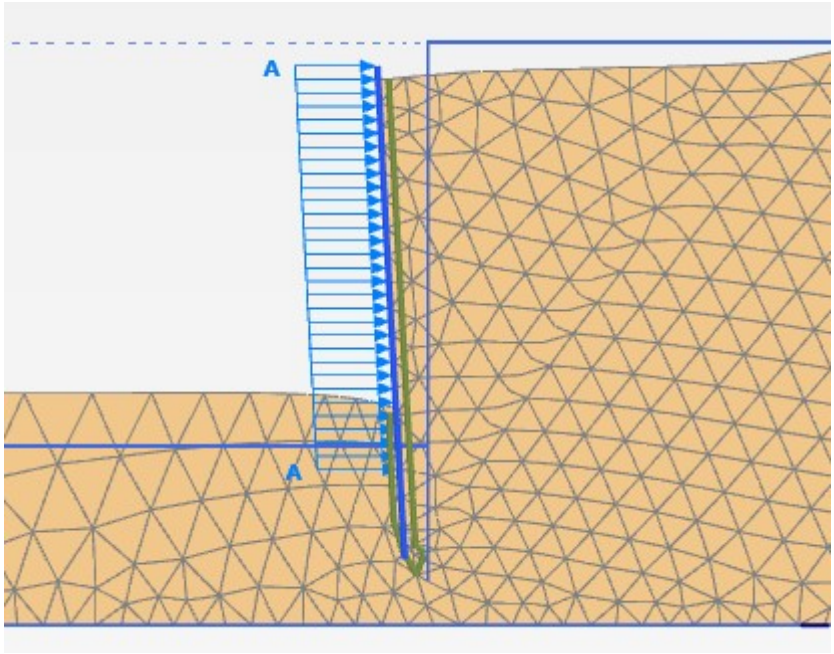

Figure 4.9: Deformed mesh of active failure after soil collapse

<Phase 2> (Step 20)

Soil element	Stress point	Local number	X [m]	Y [m]	σ'_{xx} [kN/m^2]	σ'_{yy} [kN/m^2]	σ'_{zz} [kN/m^2]	σ_{xy} [kN/m^2]	Status
Clus. 1 - El. 1333	3997	1	15.084	10.478	-13.540	-40.282	-16.514	-1.505	Failure
Clus. 1 - El. 1265	3793	1	15.084	10.678	-12.191	-35.895	-14.764	-2.011	Failure
Sand	3795	3	15.084	10.978	-10.311	-29.698	-12.297	-2.467	Failure
Clus. 1 - El. 1266	3797	2	15.091	11.370	-7.303	-20.405	-8.550	-2.251	Failure *
Sand	3796	1	15.091	11.670	-5.710	-16.767	-6.937	-1.006	Failure
Clus. 1 - El. 1364	4091	2	15.096	12.600	-2.278	-6.331	-2.641	-0.724	Failure
Clus. 1 - El. 1336	4007	2	15.099	11.966	-4.747	-13.914	-5.749	-0.870	Failure
Sand	4006	1	15.099	12.266	-3.740	-10.790	-4.466	-0.875	Failure
Clus. 1 - El. 1269	3805	1	15.190	11.835	-5.918	-16.841	-6.997	-1.596	Failure
Clus. 1 - El. 1212	3634	1	15.206	10.012	-15.941	-47.569	-19.488	-1.416	Failure
Clus. 1 - El. 1215	3643	1	15.238	11.060	-9.632	-26.937	-11.253	-2.952	Failure
Clus. 1 - El. 1217	3650	2	15.245	11.252	-9.729	-27.071	-11.295	-3.075	Failure
Clus. 1 - El. 1333	3999	3	15.335	10.411	-13.485	-39.727	-16.340	-2.193	Failure
Clus. 1 - El. 1265	3794	2	15.335	10.611	-12.326	-35.954	-14.832	-2.473	Failure
Clus. 1 - El. 1266	3798	3	15.364	11.579	-8.242	-23.668	-9.780	-2.038	Failure
Clus. 1 - El. 1364	4092	3	15.383	12.900	-0.606	-1.433	-0.626	0.298	Failure
Clus. 1 - El. 1336	4008	3	15.396	12.163	-4.174	-12.473	-5.116	-0.321	Failure
Clus. 1 - El. 1212	3636	3	15.458	10.245	-15.312	-45.633	-18.685	-1.518	Failure
Clus. 1 - El. 1269	3806	2	15.463	11.745	-5.524	-16.145	-6.683	-1.069	Failure
Clus. 1 - El. 1290	3870	3	15.482	12.766	-1.714	-4.992	-2.046	0.354	Failure
Clus. 1 - El. 1269	3807	3	15.487	12.032	-5.815	-17.426	-7.113	-0.233	Failure
Clus. 1 - El. 1215	3644	2	15.489	10.693	-11.350	-32.421	-13.467	-2.957	Failure
Clus. 1 - El. 1290	3869	2	15.492	12.363	-3.562	-10.615	-4.346	0.354	Failure
Clus. 1 - El. 1217	3649	1	15.519	11.461	-8.147	-23.744	-9.791	-1.658	Failure
Clus. 1 - El. 1212	3635	2	15.575	9.814	-17.178	-51.429	-21.046	-0.952	Failure

Figure 4.10: Filtered table view of active collapse case – under "Effective Cartesian Stress" selection

Structural element	Node	Local number	X [m]	Y [m]	u_x [10^{-3} m]	u_y [10^{-3} m]	|u| [10^{-3} m]
Plate 1-1	862	3	15.000	13.000	-22.440	-10.591	24.814
(diaphram wall)	861	2	15.000	12.700	-22.120	-10.591	24.525
	860	1	15.000	12.400	-21.800	-10.590	24.237
Plate 1-2	860	3	15.000	12.400	-21.800	-10.590	24.237
(diaphram wall)	858	2	15.000	12.100	-21.481	-10.590	23.949
	859	1	15.000	11.800	-21.161	-10.590	23.663
Plate 1-3	859	3	15.000	11.800	-21.161	-10.590	23.663
(diaphram wall)	857	2	15.000	11.500	-20.841	-10.590	23.377
	856	1	15.000	11.200	-20.522	-10.589	23.093
Plate 1-4	856	3	15.000	11.200	-20.522	-10.589	23.093
(diaphram wall)	855	2	15.000	10.900	-20.202	-10.589	22.809
	854	1	15.000	10.600	-19.882	-10.588	22.525
Plate 1-5	854	3	15.000	10.600	-19.882	-10.588	22.525
(diaphram wall)	801	2	15.000	10.300	-19.561	-10.588	22.243
	800	1	15.000	10.000	-19.240	-10.587	21.960
Plate 1-6	800	3	15.000	10.000	-19.240	-10.587	21.960
(diaphram wall)	793	2	15.000	9.700	-18.918	-10.587	21.679
Plate 1-7	792	3	15.000	9.400	-18.595	-10.586	21.397
Plate 1-6	792	1	15.000	9.400	-18.595	-10.586	21.397
Plate 1-7	773	2	15.000	9.100	-18.272	-10.585	21.116
(diaphram wall)	772	1	15.000	8.800	-17.947	-10.584	20.836
Plate 1-8	772	3	15.000	8.800	-17.947	-10.584	20.836
(diaphram wall)	771	2	15.000	8.500	-17.621	-10.583	20.555
Plate 1-9	770	3	15.000	8.200	-17.294	-10.582	20.275
Plate 1-8	770	1	15.000	8.200	-17.294	-10.582	20.275

Figure 4.11: Results table of wall displacement for active collapse model

The horizontal wall displacement (Δ) is readily available from PLAXIS results in the form of both graph (see Figure 4.12) and values in table (Figure 4.13). While the magnitude of wall horizontal displacement could be obtained from tables, and is able to be easily transferred into spread sheet. Consequently, only $\beta_a$and $\beta_p$are needed for the estimation of R based on equation (7) and (8). Zhang et al. (1998)'s pragmatic charts method is firstly carried out for the sand with friction angle of 30 degree. The specific procedures are quite straightforward and not listed here. The obtained $\beta_a$and β_p are 0.4 and 0.51 respectively. However, the author find the pragmatic charts method provided by Zhang et al. (1998) is a very rough estimation and it needs some guess to obtain these values, so it is valuable to compare the resulting lateral earth pressure obtained from these parameters to the PLAXIS results. Based on Figure 4.12, it is obvious that the wall subjects to active displacement only. And only excavated wall section (top 9 meters) is investigated for this study, thus only active soil pressure is investigated and only equation (5) is used for calculation of K.

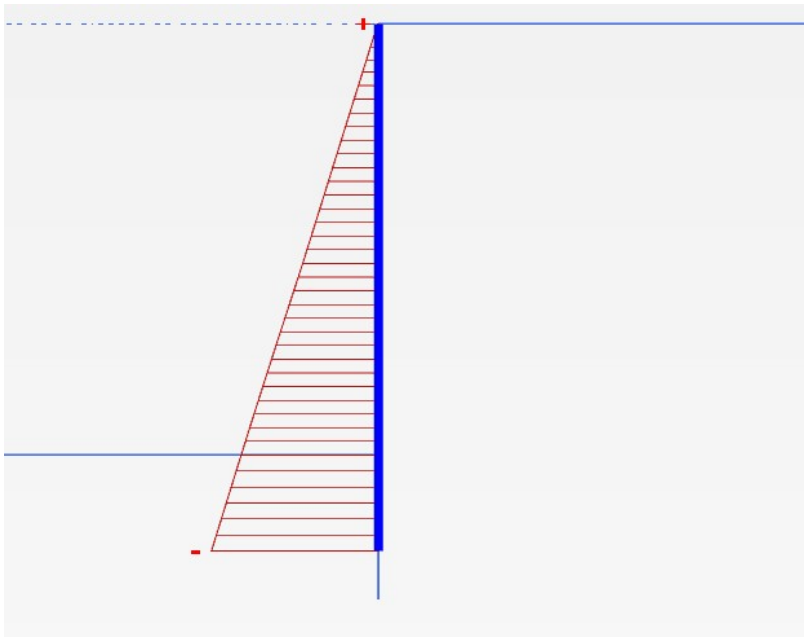

Figure 4.12: Result horizontal displacement of static phase (phase 2)

4.4. Comparison between Theoretical and PLAXIS Results for Static Case

File View Project Deformations Forces Tool Window Help

<Phase 2> (Step 17)

Structural element	Node	Local number	X [m]	Y [m]	u_x [10^{-3} m]	u_y [10^{-3} m]	|u| [10^{-3} m]
Plate 1-2	867	1	15.000	12.500	-0.867	-10.724	10.759
(diaphram wall)	864	2	15.000	12.250	-1.259	-10.724	10.798
	863	3	15.000	12.000	-1.651	-10.724	10.850
Plate 1-3	863	1	15.000	12.000	-1.651	-10.724	10.850
(diaphram wall)	862	2	15.000	11.714	-2.101	-10.724	10.928
	861	3	15.000	11.429	-2.551	-10.724	11.023
Plate 1-4	861	1	15.000	11.429	-2.551	-10.724	11.023
(diaphram wall)	860	2	15.000	11.143	-3.000	-10.724	11.135
	859	3	15.000	10.857	-3.449	-10.723	11.265
Plate 1-5	859	1	15.000	10.857	-3.449	-10.723	11.265
(diaphram wall)	858	2	15.000	10.571	-3.898	-10.723	11.410
	857	3	15.000	10.286	-4.346	-10.723	11.570
Plate 1-6	857	1	15.000	10.286	-4.346	-10.723	11.570
(diaphram wall)	838	2	15.000	10.000	-4.794	-10.723	11.746
	837	3	15.000	9.714	-5.242	-10.722	11.935
Plate 1-7	837	1	15.000	9.714	-5.242	-10.722	11.935
(diaphram wall)	830	2	15.000	9.429	-5.690	-10.722	12.138
	829	3	15.000	9.143	-6.137	-10.722	12.354
Plate 1-8	829	1	15.000	9.143	-6.137	-10.722	12.354
(diaphram wall)	769	2	15.000	8.857	-6.585	-10.721	12.582
	768	3	15.000	8.571	-7.034	-10.721	12.822
Plate 1-9	768	1	15.000	8.571	-7.034	-10.721	12.822

Figure 4.13: PLAXIS results table showing displacement of Wall in Static Phase (phase 2)

Based on horizontal displacement values from tables shown in Figure 4.13, R value corresponding to each displacement could be obtained from equations (7) and (8) using spreadsheet. The variation of R throughout the depth of the wall is shown in Figure 4.14. Then the lateral earth pressure coefficients K are calculated from equations (5) and the distribution of K along the wall is shown in Figure 4.15.

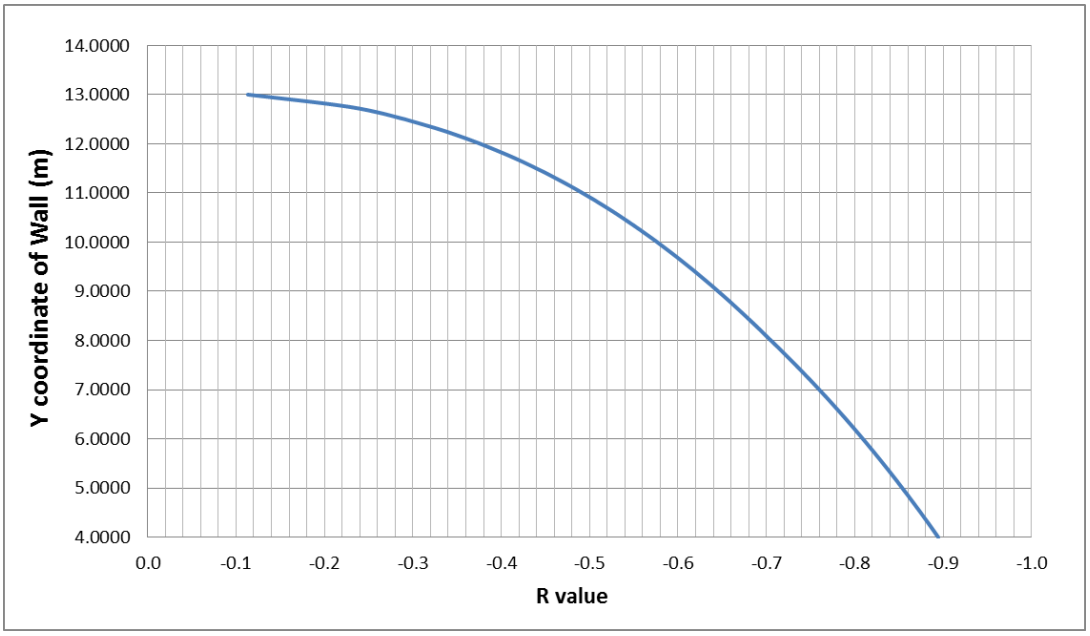

Figure 4.14: The obtained curve of R value versus Y axis of the Wall

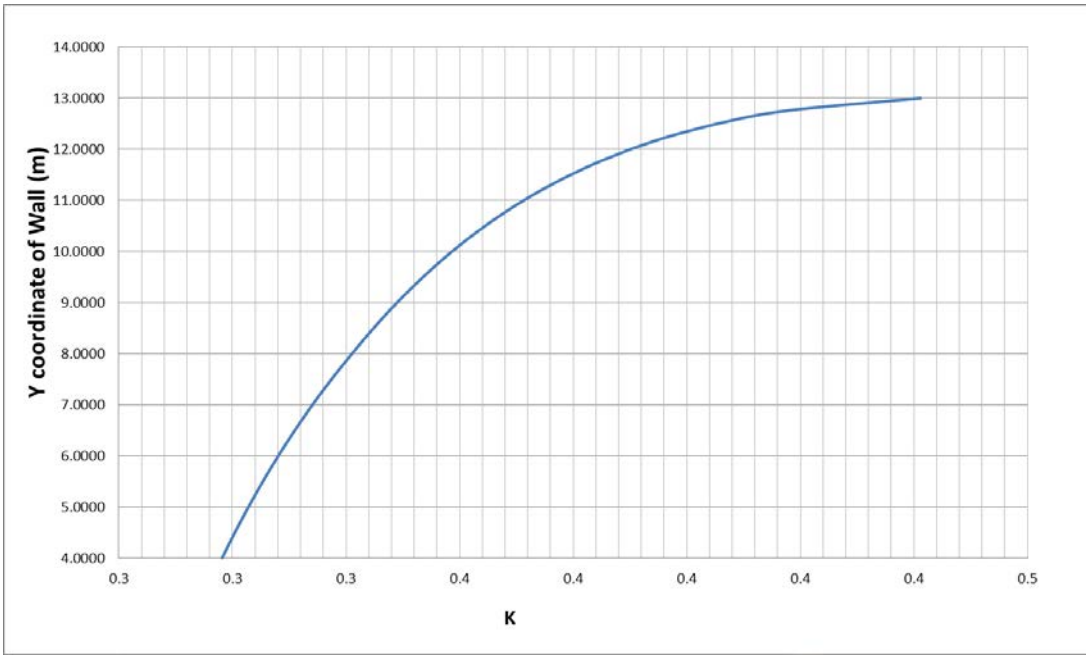

Figure 4.15: The obtained curve of K value versus Y axis of the Wall

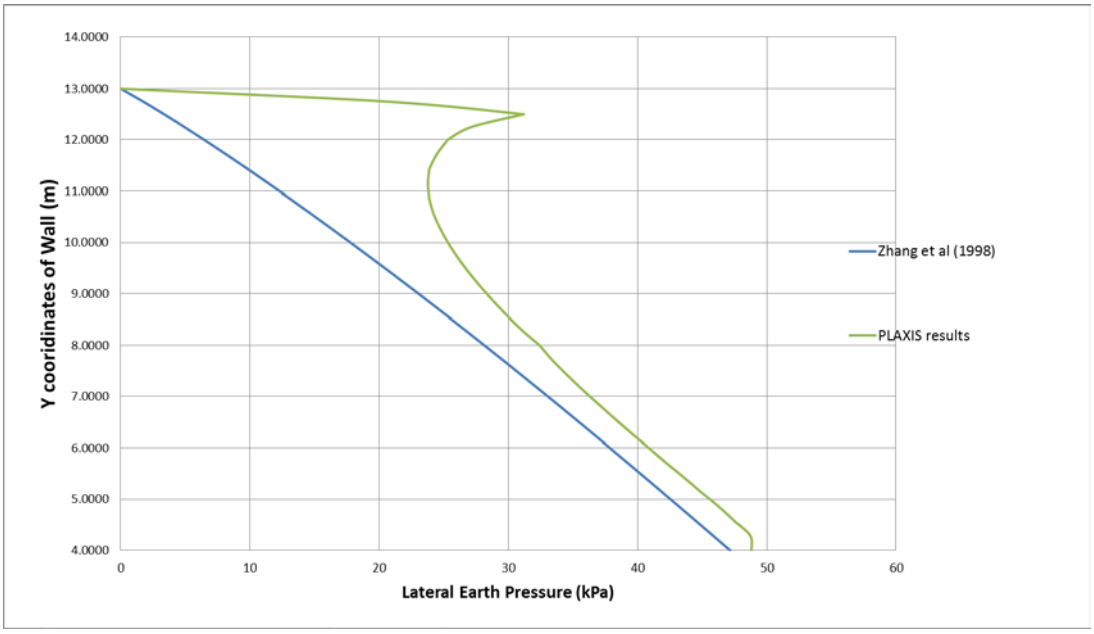

Figure 4.16: Distribution of earth pressure along walls based on different methods

With the distribution of K, the lateral earth pressure could be obtained from $p_z = \gamma z K$. Figure 4.16 shows the distribution of lateral earth pressure along the wall as calculated using strain ratio dependent earth pressure theory produced by Zhang et al (1998). A linear distribution is observed. Besides, the pressure distribution obtained from the PLAXIS results is also drawn. PLAXIS result produces the lateral pressure distribution as shown in the green curve of Figure 4.16. These two curves agree well under Y coordinates of 9 m which means below 4 m depth of the wall. However, for the upper 9 m coordinates part, PLAXIS gives significantly larger lateral earth pressure which increases drastically for the top 0.5m, after which it reduces to a value similar to analytical results. The inconsistency between the horizontal displacements used by Zhang et. al (1998)'s analytical method and the PLAXIS generated large pressure for the top part of the wall might be caused by large amount of vertical displacements the top of the wall as shown in Figure 4.17, which indicates a strong dominance of vertical displacement for the top section of the wall. But in strain increment ratio theory, only horizontal displacement is accounted for.

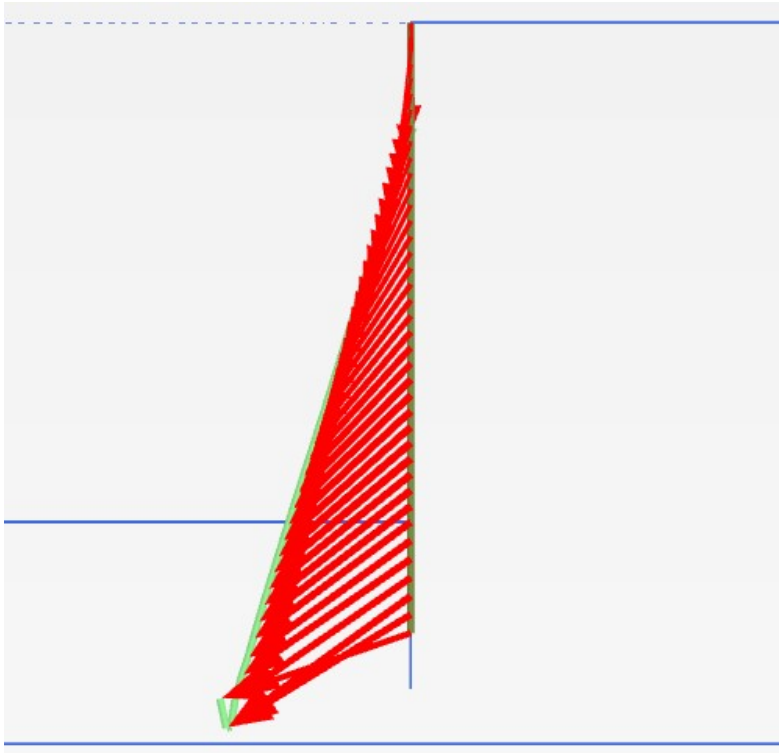

Figure 4.17: Displacement arrows along the wall after PLAXIS calculation (static phase)

Considering that the parameters for Zhang et al. (1998) are based on rough estimation, especially for two charts determined exponential parameters $\beta_a$and β_p, this final lateral pressure is acceptable and so the software obtained parameters are justified. However, more investigation could be conducted on other type of soils or retaining systems with various geometries to further verify this study, and these investigations should be for normally consolidated soil only, which is a premise for current strain increment ratio lateral earth pressure theory.

In this study, PLAXIS acts as a tool to calculate critical state earth/wall displacement Δ_a and$\Delta_p$which, previously, could only be roughly estimated based on empirical or value fitting equations shown in Table 4.4. The ideas in this study could also be used as a tool for further investigation of Δ_a and Δ_p for various soils and retaining systems. Also, the study on influencing factors forΔ_a and Δ_p could be made by parametric study as an extension of the present study.

Actually, if the PLAXIS results as shown in Figure 4.16 were verified in practice, it could lead into a way of calculating β_a and β_p for equations (7) and (8) by means of

curve fitting using a similar graph as Figure 4.16. For example, for the current retaining wall case, change the value of β_a since only active displacement is encountered and only equation (7) is utilized for R. Keep changing β_a until the curve comes closest to PLAXIS curve as shown in Figure 4.18, then the input β_a value can be used as β_a for similar cases. In this case, a $\beta_a$value of 1.1 produces two very close curves as shown in Figure 4.18. Compared to Figure 4.16, it seems changing β_a value from 0.4 to 1.1 only slightly increase the lateral pressure, so the influence of β_a value is not significant at least for current model.

The curve fitting method can be easily applied even when the wall subjects to both passive and active cases by building special models, such as a passive state only wall, to gain β_p values, which could then be applied into similar soil and wall systems. As mentioned above, it is certainly feasible to useβ_a and β_p values in retaining wall systems which has the same wall and soil, however, the influence of other parameters, such as flexural rigidity, on β_a and β_p, andΔ_a and Δ_p needs to be further assessed while numerical soft-wares like PLAXIS could be a tool for producing a better way to estimate those parameters.

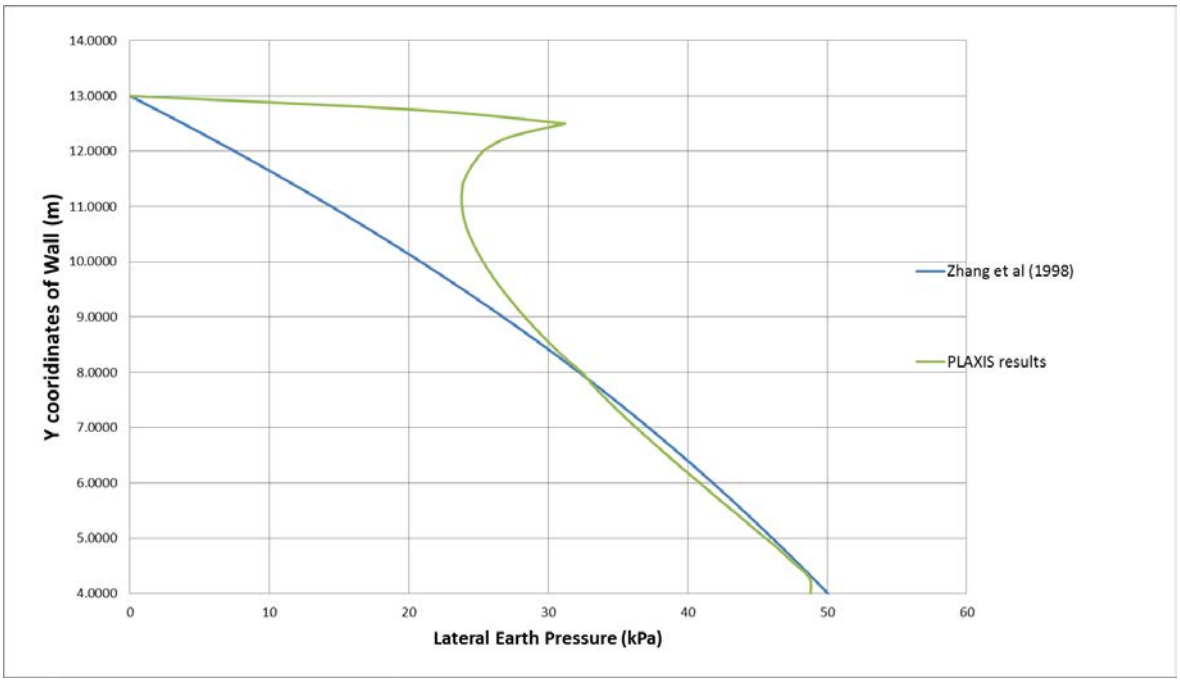

Figure 4.18: Distribution of earth pressure along wall based on analytical and computational solutions using β_a = 1.1

Soil element	Local number	X [m]	Y [m]	ε_V [10^{-3}]
Clus. 1 - El. 1495	2	15.089	7.460	-4.369
Clus. 1 - El. 1500	1	15.087	7.307	-4.330
Clus. 1 - El. 1495	1	15.093	7.948	-4.285
Clus. 1 - El. 1465	1	15.089	7.460	-4.271
Clus. 1 - El. 1496	2	15.094	8.062	-4.229
Clus. 1 - El. 1465	2	15.087	7.307	-4.208
Clus. 1 - El. 1467	2	15.098	8.505	-4.085
Clus. 1 - El. 1500	2	15.084	6.862	-3.985
Clus. 1 - El. 1466	2	15.093	7.948	-3.959
Sand	1	15.094	8.062	-3.910
Clus. 1 - El. 1498	1	15.084	6.862	-3.906
Clus. 1 - El. 1464	1	15.080	6.406	-3.856
Clus. 1 - El. 1467	1	15.099	8.621	-3.751
Clus. 1 - El. 1498	2	15.080	6.406	-3.724
Clus. 1 - El. 1463	1	15.078	6.268	-3.693
Clus. 1 - El. 1496	1	15.098	8.505	-3.677
Clus. 1 - El. 1464	2	15.078	6.268	-3.660
Clus. 1 - El. 1468	2	15.099	8.621	-3.638
Clus. 1 - El. 1494	2	15.069	5.191	-3.616
Clus. 1 - El. 1497	1	15.068	5.113	-3.574
Sand	2	15.064	4.601	-3.395
Clus. 1 - El. 1463	2	15.074	5.763	-3.262
Clus. 1 - El. 1392	2	15.103	9.079	-3.031
Clus. 1 - El. 1462	2	15.073	5.677	-2.986
Sand	1	15.074	5.763	-2.883
Clus. 1 - El. 1468	1	15.103	9.079	-2.865
Clus. 1 - El. 1494	1	15.073	5.677	-2.848
Clus. 1 - El. 1392	1	15.104	9.213	-2.800
Clus. 1 - El. 1366	1	15.063	4.530	-2.685
Sand	2	15.059	4.038	-2.574
Clus. 1 - El. 1469	1	15.108	9.665	-2.201

Figure 4.19: A table showing volumetric strain for stress points close to the wall and interface

4.5. Results from Seismic Phase of PLAXIS

4.5.1. Comparison of Wall Displacement for various Scenarios

Figure 4.20 demonstrates the wall displacement after both static and seismic cases. Also, the maximum passive and active displacements of the wall during the strike of the Offshore Maule earthquake are drawn. The red curve represents the final displacement produced by PLAXIS after the whole 60 seconds of Offshore Maule earthquake. Based on PLAXIS results, strong seismic load like Offshore Maule has multiplied the wall displacement towards active side by comparing the final displacement curve to static displacement curve in Figure 4.20. The passive

displacement curve indicates that seismic effect has moved some part of the wall towards passive side during the 60 seconds, but it does not count the maximum active displacement since zero value, which is the maximum of all phases by sign convention is used in this model to represent initial non-displaced status. It is obtained from the maximum active displacement curve that the wall displaces more than its final value during the seismic duration. Also, it is obvious that, despite some fluctuations at the top of the wall, the displacement of the wall follows linear distribution for most of the wall depth. Considering the increased wall displacement in seismic case, it is making the serviceability condition worse. It needs to be mentioned that, normally, a critical displacement, such as Δ_a, is related with the failure of the wall, however, from mechanical point of view, this $\Delta_a$is obtained from static cases but not seismic one, where seismic influence may change Δ_a, but the same $\Delta_a$is used in Zhang et al (1998)'s strain increment ration method for seismic cases. The extent of different Δ_a for static and seismic cases and needs further investigation, but not conducted in this paper. Since the original strain increment ratio solution uses Δ_a from static cases for seismic calculation.

4.5.2. Parameters for Seismic Analytical Solutions

Based on the displacement results for both final and maximum active displacement after seismic calculation, the R and K profile for both cases are able to be obtained. These procedures and results are similar to Figure 4.14 and Figure 4.15, but not listed here for simplicity. i value needs to be known for the use of equations (9) and (10). According to the SMC file of Offshore Maule earthquake as shown in Figure 4.2, a representative acceleration of 2m/ s^2 could be used which equals to k_h=200cm/s^2/g=0.2041, and, based on equation tani= k_h, i is calculated as 0.2013 in radian. If the maximum acceleration of 5m/ s^2 is read from SMC file, the corresponding values are: k_h=0.5102, i=0.4718.The R value in equations (9) and (10) are calculated in the same way as static cases. However, now we have two choices of $\beta_a$and β_p, one is obtained from pragmatic method as mentioned by Zhang et al. (1998), the values are 0.4 and 0.51 for $\beta_a$and β_p respectively; the other one is obtained from curve fitting of final static active displacements, by which $\beta_a$is obtained as 1.1. $\beta_p$for curve fitting could also be conducted but we need to build a passive movement retaining wall model like the one used for $\boldsymbol{\Delta}_a$, however, this

procedure is neglected since only a small fraction of wall subjects to small amount of passive movement in seismic case only, and this is only for final displacement after seismic load, so the β_p from curve fitting is neglected and still taken as 0.51 from chart method for simplicity. To clarify, the sets of lateral pressure results obtained based on Zhang et al. (1998) are listed in Table 4.5.

Table 4.5: Parameters used for each set of analytical calculation

	Set 1	**Set 2**	**Set 3**	**Set 4**
Angle of seismic coefficient i (radian)	0.20 (representative)	0.20 (representative)	0.47 (peak)	0.47 (peak)
$\boldsymbol{\beta_a}$ ***and*** $\boldsymbol{\beta_p}$	β_a= 0.4 β_p=0.51 (Chart Method)	β_a= 1.1β_p=n/a (curve fitting)	β_a= 0.4 β_p=0.51 (Chart Method)	β_a= 1.1β_p=n/a (curve fitting)

The K and R profiles for each set of calculation are not posted here for simplicity, but they are similar to Figure 4.14 and Figure 4.15. The displacement values applied into equations (7) and (8) are final displacements from PLAXIS rather than maximum displacement since they are at the same time when the final wall pressure is drawn. The produced results for analytical solutions with various parameter sets are demonstrated in Figure 4.21 together with results from PLAXIS seismic.

4.5.3. Seismic Lateral Earth Pressure along Wall

Based on Figure 4.21, β_a and β_p values have only small influence on seismic pressure distribution since curves from different β_a and β_p values (but the same acceleration) nearly coincide with each other. In contrast, angle of seismic coefficient (i) has greater influence on lateral earth pressure based on analytical solution of Zhang et al. (1998)'s strain ratio dependent method. In Figure 4.21, set 3 and 4 (see Table 4.5), using peak acceleration value of $5\,m^2$/s, have produced pressure distributions much more similar to the PLAXIS results. This further justifies that lateral earth pressure is influenced by maximum acceleration level rather than a representative acceleration value. However, PLAXIS has displayed a pressure

distribution which does not match linear distribution, this is more correct than the linear distribution used by analytical solution, since pesudo-static analytical solution does not take into account phase change and dynamic amplification factors in pressure distribution. Steedman and Zeng (1990) found the effect of these two factors using centrifuge modelling tests. In addition, free field displacement from seismic case is able to influence local pressure on the wall, which will be discussed in detail in section5.5.

PLAXIS provides the change of various results parameters with dynamic time. In this study, node no. 919 (see Figure 4.22) with Y coordinate of around 7.2 m is chosen since this is the point corresponding to maximum pressure according to Figure 4.21. Figure 4.23, Figure 4.24 and Figure 4.25 are showing the changing of lateral earth pressure, horizontal acceleration and displacement with dynamic time respectively.

Interestingly, comparing Figure 4.23 and Figure 4.25, it is obvious that lateral earth pressure and displacement are in similar phase, and the shapes of these two curves are similar to each other. This further proves the correctness of using wall displacement to determine the lateral earth pressure for any state between passive and active states. According to Figure 4.23, the final earth pressure is not the extreme value during the strike of the earth quake. However, considering that the wall displacements are always in active state, a larger earth pressure is safer (if the wall does not subject to structural failure) since active limit could be viewed as a state of failure subject to the smallest earth pressure. In other words, seismic load has actually made the wall safer in terms of stability. However, this only applies to the final wall pressure in this case, for other cases maximum earth pressure during the seismic strike might trigger wall failure and this effect is due to be investigated. For node no. 919, the smallest earth pressure is that of static case. In other words, earthquake load is likely contributing to the stability of the retaining system (if the seismic influence on active pressure is neglected).

Regarding acceleration versus dynamic time curve, there is no similarity found between Figure 4.24 and the other two curves, which means the acceleration is not in phase with the wall displacement. Actually, the acceleration is shown to be on both directions (both minus and positive in Figure 4.24), but the wall only displaces further in active side during the whole earthquake strike as shown in Figure 4.23,

which means there is no passive side displacement encountered for node no. 919 during the whole process. This coincides well with the curve for maximum passive displacement in Figure 4.20, in which no passive displacement is encountered for around 11 to 7 meters of Y coordinate of the wall. But it does not mean no passive stress state is encountered since the influence of free field that will be discussed in section 5.5

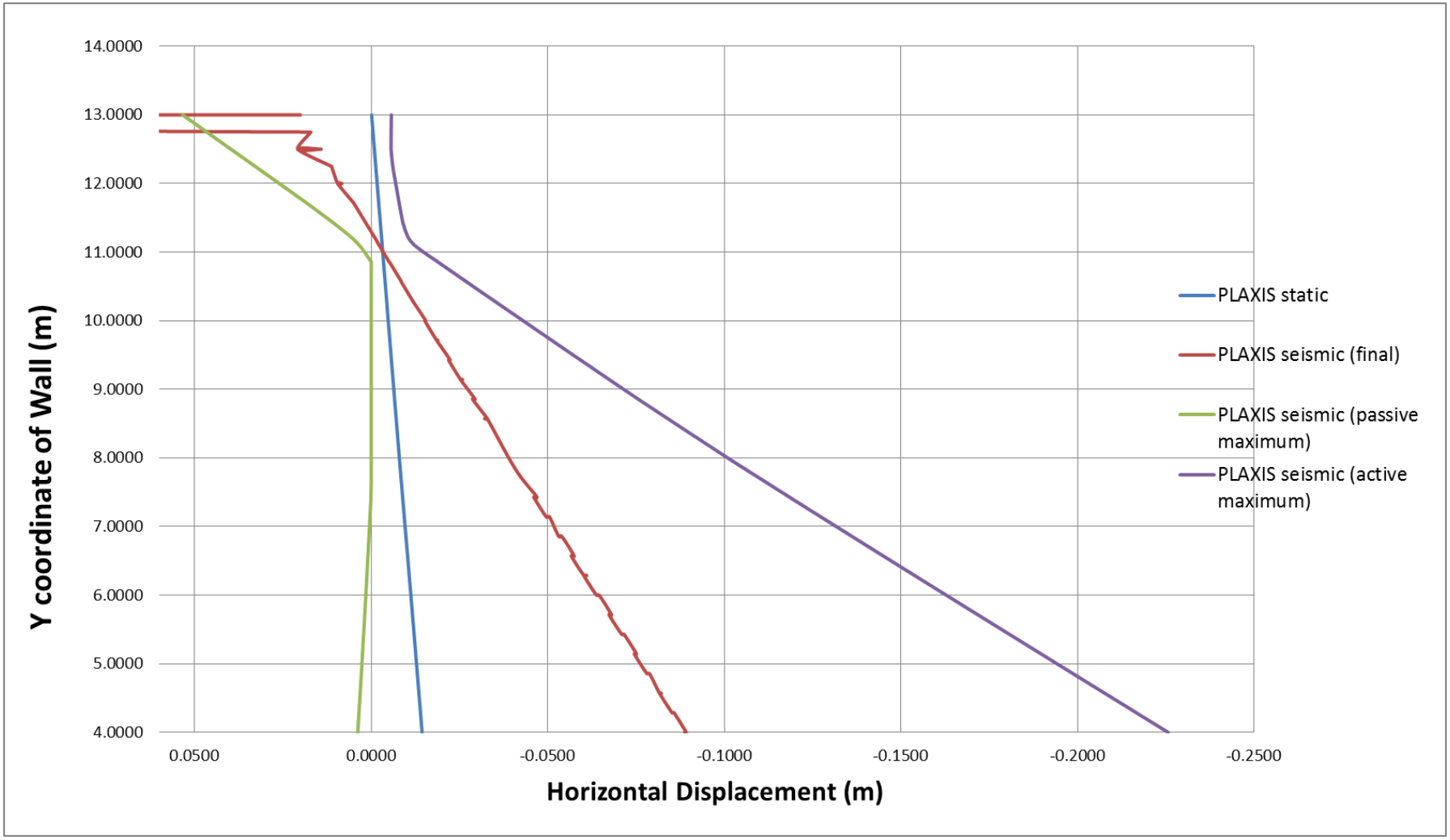

Figure 4.20: Comparison of horizontal displacement for static and seismic cases

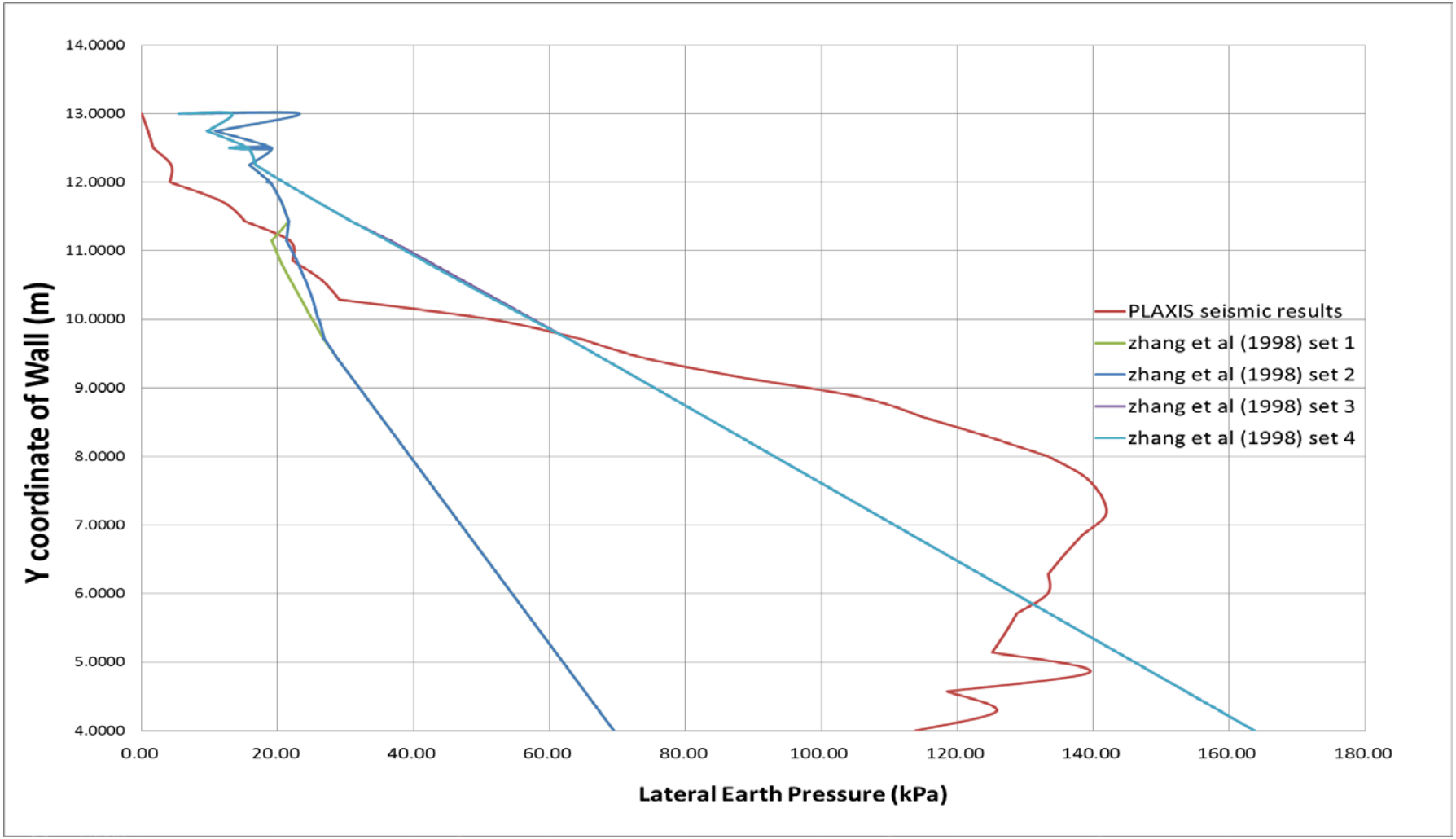

Figure 4.21: Lateral earth pressure distribution by PLAXIS results and analytical solutions with various parameters

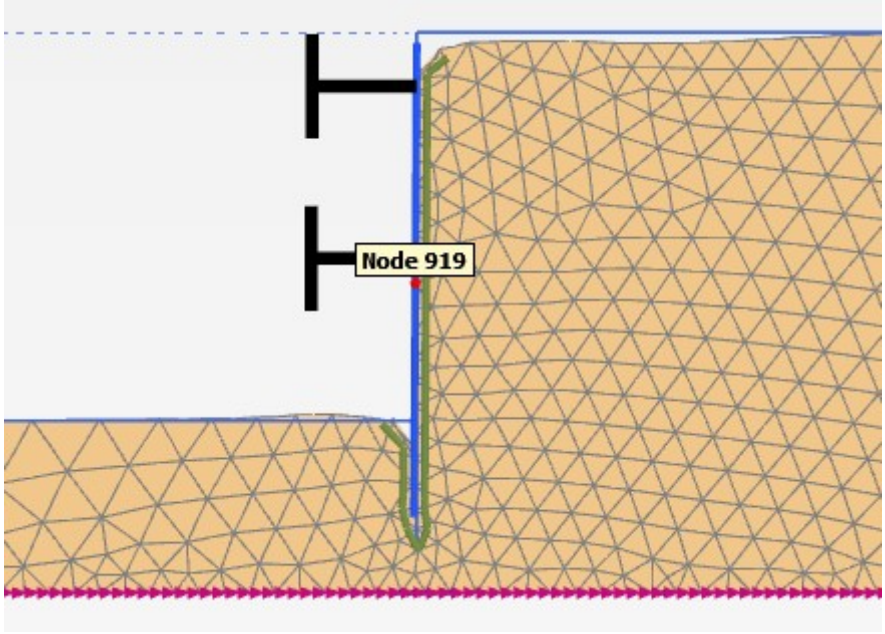

Figure 4.22: Location of the node picked for phase effect analysis

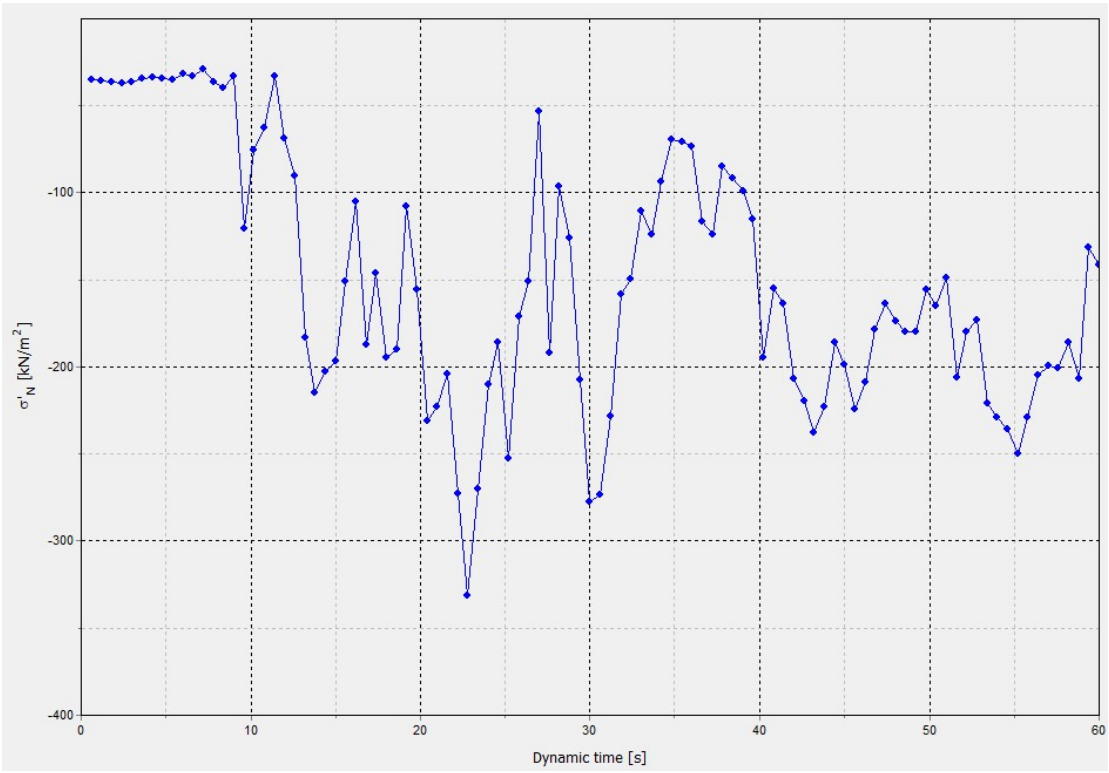

Figure 4.23: Dynamic time versus lateral earth pressure curve for node no. 919

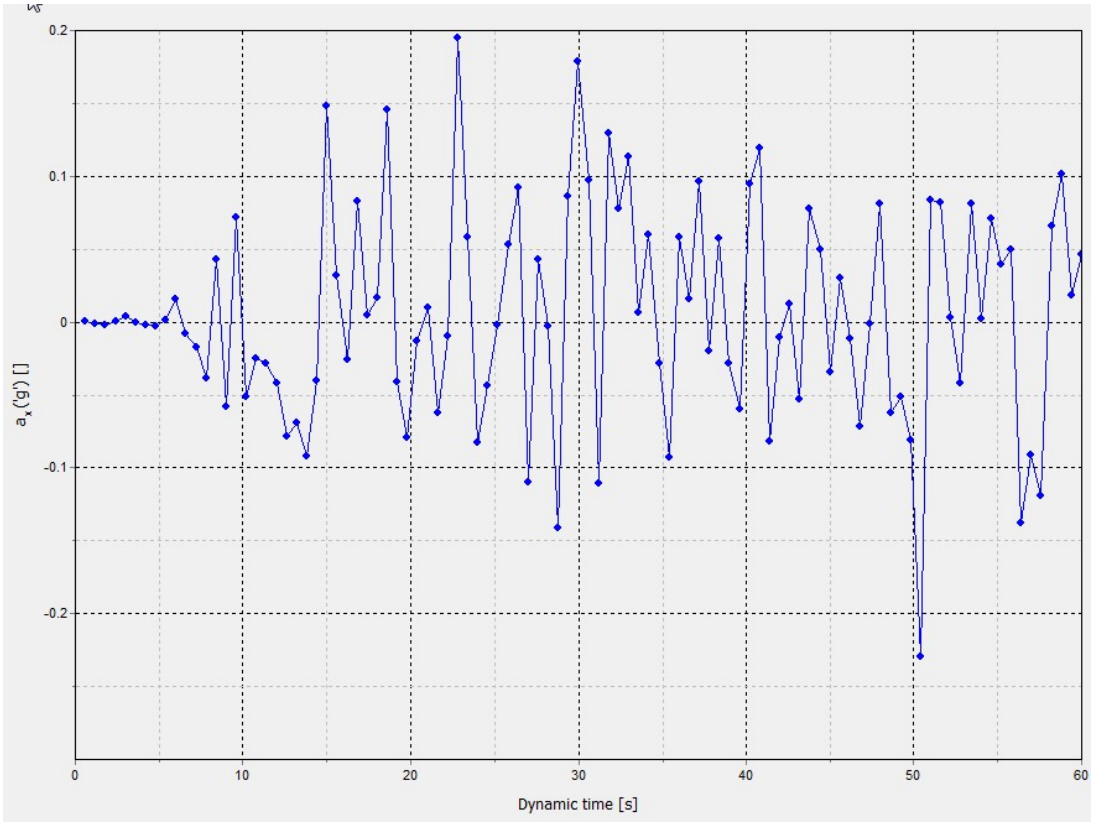

Figure 4.24 :Dynamic time versus acceleration curve for node no. 919

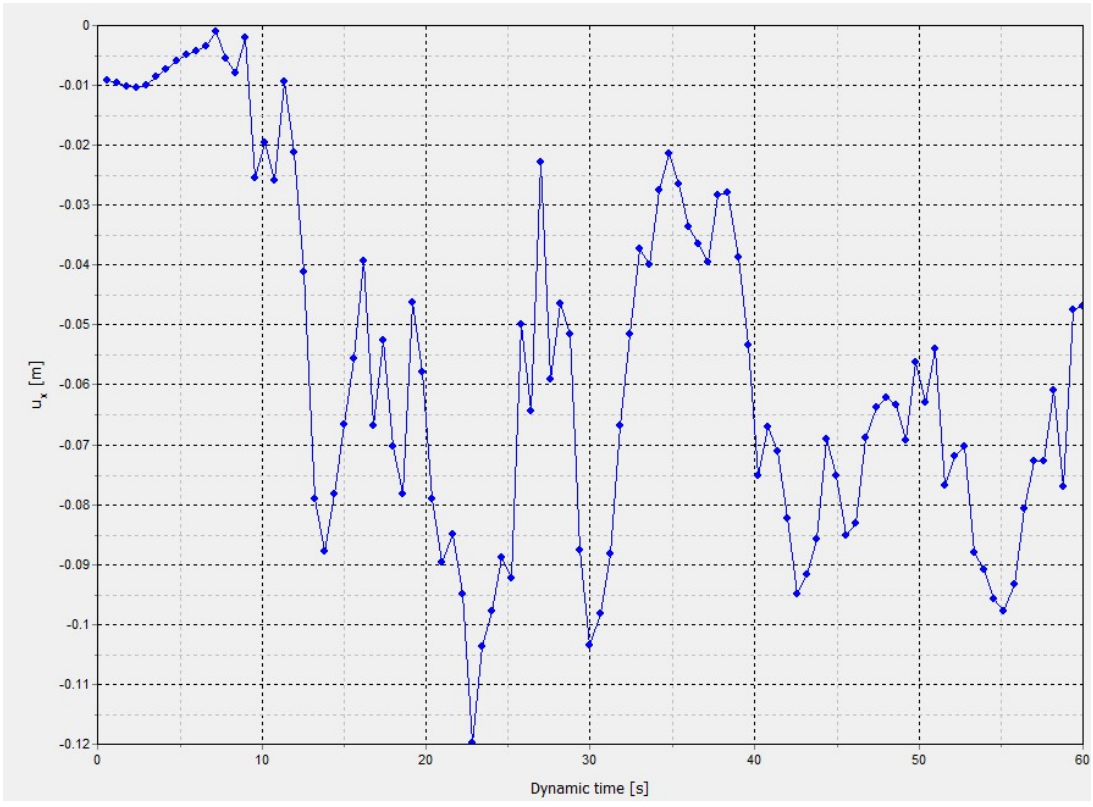

Figure 4.25: Dynamic time versus lateral displacement curve for node no. 919

4.6. Results Study for Subgrade Modulus and Free Field Theory

4.6.1. Free Field Displacement

It is difficult to obtain plastic shear modulus G_{sp} without numerical solution. So, firstly, only elastic solution (equation 12) is used, the assumption is that all sections are subject to elastic response. The resulting free field displacements from both the analytical solution and PLAXIS output are demonstrated in Figure 4.27. It is indicated that, by using the peak acceleration, the obtained free field displacement agrees well with the final freefield displacement from PLAXIS results, at least for a depth below around 10.4m of Y coordinates in this case. The results start to deviate significantly beyond 10.4m upward, which is probably due to the plastic response at this location, as demonstrated by larger displacement for the upper part of the wall in Figure 4.26, since only elastic G is used for the blue line in Figure 4.27, but plastic response is accounted for in PLAXIS.

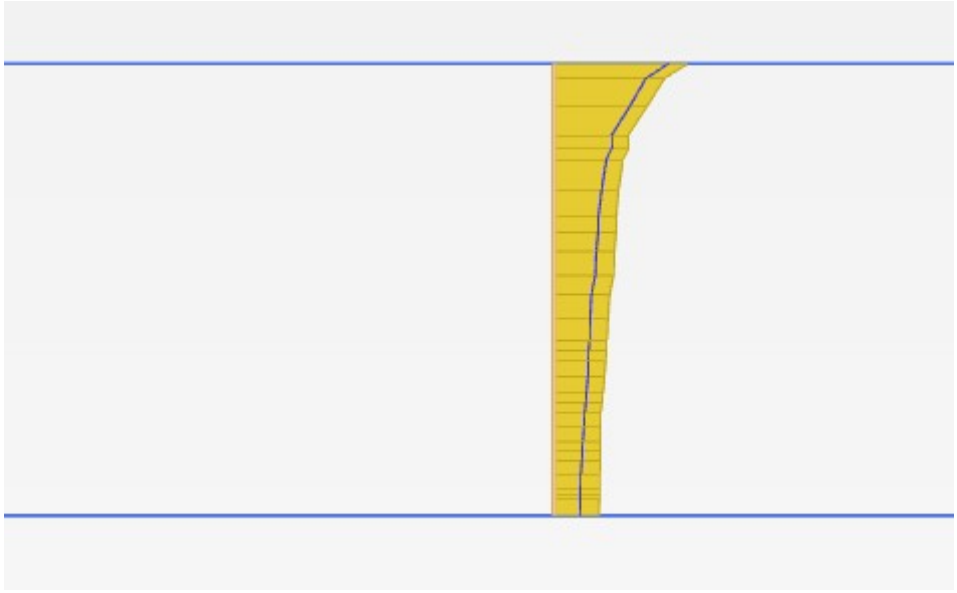

Figure 4.26: Free field displacement profile (final and maximum) provided by PLAXIS

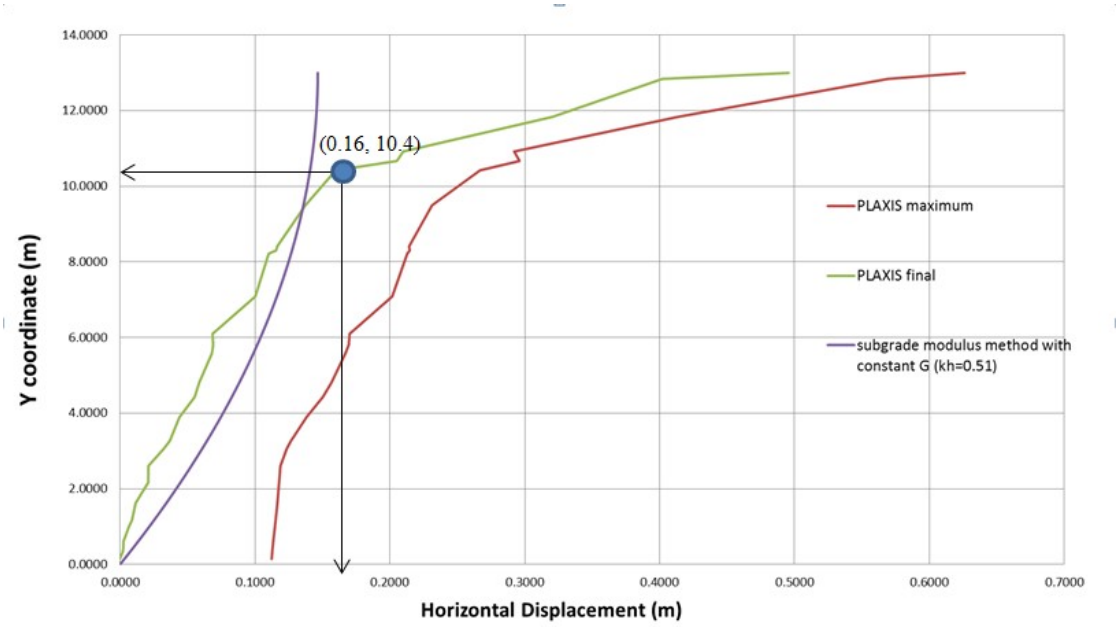

Figure 4.27: Horizontal displacement of free field based on various methods

4.6.2. Comparison of Modelling and Theoretical Results based on Subgrade Modulus Method

$\mathbf{C_2}$ from equation (13) is normally taken as 1.35 based on previous studies. Since a constant G of 5000 kPa is used in this study, from this equation (13), Ks should have a relatively constant value of 519 for soil sections in elastic states.

In this method, soils between wall and free field are modelled as spring with certain stiffness. The earth pressure could be calculated using Equation (14) with $\boldsymbol{\Delta}$u shown in Figure 4.28 as the distance between two lines.

With $\boldsymbol{\Delta}$u and σ_{xo} ready for all wall depth as obtained from PLAXIS results, Ks is able to be evaluated based on PLAXIS results of lateral wall pressure. Figure 4.29 is showing the obtained Ks values along the depth. Generally, Ks value higher along the wall indicates a much lower value of Ks. This is probably due to the plastic response, which starts at a location of between 9-10 meters that corresponds well to the previous finding based on Figure 4.27. Obviously, the calculated value of Ks = 519 from equation (13) agrees well with the average value of the points for the "lower than 9 meters" section of the wall. These points are in elastic response, which also agrees with the elastic G used in equation (12). Similarly, the plastic Ks (shown in Figure 4.29) is estimated from the location of points upper of the soil strata, since

the displacement is larger for the upper part of the soil strata based on Figure 4.27 and this is a norm for soil dynamics. However, some extreme points are showing that Ks values could be quite different than 519, which means the use of equation (13) remains as a rough estimation for local pressure, since either under estimation or overestimation are possible by keeping Ks as 519. In addition, there is a transition area between plastic and elastic status with an intermediate Ks of around 270, for a depth of between 9 to 10 meters as shown in Figure 4.29. It is difficult to accurately represent the pressure for the transition section since the Ks seems varying a lot even for a small change in depth.

The Ks for plastic domain could be used as a way to back analyse a Gsp used in equation (13). In this case, Gsp is calculated as 289kpa. But this value leads into an extremely large plastic displacement based on equation (13) thus is not correct for use in analytical displacement calculations. Considering a homogeneous soil with constant G is used in all phases, further study on other models that permits a varying G with soil depth is definitely useful.

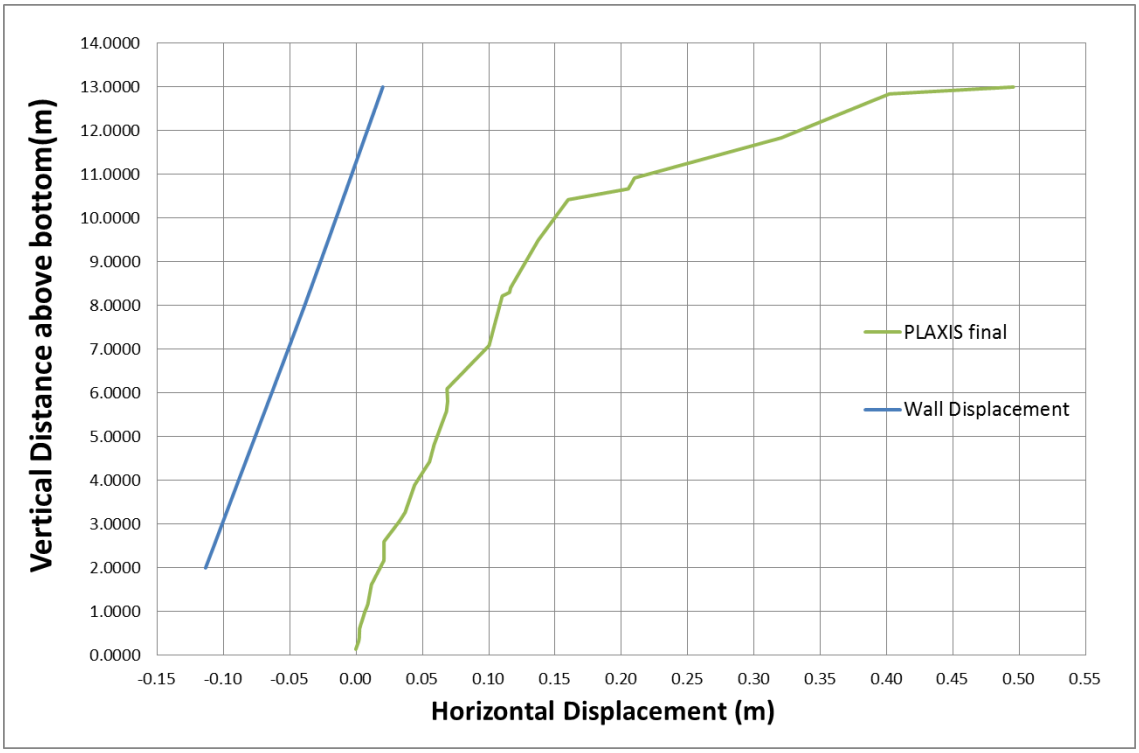

Figure 4.28: Displacement profile for wall and freefield

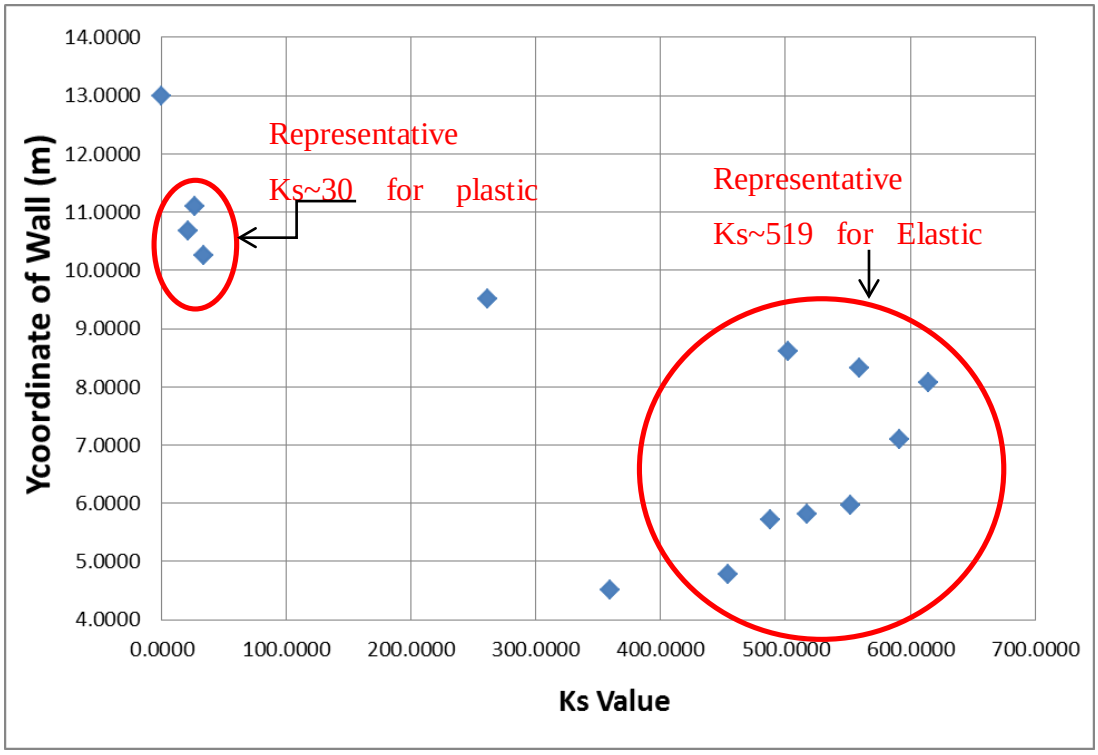

Figure 4.29: Ks values based on PLAXIS results

4.7. Summary

To conclude, despite the variance on local pressure distribution, Zhang et al. (1998)'s strain ratio dependent earth pressure theories for both static and seismic earth pressure agree well with PLAXIS results as demonstrated in Figure 4.16 and Figure 4.21. This means the earth pressure is based on lateral displacement of the retaining wall, and PLAXIS software coinsides with this feature. It is sufficient to use displacement ratio R as shown in equations (7) and (8) to produce reasonable earth pressure values. In addition, PLAXIS is a convinient tool to gain relevant parameters required by strain ratio dependent earth pressure theories such as wall displacement (Δ), active failure wall displacement Δ_a, passive failure wall displacement Δ_p and amendment for β_a and β_p using curve fitting. The detailed procedures for these paramters are also established.

Regarding free field response, PLAXIS has produced similar results to that from theory in this case. It has also been verified that PLAXIS results have indicated an elastic spring modulus (Ks) that agrees very well analytical approximation using equation (13). Consequently, a simple backanalysis method is displayed to use

PLAXIS results to evaluate spring modulus used in such theories even for plastic cases.

Chapter 5. ABAQUS Simulation and Results Discussion

In this chapter, a 2D ABAQUS model of the same soil-wall retaining system (as shown in Figure 5.1) was built to further verify the PLAXIS results and theoretical solutions. Similar to PLAXIS study, both strain increment ratio lateral earth pressure theory and free field subgrade modulus theory were studied using modelling output of wall displacement and lateral earth pressures. Critical discussion was made in terms of local variation of pressures, and this lead into findings regarding amendment of existing method. The structure of this chapter is listed below:

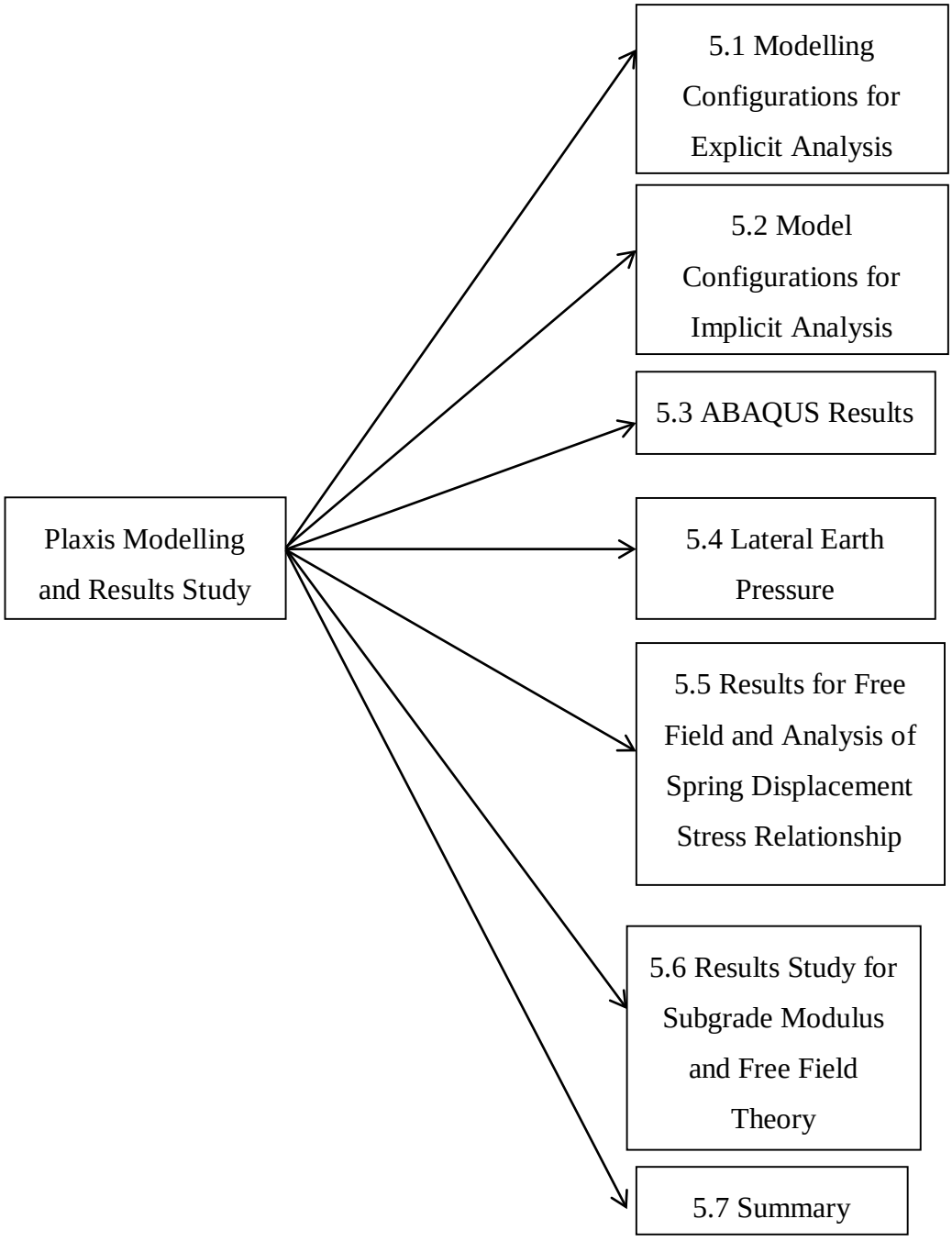

5.1. Model Configurations for Explicit Analysis

5.1.1. Wall Model (including relevant connectors)

The wall was modelled with 2D planner shell. The length of the wall is 11 meters, in which 9 meters were daylighting, as the same with PLAXIS model. Different than the plate element used in PLAXIS, the wall model in ABAQUS has a width of 2.24m, which is the equivalent width obtained from wall parameters (can be directly read from plate material set in PLAXIS). The geometry profile and material properties (see Table 4.5) of the planner shell were set so that it has the same geometry, elasticity and thus moment of inertia as that of the PLAXIS model.

Two connecters were built at 1 m and 4 meters under the upper end of the wall to model the struts of the wall (see Figure 5.1). The stiffness of the strut is set so it matches an EA of 2e6 kPa and equivalent length of 15 meters used for "Fixed End Anchor" element by PLAXIS model.

The wall displacement constraints and intersection information will be discussed in Stages and Intersections section of this chapter respectively.

Table 5.1: Diaphragm wall retaining system model properties

Density (kg/m3)	***Elasticity (Pa)***	***Poisson ratio v***	***Stratum Length (m)***	***Stratum Height (m)***
378.774	5366726000	0.3	60	13

5.1.2. Soil Model (including relevant connectors)

The same soil of 13 meters high and 60 meters long (excluding two extra side blocks) was built. The material properties of this soil were shown in Table 5.2. Mohr-Coulomb plastic model was chosen following the elastic state, this corresponds to the same material model in PLAXIS. A small number of dilation angel and cohesion were input to pass the program's numerical requirement, but these have negligible effects on the wall behaviour. The bottom line of the soil model is constrained from vertical displacement and keep symmetry about Y = constant plane (U2 = UR1 = UR3 = 0). In seismic stage, the periodic horizontal acceleration was applied on the bottom of the backfill part (excluding the bottom of the extra blocks) to simulate earthquake excitations.

There are a series of connectors created along both right and left hand sides of the soil model (see Figure 5.1). These connectors are used to model more realistic dynamic responses at side boundaries. Since, as widely known, a fixed boundary will incur "Box Effect" that harbours the seismic energy inside the block. In ABAQUS Explicit Dynamic step, spring element is not applicable to connect to ground so connectors with translational (U1 direction) stiffness are used. However, another set of implicit simulation will be discussed later using spring/dashpot for absorbing boundary conditions. The connectors are distributed evenly on both boundaries and they are given a stiffness to try to simulate the seismic response correctly. Every connector points at the boundary needs to be assigned a point mass with the same density of 1734.7 as the soil.

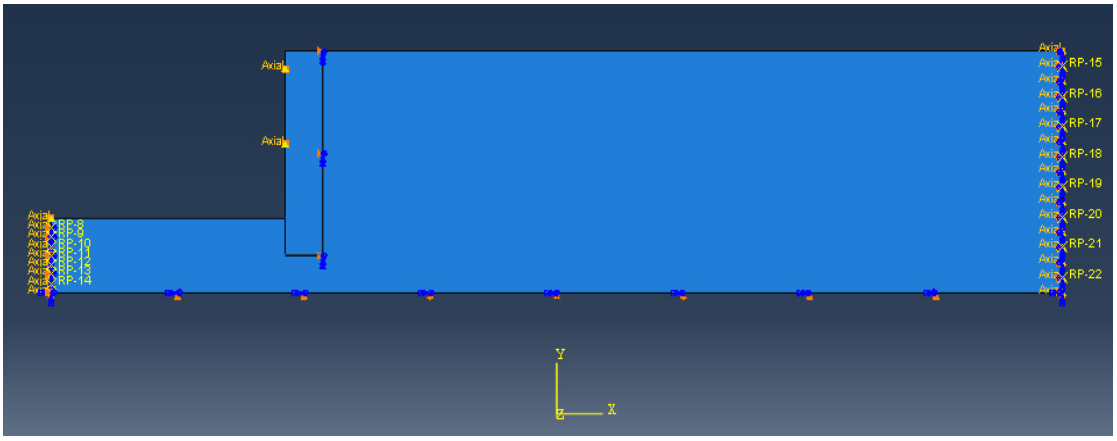

Figure 5.1: Assembled ABAQUS model of retaining wall

Table 5.2: Soil material properties in ABAQUS

Density (kg/m3)	***Elasticity (Pa)***	***Plastic Model***	***Effective angle of friction ϕ′ (degree)***	***Dilation Angle (degree)***	***Poisson ratio v***	***Cohesion Yield Stress (Pa)***	***Abs Plastic Strain***
1734.7	1.75e7	Mohr-Coulomb	30	0.1	0.3	50	0

5.1.3. Mesh

Explicit Plain Strain linear quadrilateral element type was adopted for both soil and wall. Finer meshes were applied at the area of wall – soil intersection and coarse

mesh for the far field. Due to the existence of connectors at side boundaries, the mesh will be generated according to connector points, which always fall on the node by automatically.

A completed mesh scheme is shown in Figure 5.2.

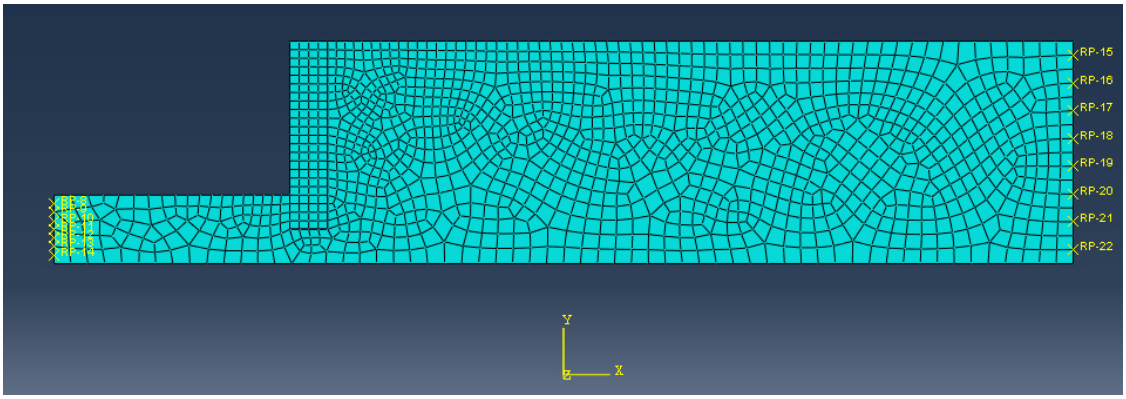

Figure 5.2: *Mesh scheme of retaining wall and soil*

5.1.4. Steps

All steps in this mode are set as dynamic explicit with a period of 1 second. There are 3 steps in total after initial step: settling, static and seismic. In the settling part, the gravity load was firstly applied and the soil settles due to elasticity and gravity. The wall is constrained from any lateral deformation (U1 = UR2 = UR3 = 0)at this stage, while both sides of the soil are also constrained as (U1 = UR2 = UR3 = 0). The horizontal pressure at the wall should represent the at rest state.

In the static part, the wall is allowed from displacement and a static lateral earth pressure should be generated. As a result, the wall will displace to the active side and there will be a horizontal pressure.

In the seismic part, the bottom acceleration is applied. The two soil boundary constraints are removed so the lateral displacement of the soil block is under the control of connectors.

5.1.5. Load

Gravity load was applied to soil (including extra blocks) and wall, but the struts are set as no gravity, the same as the PLAXIS' strut function. The amplitude – time curve for gravity load is shown in **Figure 5.3**, which is for the total time starts from "settling" stage.

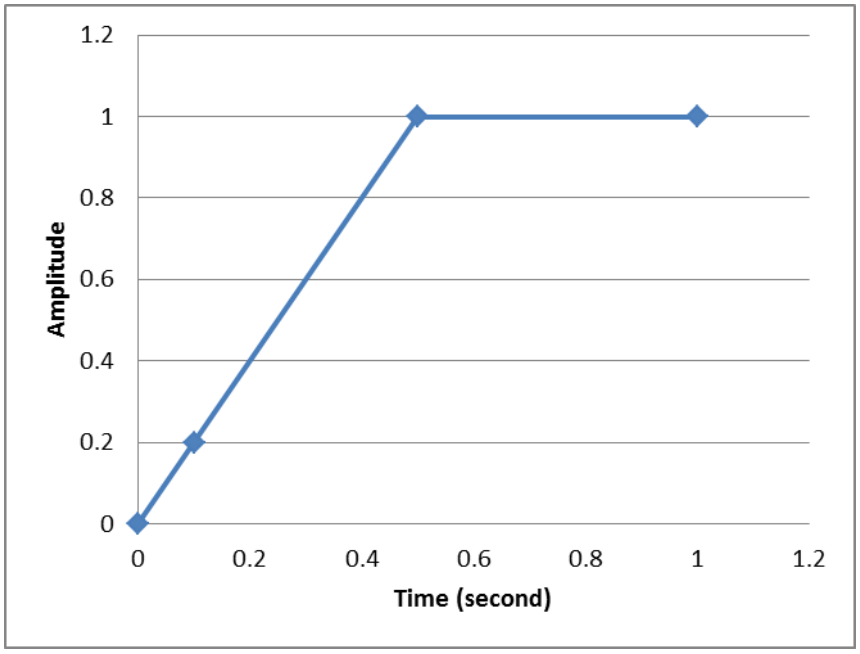

Figure 5.3: *Development of gravity force with step time*

5.1.6. Ground Acceleration

The harmonic sinusoidal ground acceleration is applied at horizontal direction as a boundary condition on the bottom line of the middle soil block. The acceleration level is firstly picked as a representative one of $2.5m/s^2$ from offshore maule earthquake, also, an acceleration level of $5m/s^2$ is adopted to represent the peak acceleration. The acceleration – time curve is demonstrated in Figure 5.4. The amplitude is set as sinusoidal with a frequency of 4 (4 circles per second or 25.13 radian per second).

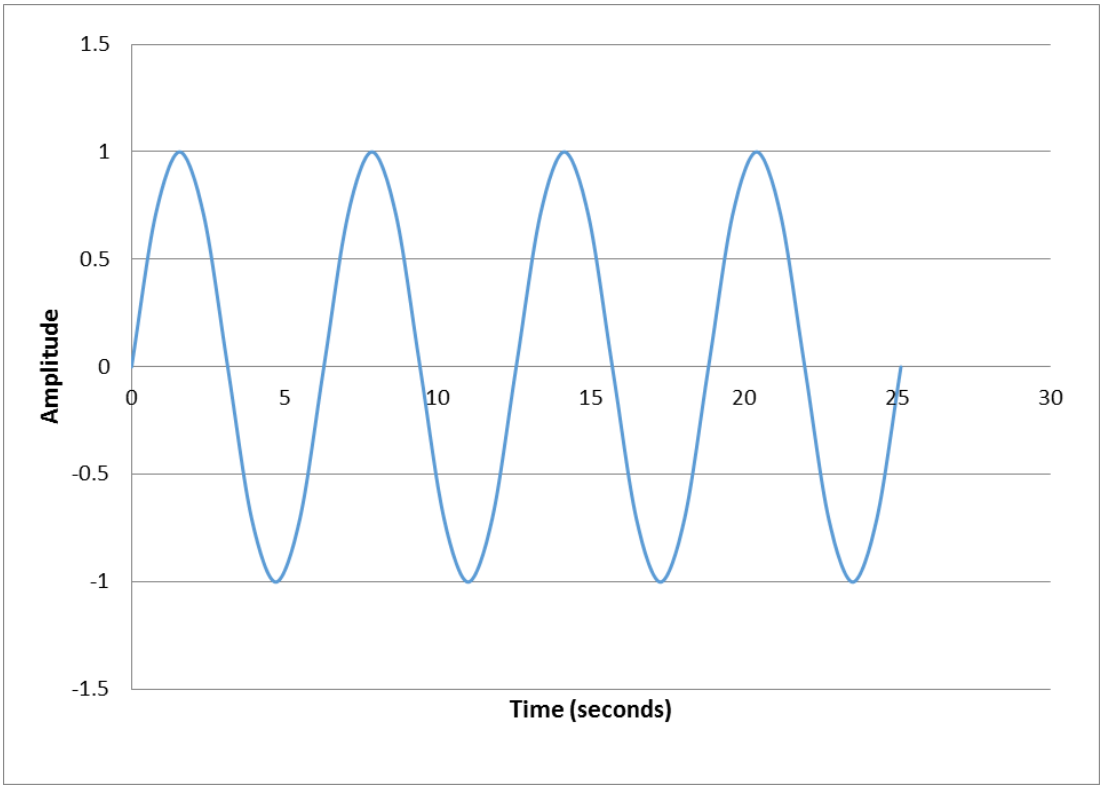

Figure 5.4: Harmonic ground acceleration curve applied at the bottom of the model soil (normalized amplitude)

5.1.7. Interactions

When in settling step, the response between the wall and soil is modelled as penalty contact method with frictionless tangential behaviour.

The response between the wall and soil is modelled by a kinematic contact. The interaction property is given a tangential response with a friction coefficient of 0.39 (obtained from δ_{mob}=21.2° used in PLAXIS model).

5.2. Model Configurations for Implicit Analysis

In the implicit analysis, in which all settling, static and seismic steps are switched into implicit dynamic mode, all geometries, soil parameters, wall parameters, boundary conditions and configurations for each step are identical to those mentioned above for the Explicit case, except spring elements are used to replace connectors. The model scheme is shown in Figure 5.5. The purple circles along both sides represent spring elements, they are given a rough stiffness of 1.75e6 N/M based

on soil properties. It has been generally tested that the stiffness (if under an order of magnitude of difference) here will have little effect on the wall behaviour.

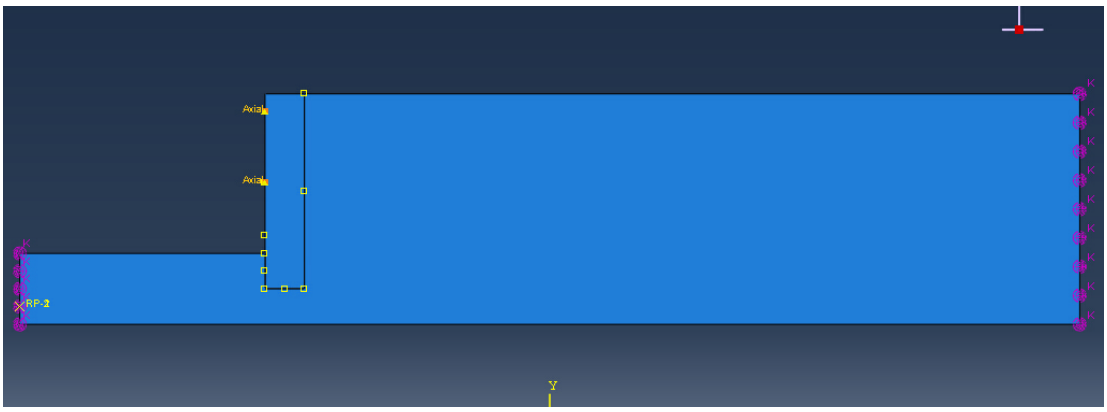

Figure 5.5: Model view of assembled instances under Implicit Analysis

5.3. ABAQUS Results

5.3.1. Deformed Mesh

Both the dynamic explicit and implicit calculation runs successfully with the produced deformed meshes shown in Figure 5.7 and Figure 5.9. Please note, there are harmonic acceleration levels of 2.5 m^2/s and 5m^2/s substitute in the normalized 1 value in Figure 5.4for both explicit and implicit analysis.

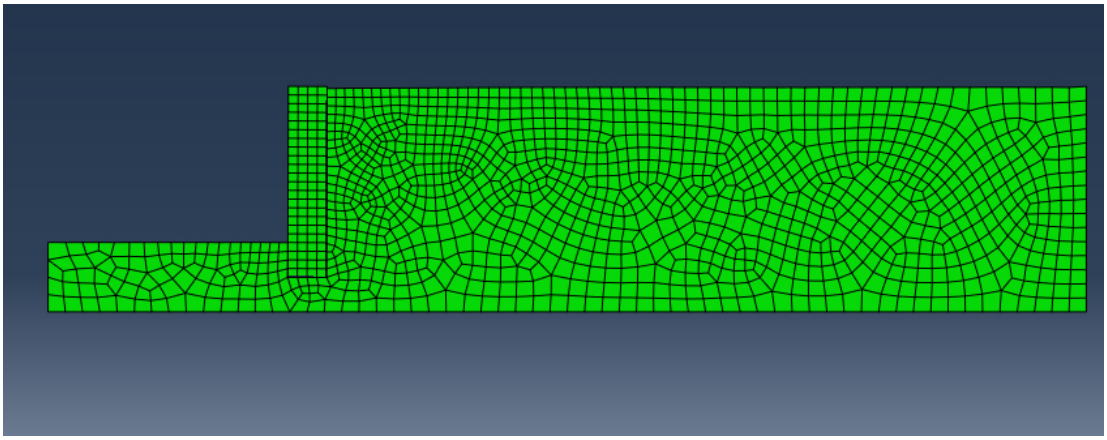

Figure 5.6: ABAQUS Explicit resulting deformed mesh after static dynamic step (scaled up 1.0 time)

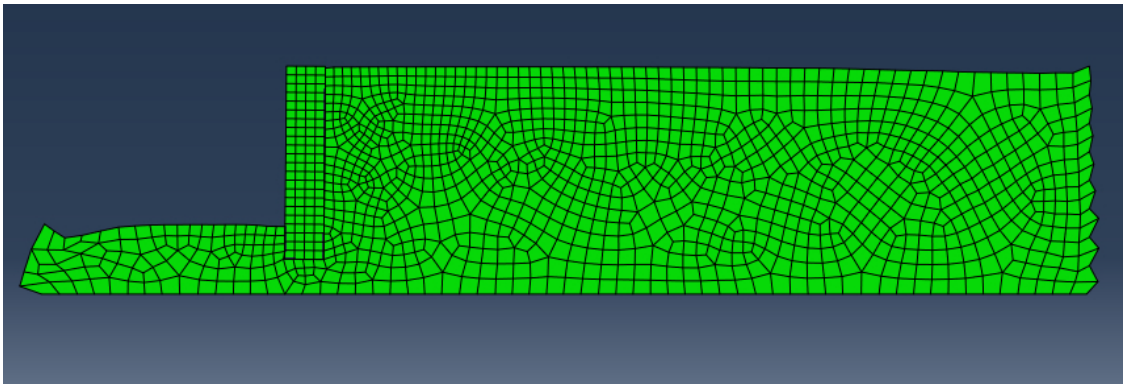

Figure 5.7: ABAQUS Explicit resulting deformed mesh after dynamic step (scaled up 1.0 time)

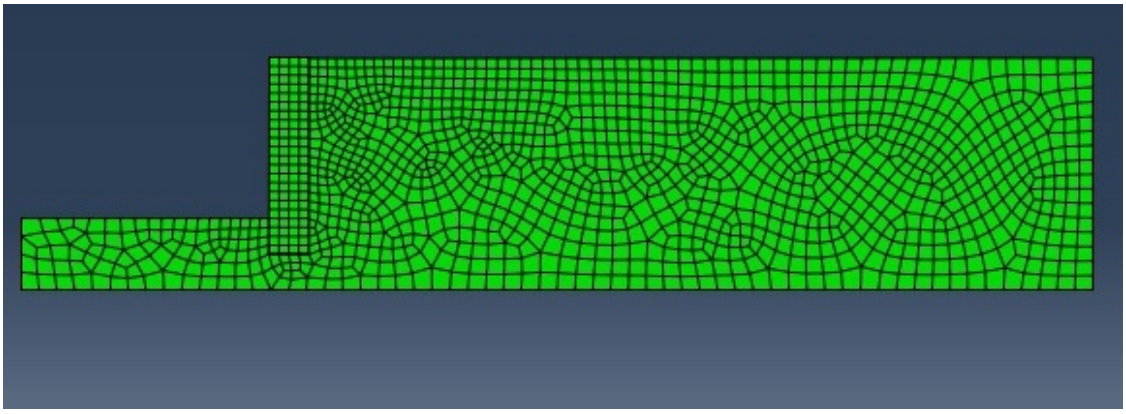

Figure 5.8: ABAQUS Implicit resulting deformed mesh after static dynamic step (scaled up 1.0 time)

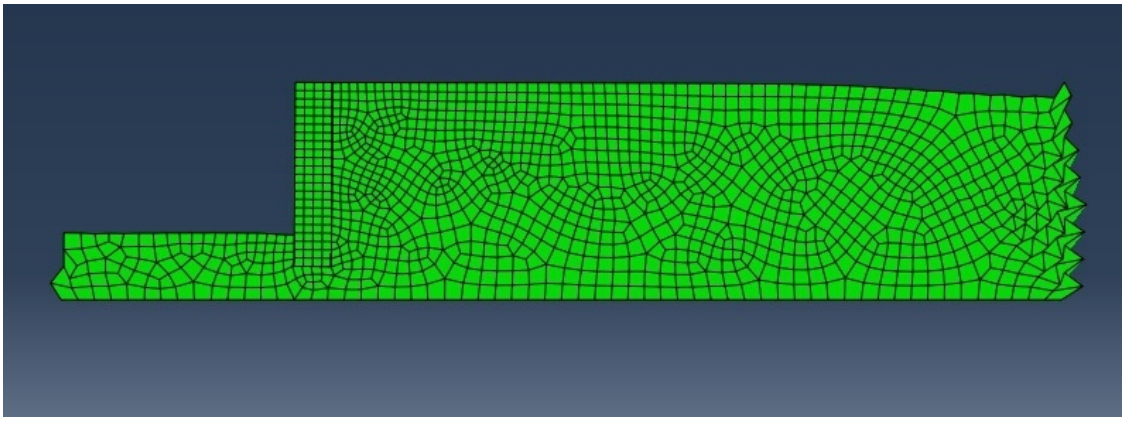

Figure 5.9: ABAQUS Implicit resulting deformed mesh after dynamic step (scaled up 1.0 time)

5.3.2. Horizontal Wall Displacement

Figure 5.10 and Figure 5.11 demonstrate the wall horizontal displacement profile from both ABAQUS Implicit and Explicit analysis results, 2.5 m^2/s and 5 m^2/s ground acceleration amplitude respectively. Also, wall displacement from PLAXIS is

plotted for comparison. The negative sign in these graphs represent active side displacement and the positive sign is the passive displacement.

In Figure 5.10 and Figure 5.11, ABAQUS implicit and explicit, using different boundary elements, produce similar results in terms of wall displacement for both $2.5m^2$/s and $5m^2$/s acceleration amplitude. The maximum active displacement all occurs at the bottom of the excavation (9 meter depth), $2.5m^2$/s has produced 0.06 to 0.065 meters of displacement at the bottom end of the wall's excavated section. When $5m^2$/s acceleration is used, the maximum active displacement occurs at the same location but with a greater displacement of around 0.085 meters. From the graph, it is obvious that there is a section of passive displacement for the top part of the wall, and the active side displacement starts below around 1.5 meters in average of all curves. This is close to PLAXIS results (green curve in Figure 4.20). Also, it is obvious that most displacement curves are approximately liner with wall depth, which is due to the relatively high rigidity of the wall.

By using a representative acceleration level of $2.5m^2$/s, ABAQUS has produced slightly lower displacement for both active and passive cases compared to the results from PLAXIS using full acceleration time series of Offshore Maule earthquake for 60 seconds as described in Figure 4.2. By using peak ground acceleration amplitude of $5m^2$/s, Figure 5.10 and Figure 5.11 have shown that ABAQUS produced higher results to that of PLAXIS, but they are still in the same order of magnitude. It should be noted that ABAQUS has many parameters available, slight changes in some parameters, such as intersection details or model types (2D or 3D), would more or less shift the displacement curve; in addition, the changing of soil model configurations such as changing dry sand to wet sand, change the plastic model (Mohr-Coulomb in this case) to other failure criterion, or material damping may incur different results in displacement curves. It is derived that both ABAQUS representative and peak ground acceleration level are able to produce reasonable horizontal displacement distribution of wall compared to the results from PLAXIS. Furthermore, using a peak ground acceleration level will produce closer displacement curves to PLAXIS' curve as shown in this case (see Figure 5.10 and Figure 5.11).

5.4. Lateral Earth Pressure

Figure 5.12 and Figure 5.13 demonstrate the lateral earth pressure made by both ABAQUS Implicit and Explicit under both representative and peak acceleration levels. Compared to PLAXIS results, both ABAQUS implicit and explicit with acceleration level of both 2.5m^2/s and 5m^2/s, have produced larger lateral earth pressure than the PLAXIS results. When 2.5 m^2/s is adopted, the ABAQUS results are from 10 to 100 kPa larger than that from PLAXIS. When a 5 m^2/s acceleration level is used (Figure 5.13), ABAQUS produces around 10 to 150 kPa greater lateral earth pressure than PLXIS results.

For 2.5 m^2/s acceleration, ABAQUS results from both implicit and explicit analysis increase approximately linearly for the above 4 meters depth, beyond which the lateral pressure starts to be almost constant from ABAQUS implicit analysis and a much lower rate of increase with depth from ABAQUS explicit (see Figure 5.12). Regarding 5m^2/s acceleration, both explicit and implicit lateral earth pressure also increase approximately linearly for the first 5.5 meters depth, after which the increase ratio between lateral earth pressure and depth is reduced significantly (see Figure 5.13). This trend agrees well with PLAXIS, which even showed a decreasing lateral earth pressure with depth under certain depth as shown by green curve in Figure 5.12 and Figure 5.13.Thus, although there is certain variance for the local lateral earth pressure, the pressure distribution curve from ABAQUS and PLAXIS' results, regardless of which analysis method or what acceleration is used, are similar. Since those lateral earth pressure curves all increase approximately linearly for a certain upper part of the wall depth, after which this increase trend has slowed down or diminished (for ABAQUS results) or turns into a decreasing trend (the PLAXIS results). For ABAQUS analysis, the depth at which the lateral earth pressure versus depth ratio starts to fall seems to be influenced by the ground acceleration level but barely by the analysis type of implicit or explicit. With a representative acceleration level of 2.5 m^2/s, this depth is around 3 meters (see Figure 5.12), at which the rate of lateral earth pressure increase slows down. And with a peak acceleration level of 5 m^2/s, this depth is around 5.5meters (see Figure 5.13). In summary, larger ground acceleration lead into a deeper depth above which the lateral earth pressure distributionis approximately linear. This agrees with normal triangular pressure

distribution by most analytical theories. There is a further analysis and discussion in 5.5regarding the relationship pressure distribution and free field displacement.

Figure 5.14 puts together all ABAQUS results of lateral earth pressure for easier comparison. It is obvious that a lower ground acceleration level has produced lower lateral earth pressure under around 4.5 meters. However, interestingly, for the upper part of the wall, 2.5 m^2/s acceleration level has shown slightly larger lateral earth pressure to that produced by 5 m^2/s acceleration level. Also, it could be observed that implicit analysis has produced somewhat lower lateral earth pressure especially after certain depth. This is probably due to the better dynamic absorbance effect provided by spring/dashpot element that is used by implicit analysis compared to connectors used for explicit analysis. In other words, more seismic energy is possibly retained in the soil block in explicit analysis (box effect).

As obtained above, Zhang et al (1998)'s strain ratio dependent solution produces results that agrees well with PLAXIS results. Zhang et al (1998)'s method in this calculation uses parameters, such as lateral wall displacement, obtained from PLAXIS. Since parameters β_a, β_p and Δ_a and Δ_p depend on soil properties and geometry of retain wall, both ABAQUS and PLAXIS share similar values of these parameters due to similar soil properties and wall geometry. Thus, with a similar lateral displacement produced between ABAQUS and PLAXIS as shown in Figure 5.11, it is reasonable to deduce Zhang et al. (1998)'s method will produce a similar results compared to that of PLAXIS if displacement values from ABAQUS was used. As a result, the analytical results based on PLAXIS displacement values are still applied in those graphs. As found earlier in the section4.5, they agree well with PLAXIS modelling results and this justified seismic analysis in PLAXIS follows strain increment ratio theories. So, compared to ABAQUS results, the analytical solution produced lower magnitude of lateral earth pressure as shown in Figure 5.12 and Figure 5.13.However, such kind of difference is normally acceptable for retaining wall problems.

In terms of design stability, larger lateral earth pressure produced by ABAQUS means less safe considering normal active failure criterion, sine the real wall pressure may be smaller as shown in PLAXIS results and analytical results, which means the stress state is closer to active critical state based on Mohr-Coulomb criteria. However,

there will be detailed account of the larger pressure by ABAQUS in section.5.5based on free field response.

Although similar in geometry and input soil / wall parameters, ABAQUS model has some differences compared to PLAXIS model. For example, sinusoidal ground acceleration with fixed amplitude is used in ABAQUS and the acceleration lasts for only 1 second, while the SMC file of real Offshore Maule earthquake is utilized in PLAXIS for a period of 60 seconds. Else, PLAXIS has readily available absorbent boundary conditions for its dynamic analysis, while in ABAQUS, connectors or springs/dashpots are used to make the conditions the same. There are also differences in bottom constraints and strut boundaries, which will be discussed in detail in section5.5.

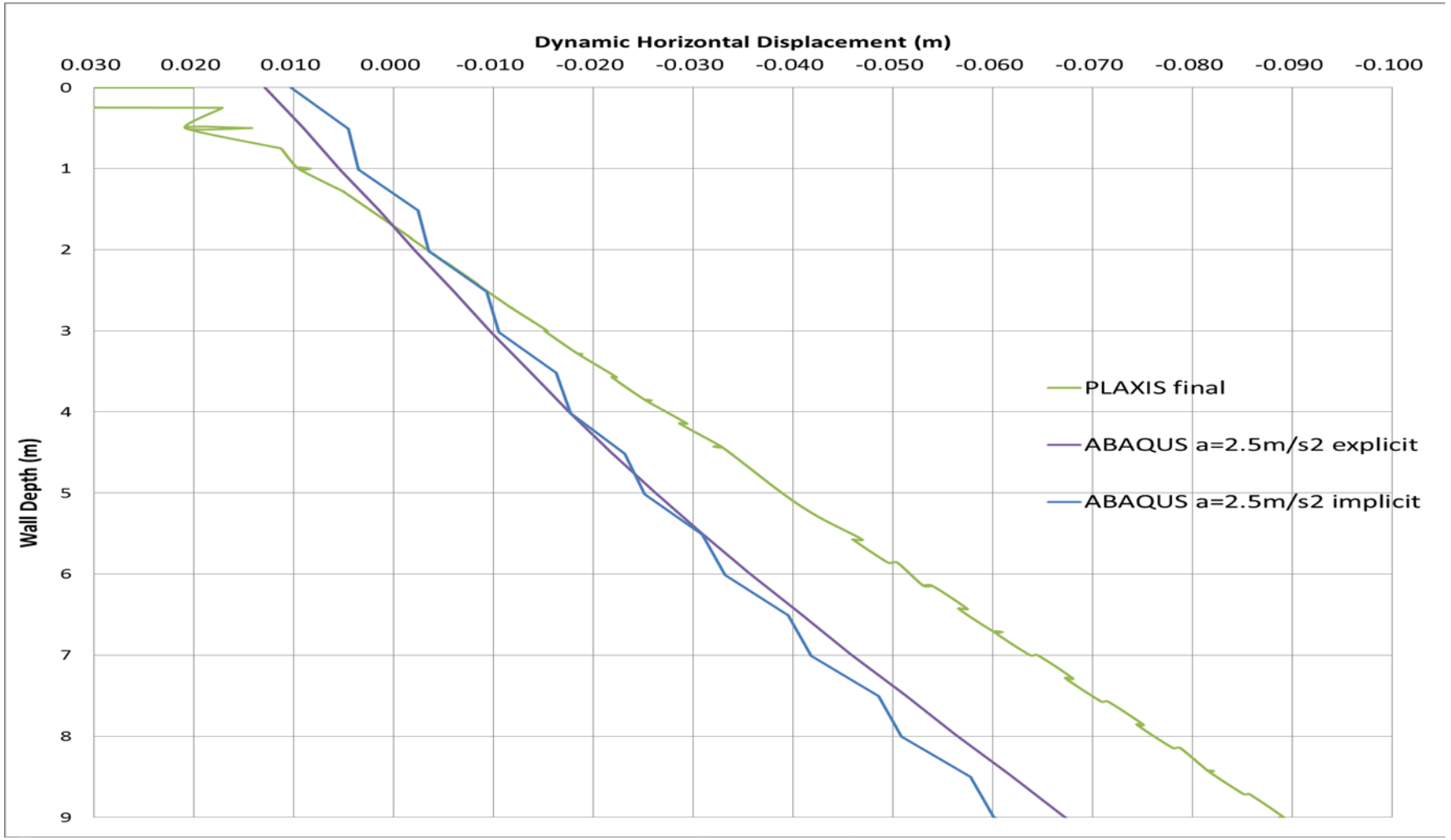

Figure 5.10: ABAQUS results for wall displacement profile for ground acceleration amplitude of 2.5 m^2/s

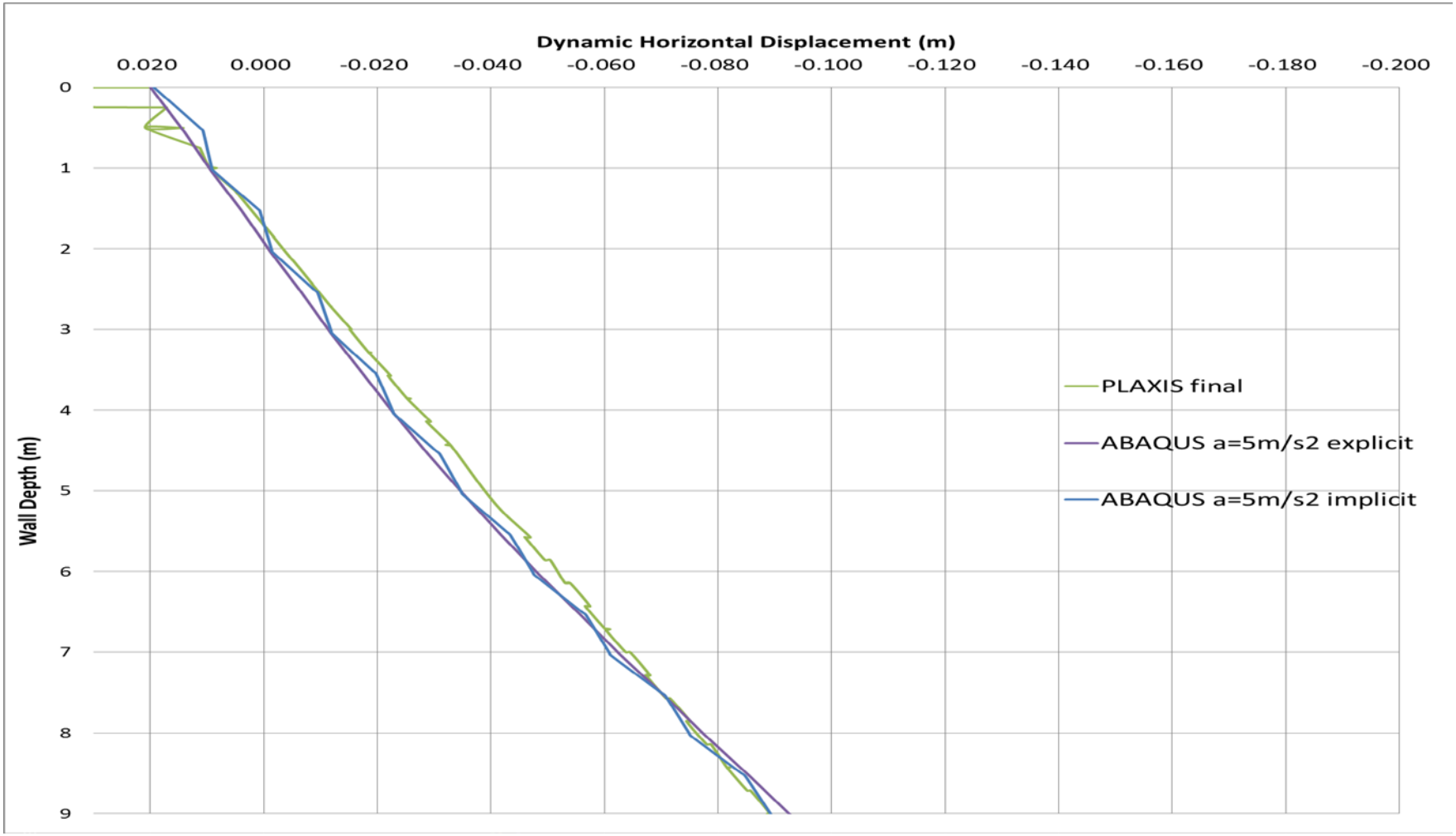

Figure 5.11: ABAQUS results for wall displacement profile for ground acceleration amplitude of5 m^2/s

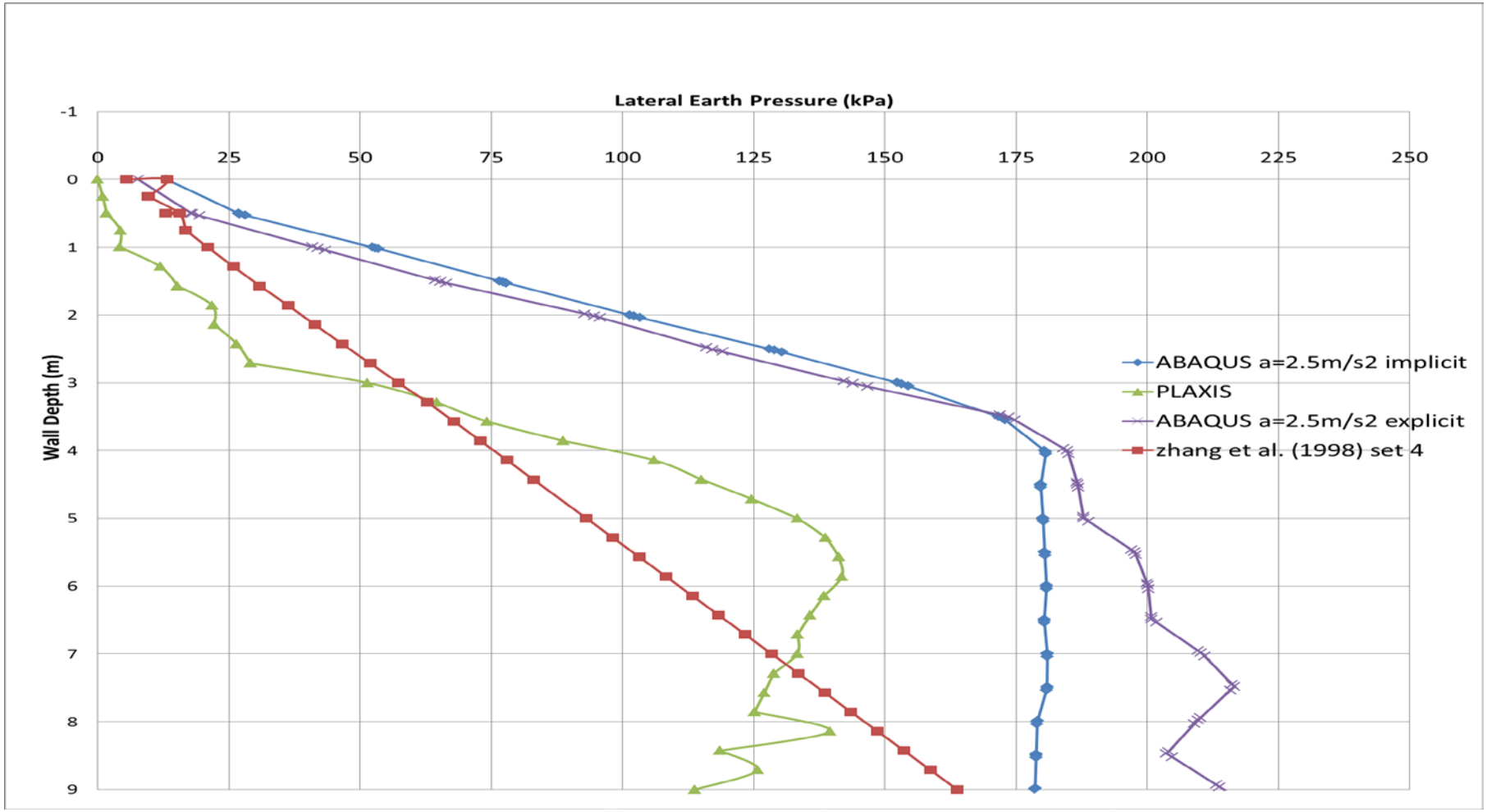

Figure 5.12: ABAQUS results for lateral earth pressure on the wall for ground acceleration amplitude of 2.5 m^2/s

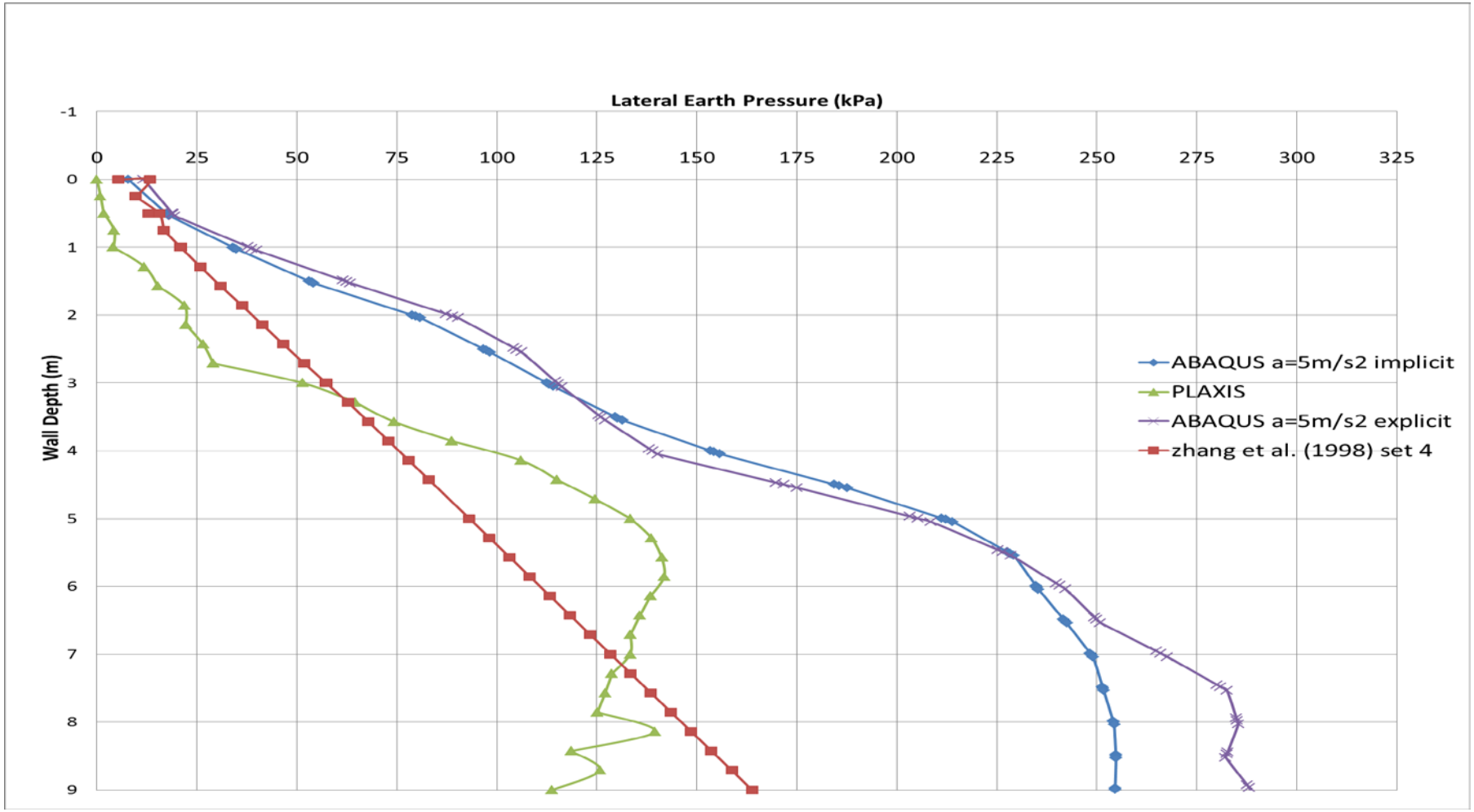

Figure 5.13: ABAQUS results for lateral earth pressure on the wall for ground acceleration amplitude of 5 m^2/s

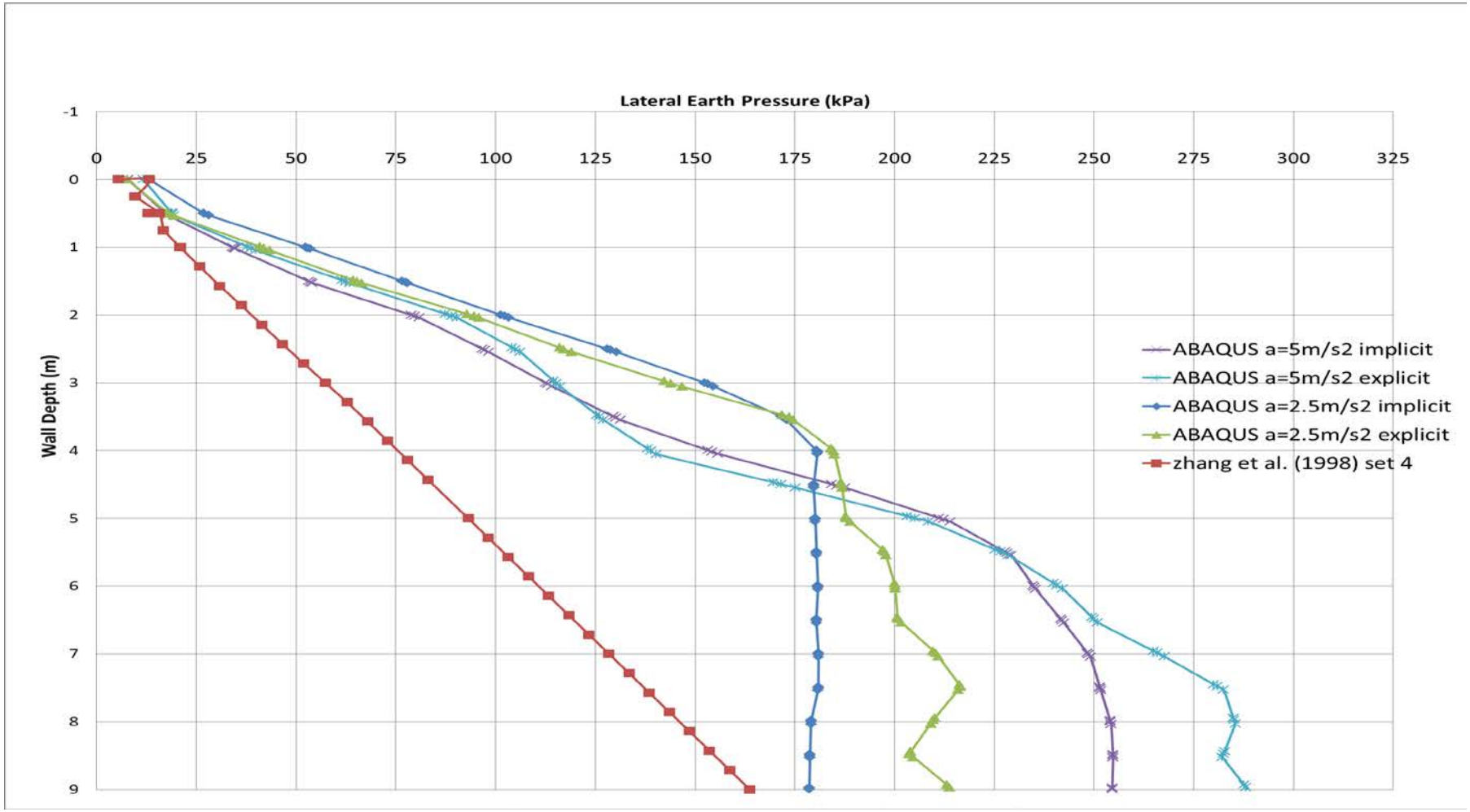

Figure 5.14: Plotting together of ABAQUS and Theoretical Result

5.5. Results of Free Field and Analysis of Spring Displacement Stress Relationship

Besides wall displacement and lateral earth pressure, a line lies across the middle of the soil block is drawn for investigating the free field response (Figure 5.15). This is not an exactly straight line due to nodes' positions, however, this line is able to represent freefield response as long as these points are around 1.5 to 2 H (H is end wall height) away from the side boundaries (Fishman et al. 1995). Also, since the ends are modelled as spring or connector elements, there should be more lenient requirement regarding free field the required free field distance from side boundaries. As a result, this line is regarded as eligible for representing free field response.

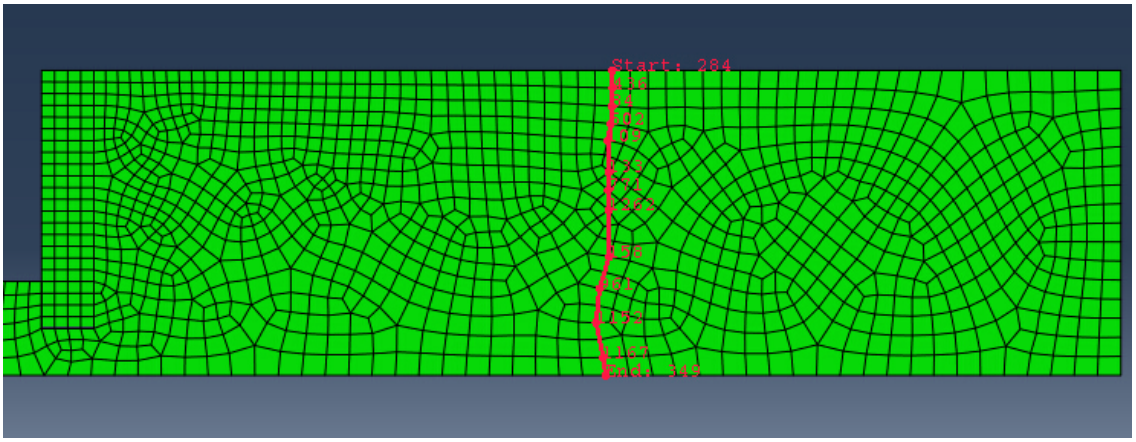

Figure 5.15: A line picked to acquire free field response (this is just an example line for one of the deformed models)

Different than PLAXIS results, ABAQUS needs to release the horizontal degree of freedom to make the ground acceleration effective, while in PLAXIS, the ground could be constrained horizontally even when the seismic acceleration is applied on the ground. In other words, to make the PLAXIS and ABAQUS results comparable, ABAQUS soil displacement needs to be calibrated to cancel the ground displacement. Also, since free field displaces symmetrically on both direction, the direction of free field displacement could be reversed for easier comparison of the magnitude of free field displacement to theory. However, the lateral earth pressured should still be addressed using the true direction from the output since active side or passive side displacement in freefield will incur changes in lateral earth pressure based subgrade modulus theories. Thus, both calibrated and original free field displacement results

from ABAQUS Explicit and Implicit using representative and peak ground acceleration amplitudes are listed in from Figure 5.16 to Figure 5.19. PLAXIS and theoretical results (elastic state only using equation (12)) are also displayed for comparison.

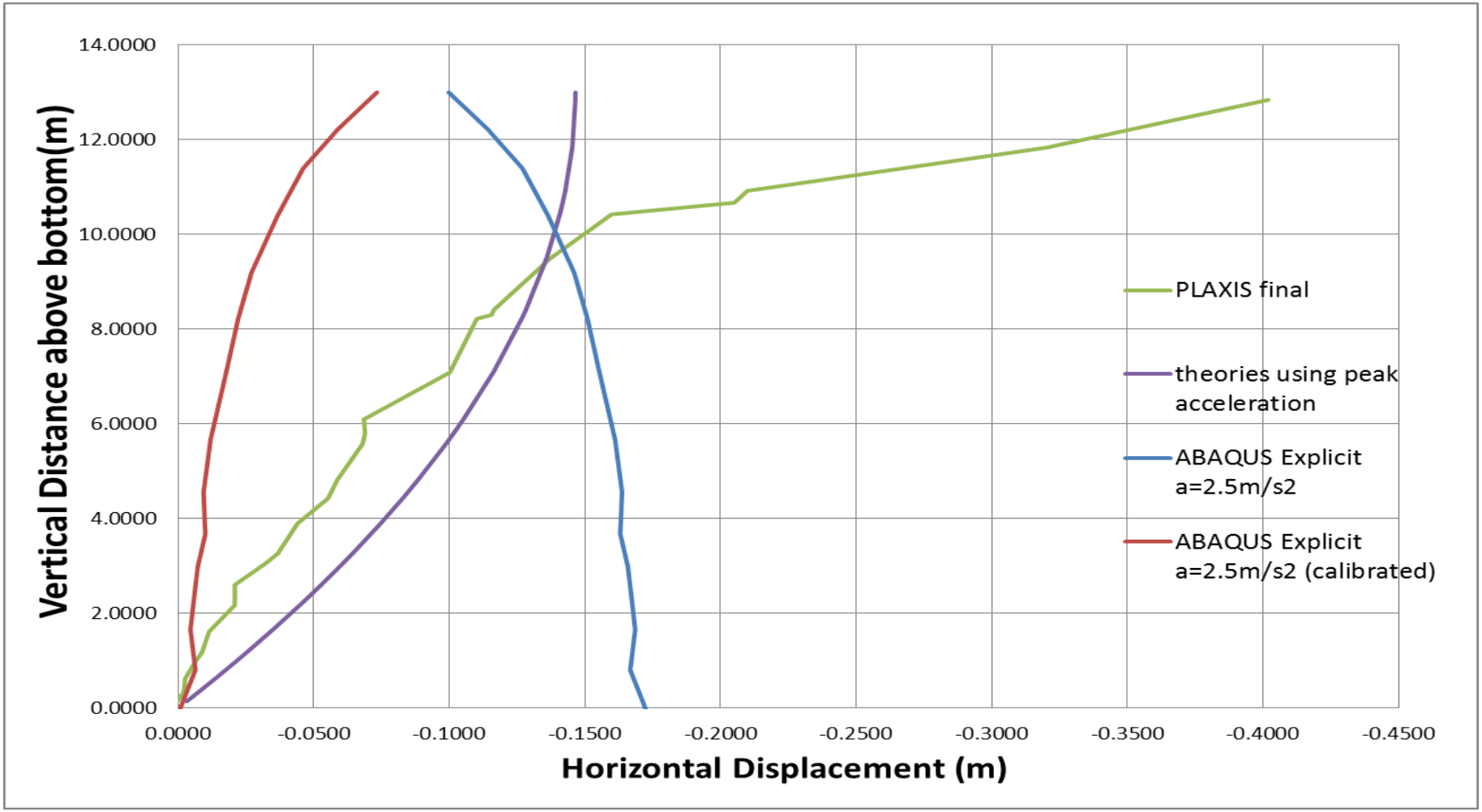

Figure 5.16： Free Field displacement for ABAQUS Explicit with representative ground acceleration level

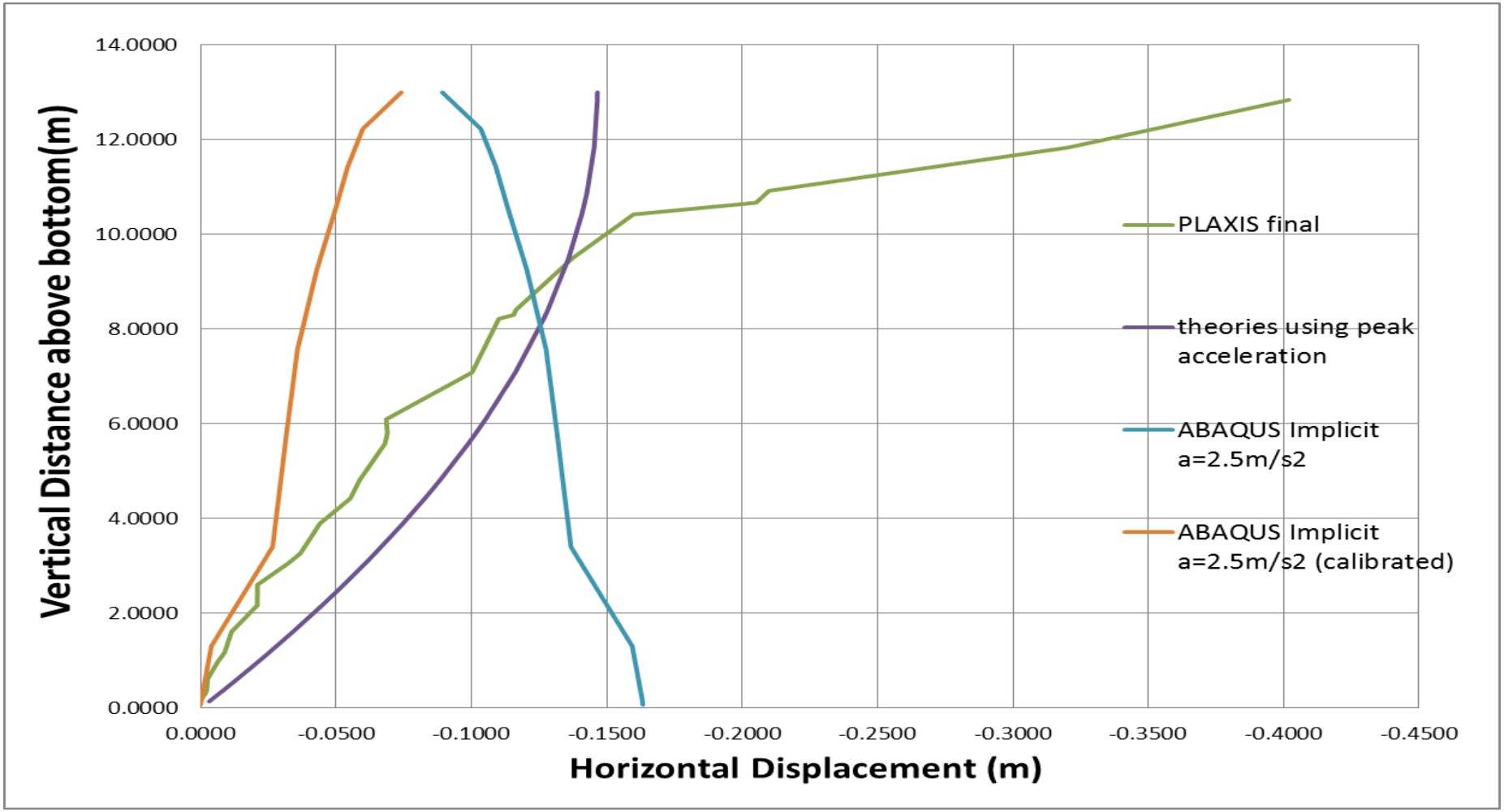

Figure 5.17: Free Field displacement for ABAQUS Implicit with representative ground acceleration level

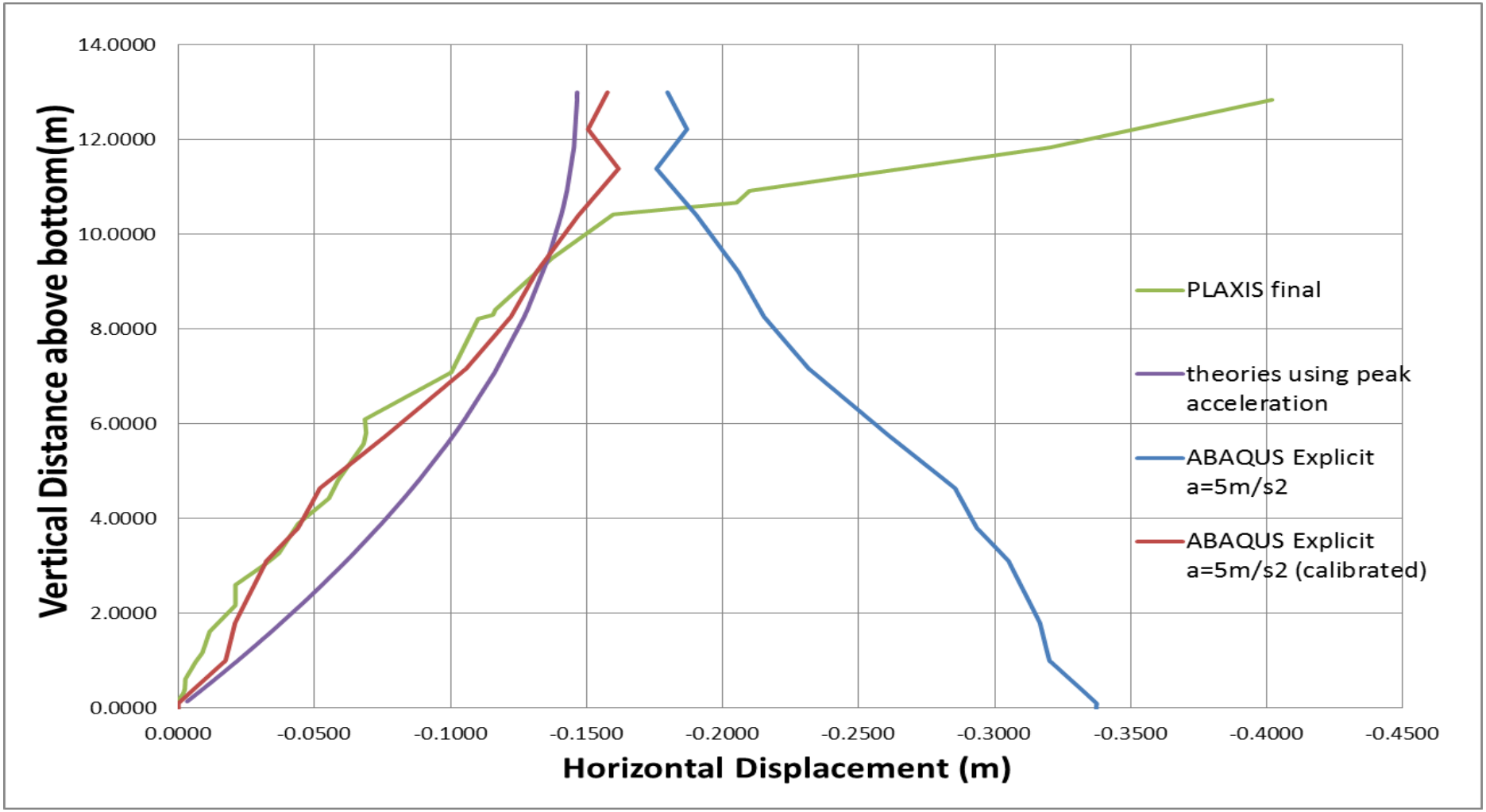

Figure 5.18: Free Field displacement for ABAQUS Explicit with peak ground acceleration level

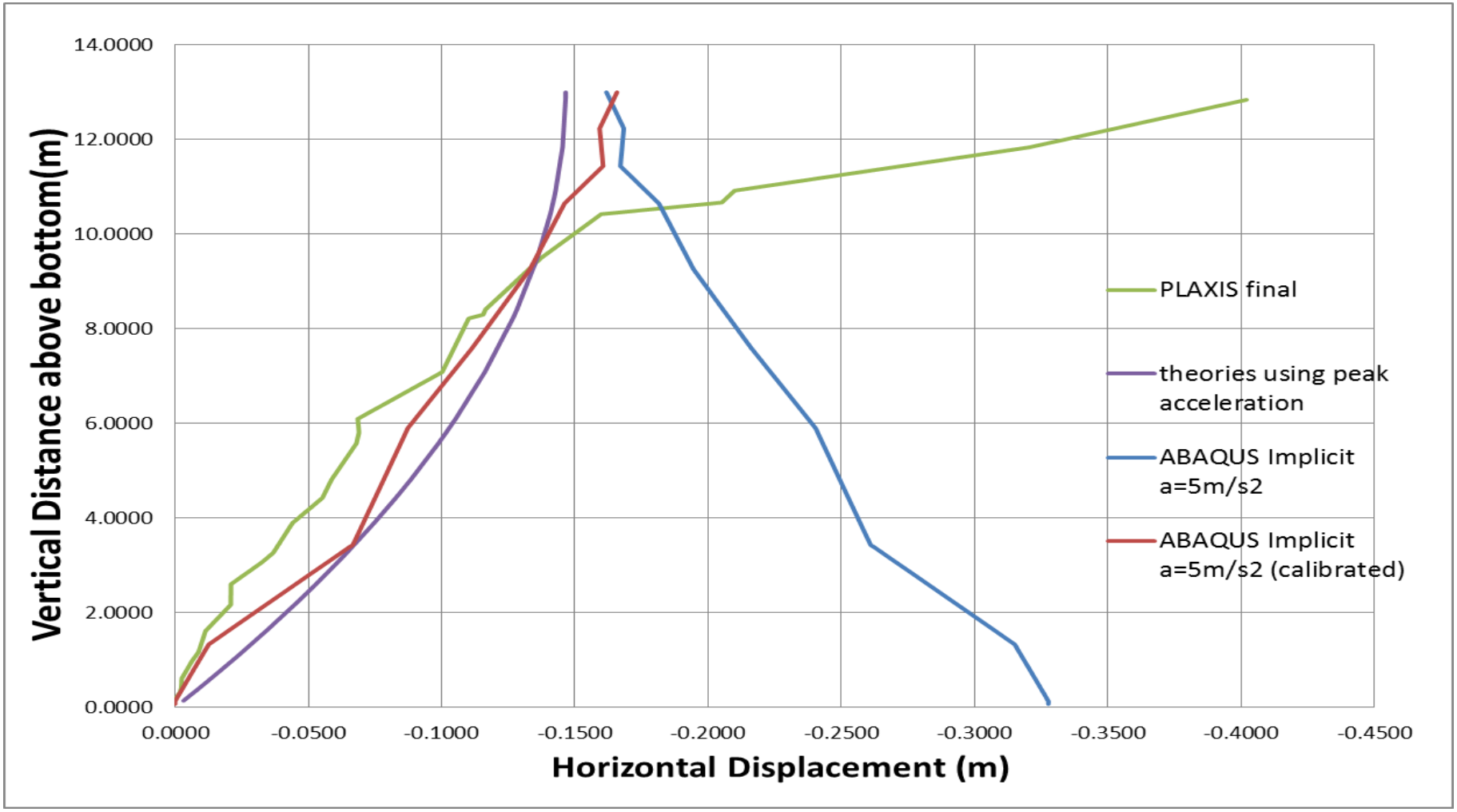

Figure 5.19: Free Field displacement for ABAQUS Implicit with peak ground acceleration level

From these graphs, it is shown that, using peak acceleration amplitude of 5 m^2/s, both ABAQUS Explicit and Implicit have produced similar (after calibration) horizontal free field displacement compared to theoretical and PLAXIS results, at least for most of the wall depth. The reason for much larger value in PLAXIS' results for the top part the wall is probably due to plastic response. This plastic trend could also be seen in ABAQUS results but to a much less extent. This is probably due to more acceleration cycles being applied in PLAXIS due to the input record of 60 seconds as shown in Figure 4.2plus that the plastic response is irreversible. Basically, there is a close match between theoretical results using peak acceleration of 5 m^2/s and ABAQUS results using the same peak value. When a representative acceleration level of 2.5 m^2 /s is used, ABAQUS produces lower horizontal free field displacement compared to both PLAXIS and theoretical results (but with peak acceleration), regardless of Explicit or Implicit analysis. To sum up, peak ground acceleration level has produced larger free field displacement and both PLAXIS and ABAQUS (using peak acceleration value) are able to reasonably predict the magnitude of this displacement by showing good agreement with theoretical results. Else, peak acceleration should be used from an earthquake record such as offshore maule since it produces closer results than using representative acceleration in terms of free field response.

The connected to ground connectors are used in ABAQUS to model the struts; thus the struts are fixed even when the ground moves. However, the horizontal displacement (un-calibrated one) of free field is larger than that from PLAXIS. Considering subgrade modulus theory such as equation (14), which indicates that the local soil pressure along the wall is controlled by corresponding local combined displacement between the wall and free field ("spring displacement"). Else in reality the struts are not absolutely fixed since it usually connects to another wall or structure that will move when strong earthquake strikes. Thus PLAXIS results are believed to be a better representation of reality, while this ABAQUS model of this study could be improved in future by addressing the fixed end condition of struts.

According to subgrade modulus theory, there must be a variance of spring displacement between ABAQUS and PLAXIS considering the variance of lateral earth pressure as shown in Figure 5.12 and Figure 5.13, since other components of lateral earth pressure such as inertia force, self-weight are very similar as input for

both softwares. However, it needs to be proved that the variance between ABAQUS and PLAXIS in terms of lateral earth pressure is controlled by “spring displacement”. Since the wall displacement and free field displacement are both available from two softwares, the combined displacement between wall and free field could then be produced. Although due to the nodes at the free field and the wall are usually not at the same height, the approximate values could still be easily and reasonably predicted by extrapolation. ABAQUS Implicit (Explicit also ok) with peak acceleration value is adopted due to its proved accuracy at producing free field displacement. The produced spring displacements from two softwares are demonstrated in Figure 5.20 and Figure 5.21.

In Figure 5.20 and Figure 5.21, negative sign means active displacement while positive sign means passive displacement. Interestingly, although the wall displaces to the active side produced by ABAQUS as shown in Figure 5.11, the effect of ground acceleration has actually triggered passive side spring displacement as shown in Figure 5.21. For retaining walls, passive displacement brings about larger lateral earth pressure when other conditions like inertia force and soil weight etc. are kept constant. So it is reasonable to deduce that PLAXIS results, with active spring displacement (see Figure 5.20), has produced lower lateral earth pressure compared to ABAQUS results. This agrees well with Figure 5.11, where ABAQUS demonstrates higher lateral earth pressure compared to PLAXIS. Also, since peak acceleration has produced larger passive displacement, this explains that greater lateral earth pressure is produced by peak acceleration to that from representative acceleration in Figure 5.11.

Since Zhang et al. (1998)’s strain increment ratio lateral earth pressure theory is built on the lateral displacement of soil right behind the wall without considering free field displacement. Also, for retaining walls at working state, Zhang et al. (1998)’s method has incorporated a concept of “intermediate wedge” to make the case transferrable to Mononoke and Okabe (1923)’s failure wedge equilibrium method, which assumes a planner failure wedge for critical states. Although this might be a reasonable solution in terms of total force on the wall and capturing the general trend of pressure distribution, which has been well proved in Figure 4.21. However, the local lateral earth pressured is still influenced by the corresponding free field displacement and thus “spring displacement”, which could also be seen in Figure

4.21, since the variance of local lateral earth pressure is obvious from PLAXIS and theory results.

In Figure 5.13, the lateral earth pressure for PLAXIS could be roughly divided into three segments with different gradients: 0-3m,3-6m and 6-9m. Compared to Figure 5.20, the spring displacement from PLAXIS generally agrees with this trend. For example, for 6-9m section, there is an increase of spring displacement in the active side seen in Figure 5.21, which corresponds to decrease of generated lateral earth pressure, so as shown for 6-9 meters segment in Figure 5.13. Else, for ABAQUS spring displacement demonstrated in Figure 5.21, a decrease of passive displacement is observed for 7-9meters. As less passive displacement means smaller generated lateral earth pressure if other conditions are kept the same, this generally agrees well with a smaller gradients shown in Figure 5.13 for 6-9m of ABAQUS lateral earth pressure. To sum up, comparing Figure 5.13,Figure 5.20 and Figure 5.21, combined displacement of wall and free field (spring displacement) has shown relevance to local lateral earth pressure. Considering that Zhang et al. (1998)'s strain increment ratio method only refers to wall displacement (or displacement of soil right behind the wall), it is more sufficient for static cases though capable of capturing the general trend of lateral earth pressure distribution for seismic cases. However, for a more accurate interpretation of pressure, the stress displacement relationship should take into account the free field displacement based on the influence of free field displacement and strong relevance between spring displacement and lateral wall pressure found in this study.

Since the local wall pressure is controlled by combined displacement of wall and freefield (spring displacement), the stress strain or displacement stress relationship for retaining wall obtained from static case should better be transferred into spring displacement stress relationship when applied for seismic case. This is yet to be investigated sufficiently to establish a quantitative relationship solution, not to mention a relevant lateral earth pressure equation. As a result, the current analysis of ABAQUS and PLAXIS results has shed some light on the influence of spring displacement and the significance of using free field displacement component for a more accurate lateral earth pressure distribution of retaining walls in seismic conditions.

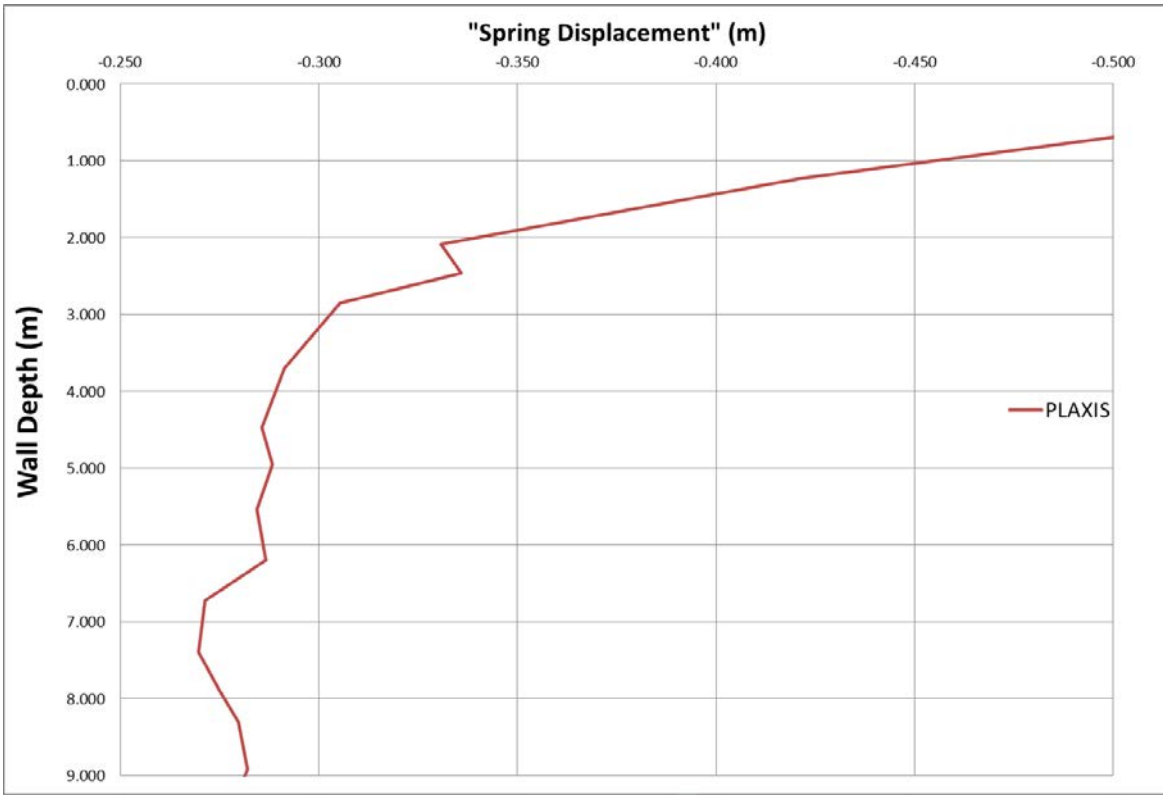

Figure 5.20: Displacement of wall and free field from PLAXIS

Figure 5.21:Displacement of wall and free field from ABAQUS Implicit

5.6. Limitations

Both ABAQUS and PLAXIS uses only Mohr-Coulomb failure criterion and considers no damping for their seismic analysis. The soil materials are strictly normally consolidated (necessary for strain increment ratio method) homogeneous dry sand without cohesion. All theories used are based on pseudo-static method. As mentioned above, the strut elements modelled by connector in ABAQUS might change the results a bit. There are more advanced seismic boundary solutions and this study uses viscous absorbent boundaries only. Numerical simulation does not always represent real soil behaviour and this analysis made in this paper has not been enhanced by experimental results. Other effects like dynamic interaction between soil and wall, vibro-densification, soil arching, dynamic amplification, phase effect etc. are all neglected since the stress of this study is to identify stress displacement relationship by taking into account free field displacement.

5.7. Summary

Both ABAQUS Implicit and Explicit models were built under different peak acceleration levels to investigate the wall responses against strain increment ratio lateral earth pressure theory and free field subgrade modulus method. The difference between Implicit and Explicit analysis is very small for both wall pressure and displacement. However, adopting peak acceleration in ABAQUS did produce larger response in terms of both displacement and lateral earth pressure. ABAQUS produced similar but somewhat larger wall pressure compared to PLAXIS and analytical solutions, while the free field displacements are very close when peak acceleration is adopted. The variance existing in lateral earth pressure is explained by study of “spring displacement”. It is obtained that seismic stress strain or stress displacement relation should take into account the influence of free field displacement.

Chapter 6. Conclusion

In this study, the author has built a model diaphragm wall with two struts retaining dry sand under seismic ground accelerations using commercial numerical modelling soft-wares ABAQUS and PLAXIS. Lateral earth pressure, wall displacement and free field displacement are produced and results are compared between various scenarios. Else, the modelling results are critically analysed and compared with analytical theories: Zhang et al. (1998)'s strain increment ratio dependent earth pressure theory, free field theory and Rowland et al. (1999)'s free-field subgrade modulus method, all of which have a focus on stress displacement relationship. The research outcomes are listed below:

1. Commercial numerical modelling soft-wares like PLAXIS has the capability to provide a way for reasonable determination of certain parameters used in strain increment ratio lateral earth pressure theories and subgrade modulus method. This is relatively accurate alternative for original empirical and rough estimations for the values of these parameters.
2. Although certain variance exists, both PLAXIS and ABAQUS produced results that demonstrate acceptable agreement with stress strain (displacement) relationship of soil proposed by Zhang et al. (1998).
3. The produced lateral earth pressure by PLAXIS is particularly close to that from strain increment ratio lateral earth pressure theory, while ABAQUS tends to generate larger lateral earth pressure using the model in this study. However, generally, the seismic earth pressure from ABAQUS agrees well with others.
4. Using peak ground acceleration from a real earth quake record as sinusoidal amplitude, ABAQUS produces close wall displacement to that from PLAXIS.
5. For this model, ABAQUS Implicit produces similar results to Explicit, while higher ground acceleration amplitudes produce greater wall response in terms of both displacement and lateral earth pressure.
6. Using peak ground acceleration as sinusoidal amplitude, ABAQUS produces free field displacement that agrees well with PLAXIS using real earthquake record and theoretical results (also using peak acceleration).
7. The variance between local wall pressure distributions among strain increment ratio dependent lateral earth pressure theory, PLAXIS and ABAQUS is controlled by the combined distance between wall and free field (spring

displacement). Spring displacement should be used for interpreting stress displacement relationship for retaining walls under seismic conditions.

In future, experimental studies could be utilized to assist numerical and theoretical studies for the purpose of validating the relationship between lateral earth pressure and spring displacement. Finally, a complete equation that interprets real stress strain behaviour for seismic retaining walls by taking into account the influence of free field displacement could be worked out. Else, this could be studied by more advanced numerical analysis like an amended ABAQUS model using more advanced and appropriate boundary conditions plus a reasonable solution of fixed end struts under seismic excitations. The ultimate goal is establish an analytical solution for the response of dynamic/seismic retaining walls under various conditions including different wall/base rigidity, displacement modes, critical and working state etc., and able to solve displacement as well as lateral pressure.

Reference

[1] Al-Homoud, A. S. and R. V. Whitman (1999). "Seismic analysis and design of rigid bridge abutments considering rotation and sliding incorporating non-linear soil behavior." Soil Dynamics and Earthquake Engineering**18**(4): 247-277.

[2] Al Atik, L. and N. Sitar (2010). "Seismic Earth Pressures on Cantilever Retaining Structures." Journal of Geotechnical and Geoenvironmental Engineering**136**(10): 1324-1333.

[3] Anderson, D. G. (2008). Seismic analysis and design of retaining walls, buried structures, slopes, and embankments. Washington, D.C., National Cooperative Highway Research Program National Research Council Transportation Research Board, American Association of State Highway

[4] Basha, B. and G. Babu (2010). "Seismic Rotational Displacements of Gravity Walls by Pseudodynamic Method with Curved Rupture Surface." International Journal of Geomechanics**10**(3): 93-105.

[5] Bolton, M. D. and W. Powrie (1988) "Behaviour of diaphragm walls in clay prior to collapse." Géotechnique**38**, 167-189.

[6] Choudhury, D. and S. Nimbalkar (2005) "Seismic passive resistance by pseudo-dynamic method." Géotechnique**55**, 699-702.

[7] Choudhury, D. and S. Nimbalkar (2007). "Seismic rotational displacement of gravity walls by pseudo-dynamic method: Passive case." Soil Dynamics and Earthquake Engineering**27**(3): 242-249.

[8] Diakoumi, M. and W. Powrie (2013) "Mobilisable strength design for flexible embedded retaining walls." Géotechnique**63**, 95-106.

[9] Fishman, K. L., J. B. Mander and R. Richards Jr (1995). "Laboratory study of seismic free-field response of sand." Soil Dynamics and Earthquake Engineering**14**(1): 33-43.

[10] Green, R. A., C. G. Olgun and W. I. Cameron (2008). "Response and Modeling of Cantilever Retaining Walls Subjected to Seismic Motions." Comp.-Aided Civil and Infrastruct. Engineering**23**(4): 309-322.

[11] Huang, C. (1996). Plastic analysis for seismic stress and deformation fields PhD dissertation, SUNY at Buffalo.

[12] Ishibashi, I. and Y.-S. Fang (1987). "Dynamic Earth Pressures With Different Wall Movement Modes." SOILS AND FOUNDATIONS**27**(4): 11-22.

[13] M.D.Bolton and R. S. Steedman (1982). Centrifugal Testing of Microconcrete Retaining Walls Subjected to Base Shaking. Soil Dynamics and Earthquake Engineering Conference.

[14] Mononobe, N. and M. Matsuo (1929). On The Determination of Earth Pressures During Earthquakes. Proc., Proc. World Engrg. Congress.

[15] Nadim, F. and R. Whitman (1983). "Seismically Induced Movement of Retaining Walls." Journal of Geotechnical Engineering**109**(7): 915-931.

[16] Ortiz, L. A., R. F. Scott and J. Lee (1983). "Dynamic centrifuge testing of a cantilever retaining wall." Earthquake Engineering & Structural Dynamics**11**(2): 251-268.

[17] Osman, A. S. and M. D. Bolton (2004). "A new design method for retaining walls in clay." Canadian Geotechnical Journal**41**(3): 451-466.

[18] Pathmanathan, R. (2006). Numerical Modelling of Seismic Behaviour of Earth - Retaining Walls. Master of Earthquake Engineering.

[19] Psarropoulos, P. N., G. Klonaris and G. Gazetas (2005). "Seismic earth pressures on rigid and flexible retaining walls." Soil Dynamics and Earthquake Engineering**25**(7-10): 795-809.

[20] Rowland Richards, J., C. Huang and K. L. Fishman (1999). "Seismic earth Pressure on Retaining Structures." Journal of Geotechnical and Geoenvironmental Engineering**125**(9).

[21] Scott, R. F. (1973). Earthquake-induced pressures on retaining walls. 5th World Conf. on Earthquake Engrg., Tokyo, Int. Assn. of Earthquake Engrg.

[22] Seed, H. B. and R. V. Whitman (1970). Design of Earth Retaining Structures for Dynamic Loads, University of California.

[23] Sherif, M. A., I. Ishibashi and C. D. Lee (1982). "Earth Pressures against Rigid Retaining Walls." Journal of the Geotechnical Engineering Division**108**(5): 679-695.

[24] Steedman, R. S. and X. Zeng (1990) "The influence of phase on the calculation of pseudo-static earth pressure on a retaining wall." Géotechnique**40**, 103-112.

[25] Yang Su, Amin Chegnizadeh and Hamid Nikraz (2013). "Review of Studies on Retaining Wall's Behavior on Dynamic / Seismic Condition." International Journal of Engineering Research and Applications**3**(6): 01-05.

[26] Veletsos, A. and A. Younan (1997). "Dynamic Response of Cantilever Retaining Walls." Journal of Geotechnical and Geoenvironmental Engineering**123**(2): 161-172.

[27] Wong, C. P. (1982). Seismic Analysis and Improved Seismic Design Procedure for Gravity Retaining Walls. Master of Science, Massachusetts Institute of Technology.

[28] Wood, J. H. (1973). Earthquake-induced Soil Pressures on Structures: Thesis, California Institute of Technology.

[29] Wood, J. H. (1975). "Earthquake induced pressures on a rigid wall structure." Bull. of New Zealand Nat. Soc. for Earthquake Engrg.**8**(3): 175-186.

[30] Zarrabi, K. (1979). Sliding of Gravity Retaining Wall During Earthquakes Considering Vetical Acceleration and Changing Inclination of Failure Surface. Master of Science, Massachusetts InstiInstitute of Technology.

[31] Zeng, X. and R. Steedman (2000). "Rotating Block Method for Seismic Displacement of Gravity Walls." Journal of Geotechnical and Geoenvironmental Engineering**126**(8): 709-717.

[32] Zhang, J., Y. Shamoto and K. Tokimatsu (1998). "EVALUATION OF EARTH PRESSURE UNDER ANY LATERAL DEFORMATION." SOILS AND FOUNDATIONS**38**(1): 15-33.

[33] Zhang, J., Y. Shamoto and K. Tokimatsu (1998). "SEISMIC EARTH PRESSURE THEORY FOR RETAINING WALLS UNDER ANY LATERAL DISPLACEMENT." SOILS AND FOUNDATIONS**38**(2): 143-163.

Appendix A: Paper for publication "Review of Studies on Retaining Wall's Behavior on Dynamic / Seismic Condition"

RESEARCH ARTICLE OPEN

Review of Studies on Retaining Wall's Behavior on Dynamic / Seismic Condition

Su Yang*, Amin Chegnizadeh**, Hamid Nikraz***

* (PhD Student, Department of Civil Engineering, Curtin University of Technology, Perth, Australia)

** (Research Fellow, Department of Civil Engineering, Curtin University of Technology, Perth, Australia)

*** (Professor, Department of Civil Engineering, Curtin University of Technology, Perth, Australia)

ABSTRACT

Current theories, experimental investigations and numerical findings for retaining walls subject to dynamic excitations are reviewed. Brief features of each method, and experimental and numerical methods are introduced and compared. Tables are listed after each section for a clear and brief view of methods in a categorized manner. Conclusive comments plus current concerns and future expectations of this area are made at last. This review aims at shedding light on the development and concepts of different researches in dynamic retaining wall design and analysis.

Keywords – dynamic, limit equilibrium, retaining wall, review, sub-grade modulus

I. Introduction

Retaining wall systems, consisting mainly of a retaining wall and backfill soil, is a prevalent structure used in our built environment including basement wall, bridge abutments, residential elevations, highway walls and so on. The engineering essence of retaining wall is to keep the retained soil in certain shape and prevent it from falling (stability), or to restrain the deformation of the wall and the backfill to maintain its service function (serviceability). Lateral earth pressure generated by retained backfill on the wall and relevant soil / wall deformations are two main facets of engineering design and analysis of retaining walls. Dynamic/seismic response of such system is one of the major areas due to the influence of dynamic force on the lateral pressure, soil / wall deformation. There are quite a number of analytical solutions, experimental investigations and numerical studies that have been conducted in this area due to different soils, wall structures, dynamic and structural conditions etc. In the meanwhile, it is widely accepted that traditional methods have insufficiencies especially under certain circumstances. As a result, there is a diversity of research to address this issue and try to accurately capture the dynamic response of various retaining systems. However, there is currently no comprehensive and categorized review of current research for dynamic retaining walls. As a result, it is valuable to produce a review of current theoretical solutions and their features; also, significant experimental findings and numerical studies are listed and evaluated. The purpose is to provide peer researchers an overview of the types of research in this area and provides introductive descriptions and critical comments for past studies.

This review work is developed from first author's doctorate research proposal submitted to Curtin University [24]. The general structure and categories of this review are indicated in the next page.

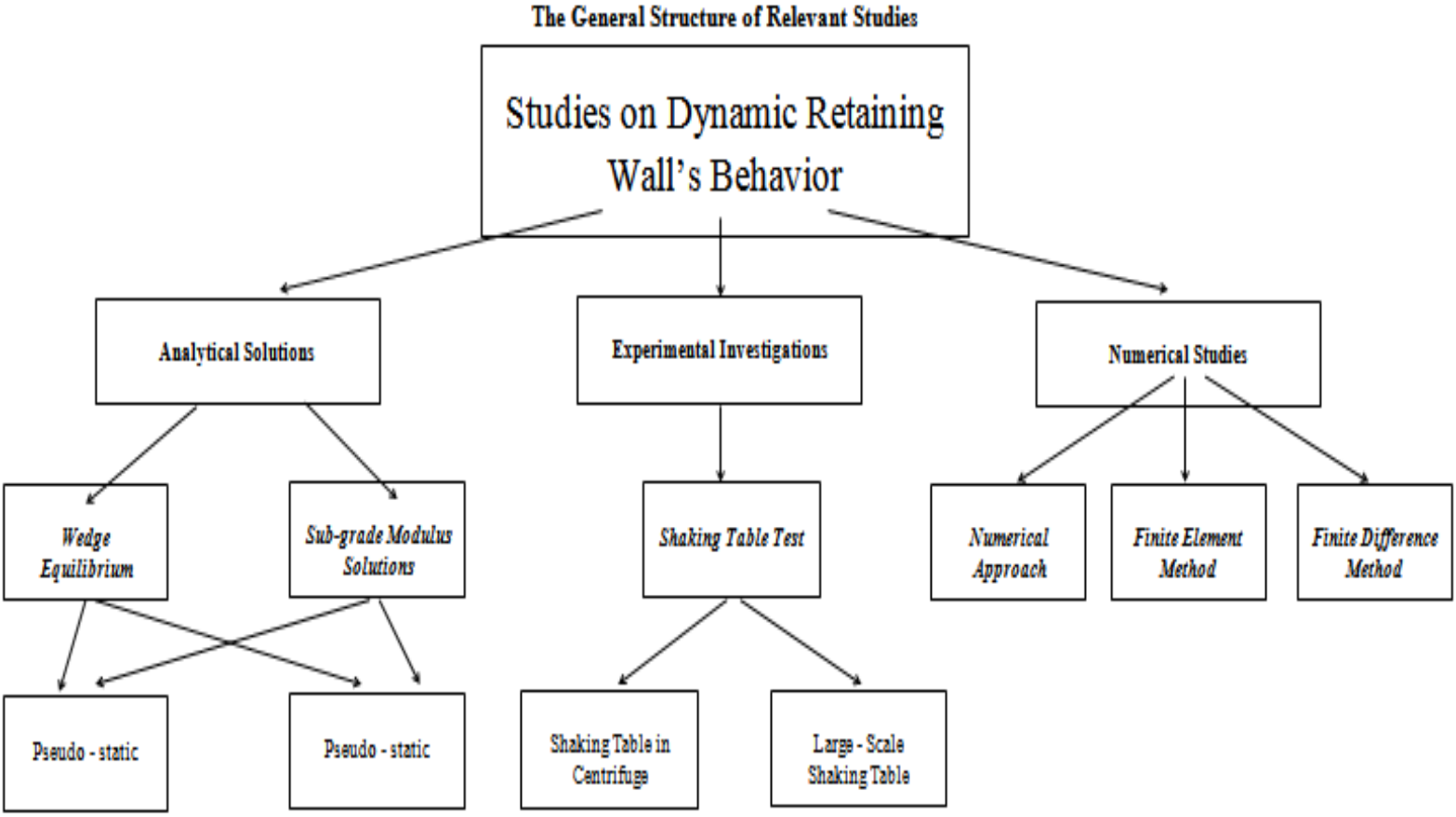

The scope of this review:

1. Studies that proposed fundamental theories or their significant improvements for retaining walls' dynamic response: that is no anchorage or any other enhancing ancillaries, no surcharge, gravity and cantilever type of wall mainly etc.
2. Analytical, experimental or numerical findings that expose new aspects of wall behavior with a significant physical or mechanism basis.

3. Analytical Theories

Currently, there are two main streams of analytical solutions for the dynamic lateral earth pressure of retaining walls: (1) Failure wedge equilibrium theory, which is mainly represented as limit equilibrium analysis (plasticity theory or extension of Coulomb's wedge theory) in which force equilibrium, including dynamic forces (both pseudo-static and pseudo-dynamic) is sought for a failure wedge. (2) Sub-grade modulus (one sub-method of this is elasticity analysis) method, in which the retained soil is considered elements with stiffness modulus such as shear beams or spring systems, so the earth pressure can be gained knowing the displacement of the interface [19]. Only significant theoretical developments are reviewed: many improvements and extensions on those original theories will be neglected or covered very briefly in this section of review.

A. Failure Wedge Equilibrium

1) Review

Mononobe and Okabe [13] (referred to as the MO method in the following text) conducted a series of shaking table tests (using original facilities) following the Kanto earthquake in 1923, and based on the experimental data, they firstly developed a method (MO method) that combines Coulomb's wedge theory with quasi–static inertial force to produce a renewed equilibrium equation, from which the coefficient of active lateral seismic earth pressure can be obtained [13].

It is widely known that some significant assumptions are inherent with the MO method:

1) Dry, cohesionless, isotropic, homogenous and elastic backfill material with a constant internal friction angle and negligible deformation [13].

2) The wall deflects sufficiently to exert full strength along the failure plane [13]. This means no wall rigidity is considered.

What's more, the MO method is a pseudo-static approach in which the time effect of dynamic force and the dynamic amplification effect are neglected. The MO method as an extension of Coulomb's wedge theory is a widely used traditional method for solving seismic retaining wall matters. It is widely used as the basic theory for new research and retaining wall design standards, such as Euro code 8 and Australian Standard 4678.

Based on the MO method, Seed and Whiteman [21] investigated the effects of various factors, such as angle of friction, slope of backfill, dry / wet condition, horizontal acceleration, source of load (seismic or blast) and wall friction, on dynamic earth pressure and proposed that dynamic earth pressure can be divided into static part and dynamic part, which then leads into an adaption of the MO method [21]. This simplified method is also widely used as a way to preliminarily solve for dynamic earth pressure issues. On the other hand, rather than one-third above the bottom of the wall from the MO method, Seed and Whiteman [21] proposed a height of 0.6H (H is wall height) above the wall bottom as the location for the resultant force [21].

Deriving from sliding block model, Richards and Elem [18] worked out a serviceability solution (R-E model) with the MO method. The R-E model provided a function for gravity wall displacement. From this, the coefficient of limiting wall acceleration can be solved for [18]. This coefficient is then used as a horizontal acceleration in the MO method to obtain earth pressure. Zarrabi [28] improved this method by taking into account vertical acceleration: this normally renders a slightly lower displacement value than the R-E model. All these methods are summarized by Nadim and Whiteman [14], who also presented a design procedure using displacement-based methods. These methods are categorized as limit equilibrium method since, for all of them, the MO method is used for pressure calculations by knowing the displacement (serviceability requirement) [14] [18] [28].

Since the above mentioned pseudo – static methods neglect the time effect of dynamic excitations and dynamic amplification, Steedman and Zeng [23] investigated the influence of phase on lateral earth pressure, and it was found that dynamic amplification has a significant influence on the coefficient of lateral earth pressure, which is supported by centrifuge tests results [23]. In addition, it can be derived that, for low frequency dynamic excitation, when dynamic amplification is not significant, pseudo – static condition is well satisfied [23]. Also, Steedman and Zeng [23] produced a solution for pseudo-dynamic pressure.

Zeng and Steedman [29] established a method to calculate the rotation of gravity wall subjects to seismic load by modeling the wall as a rotating block [29]. Acceleration needs to reach the threshold to start the rotation, which stops until the angular velocity for rotation is reduced to zero [29]. This method is a pseudo-dynamic one that takes into account time effect of dynamic response [29].

Choudhury and Nimbalkar [5], [6] have established a pseudo - dynamic method for lateral earth pressure and wall displacement in a passive case. In addition to Steedman and Zeng's [23] [29], they studied and incorporated vertical acceleration, inertia effect between wall and soil and comprehensive relevant factors, but the equations seem lengthy and so hamper practical use. Basha and Babu [4] also did a similar pseudo – dynamic research for the case of failure plane as a curved rupture surface, which is believed to be more realistic [4].

Anderson et al. [3] produced a chart method for the application of the MO method for cohesive soils. The chart method is also limited to cases of non-homogeneous soils and complex back-slope geometry as MO method [3].

Based on the "intermediate soil wedge" theory that relates wall pressure to the strain increment ratio, Zhang et al. [31] developed a new theory to evaluate seismic earth pressures against retaining walls under any condition between passive and active limit states. This method can be viewed as a combination of the failure wedge equilibrium theory and the strain-based pressure theory by Zhang et al [30]. However, the way used to determine a relevant lateral displacement factorusing this solution is difficult in practical use and not interpretative [30] [31].

2) Limitations

The MO method is a limit state method: it only applies when the failure plane is triggered. So it can not be directly used for working state analysis. Although many new solutions have been produced to overcome the inherent assumptions of the MO method, most new solutions seem tedious and so hamper their practical uses. The same goes to the method used to calculate displacements. Also, the location of the resultant force for the MO method is arguable, as well as the stress distribution, especially when the rigidity of the wall exceeds a certain level (this will also be covered in the experimental study section). What's more, it is widely believed that the wall pressure is directly related to the soil displacement behind the wall. However, many experimental and numerical findings pointed that the MO method and many of its variants do not take into account displacement modes and rigidity of the wall.

B. Sub-grade Modulus Method

In the sub-grade modulus method, the soil-wall interaction is modeled by elements like springs with a stiffness modulus (e.g bulk constant) to relate displacement and generated pressure. These methods are regarded as an alternative way to the MO method for dynamic retaining wall analysis, and were originally used as an elasticity analysis method [19]. Generally, these solutions count soil as elastic, visco-elastic, or plastic material. One significant and simple method under elastic solutions is to represent the interaction between soil and structure in the form of a spring system.

1) Review

To overcome the MO method's inaccuracy for relatively rigid walls, Wood [26] [27] developed a linear elastic theory to estimate the dynamic soil pressures on rigid walls under relatively idealized conditions such as modeling the soil as massless springs [26] [27]. Scott [20] treated the retained soil as shear beams of visco-elastic material that connect to the walls and free at its upper surface [20]. The same as Wood's, only a linear elastic condition with a constant soil stiffness is used in this Winkler - type method. To overcome the drawbacks of Scott's method, Veletsos and Younan [25] utilized semi-infinite, elastically supported horizontal bars, which have mass, to account for the radiational damping effect of the stratum [25]. The same as the previous elasticity methods, springs with constant stiffness are used to model the soil wall interaction [19]. Numerical tool such as MATLAB are needed to solve problems using some sub-grade modulus theories, so some similar studies are included in the numerical section and Table 3 of this review [19].

It is proved that the soil behavior for most geotechnical structures is stress and strain behavior. So understanding soil displacement and stress strain relationship remains an important part for relevant studies. As a result, for the sub-grade modulus method, it is important to shed light on "free-field theories". Free field refers to a field where the dynamic response of the soil is unrestrained, in other words, it is the soil response in a natural field without restriction [19].

The solution for free-field deformation is studied by a couple of researches. Fishman [7] proposed a simplified pseudo-static equation for free field displacement under an active condition with a constant shear modulus (G) and a linearly varying (with depth) shear modulus respectively [7]. Later on, Huang [9] studied plastic deformation in a free field of dry granular soil using the theory of plastic flow. It follows with a solution to calculate the free-field displacement under plastic conditions by incorporating a factor f(kh) into the elastic solution. It is worth mentioning that among the above methods, the soil is elastic – perfectly plastic with Mohr – Coulomb failure criterion and the dynamic force is assumed as pseudo – static [9].

Utilizing the free-field theories developed above, Rowland Richards et al. [19] present a simple kinematic and pseudo – static approach to evaluate the distribution of dynamic earth pressure on retaining structures. Also, both elastic and plastic soil responses are considered. A series of springs are used to model the soil between the free field and the wall [19]. And the spring stiffness is derived from elastic or secant shear modulus in the free field [19]. The wall pressure is obtained by free field stress (using un–mobilized friction angles) and relative deformation between the free–field and the retaining structure [19].

2) Limitations

For the sub-grade modulus method, the formulation of a free- field response is idealized on assumptions such as zero vertical acceleration, pseudo-static etc.: so it does not represent the real free field behavior. And, except in some laboratory studies, only rigid non-deflecting walls are considered by current analytical sub-grade modulus methods [25]. Also, the adoption of a shear modulus is difficult, since G actually varies with confining pressures, strain level and stress history. What's more, the choice of sub-grade modulus is arbitrary; for example, a constant elastic sub-grade modulus is not accurate to represent the true non-linear soil stress strain behavior. The dilemma is, with more factors being taken into account, the solution also becomes more complex and less likely to be used in practice. Alternatively, some elasticity (or sub-grade modulus) theories are to be realized in numerical tools such as MATLAB.

Table 1 listed significant analytical methods that have practical use.

Table 1 List of Analytical Methods for Dynamic Retaining Wall Pressures and Displacement (only Simplified Practical Solutions are listed)

Failure Wedge Equilibrium Method	
Pseudo – Static Pressure/Force	
Mononoke and Okabe [13] :Kae = $\frac{cos^2(\phi-\theta-\beta)}{cos\theta cos^2\beta \cos(\delta+\beta+\theta)[1+\sqrt{\frac{\sin(\phi+\delta)\sin(\phi-\theta-i)}{\cos(\delta+\beta+\theta)\cos(i-\beta)}}]^2}$	Most widely used approach. For the walls that have sufficient flexibility and subject to a low acceleration level. Other assumptions need to be met as well. Total pressure at one-third of the wall height above the wall base based on original assumptions.
Seed and Whiteman [21]: Kae = Ka+$\frac{3}{4}k_h$	Vertical wall and horizontal dry backfill. A simple version for the MO method. Other conditions are similar to the MO method, except a dynamic component acting at 0.6H (H is wall height).
Strain ratio related method for pressures by Zhang et al.'s [31], please refer to relevant papers for approaches.	Lateral pressure at any state can be calculated. Lateral to vertical strain ratio is a crucial parameter, which needs to be determined by site measurement.
A chart method for cohesion soils by Anderson [3], please refer to relevant papers for approaches.	Charts are gained from adaptions of the MO methods for cohesive soils. Conditions for the MO method still apply, except cohesive soil.
Pseudo –Static Displacement	
Richards and Elem [18]:Wall Displacement = $\frac{0.087V^2(\frac{N}{A})^{-4}}{Ag}$	N=ka (horizontal acceleration). This method, combined with pseudo – static approaches with sufficient yield of wall such as the MO method, is able to address serviceability problems for relevant cases.
Pseudo – Dynamic Force/Pressure	
Steedman and Zeng [23]: Pae = $\frac{Q_h \cos(\alpha-\varphi)+Wsin(\alpha-\varphi)}{cos(\delta-\alpha+\varphi)}$	This method takes into account the influence of phase and dynamic amplification factors on lateral earth pressure. Different results to the MO method mainly in terms of pressure distribution.
Choudhury and Nimbalkar's [5] method for pseudo – dynamic earthpressures. For equations please refer to relevant papers.	Vertical acceleration is considered. And taking into account various factors.
Pseudo –Dynamic Displacement	
Zeng and Steedman [23]: rotational acceleration α=[P_{AE} cos(δ+β□□ h+(W/g)$\alpha_g * yc$ -W* x_c - P_{AE} sin(δ+β□□ B h*tanβ)]/[I_c+W/g*r_c^2]	A rotating block method for gravity wall, taking into account the time effect of dynamic load. No inertia force is considered.
Choudhury and Nimbalkar's method [6] for pseud –dynamic displacement. Equations please refer to relevant papers.	Wall soil inertial effect is considered. And taking into account various factors.
Sub-grade Modulus Methods	
Rowland Richards et. al. 's method [19]: α_{xw}= K_oz+$C_2 \frac{G_{fl}}{H}\sqrt{\frac{z}{H}}[\frac{2k_h\gamma(H^2-\sqrt{Hz^3})}{3G_{fl}}$-$\mu_w$ $_{max}$ (1-$\frac{z}{H}$)]	Applicable for rigid walls. The value of shear modulus is idealized. The failure criterion can be Mohr–Coulomb, with which the magnitude of pressure is on the conservative side of the MO method.

II. Experimental Findings

The shaking table test and its results are realistic ways of proposing current theories and verify newly proposed theory. The most advanced shaking table tests are the shaking table incorporated with the centrifuge and large-scale shaking table test. Currently, strain gauge, pressure transducers and accelerometers are measuring tools. The walls can be modeled into various conditions such as gravity wall, cantilever wall which are fixed, rigid, flexible etc. respectively.

It is feasible to compare the calculation results, both from previous and current studies, with the results from shaking table tests or the data from previous shaking table test. This review emphasizes experimental studies that have produced useful findings and data on dynamic retaining wall response, and experiments involved in developing or justifying the above-mentioned theories, the MO and Seed and Whiteman mainly, are mostly neglected.

Ortiz Scott and Lee [15] conducted shaking table tests on flexible wall in centrifuge. It is found that the MO method produces reasonable total resultant force [15]. However, the moment the MO method produced is different. In addition, they found that there are post–shaking residual values of all parameters, which are greater than the initial values [15].

Bolton and Steedman [11] carried out a similar centrifuge shaking table test with micro-concrete retaining walls rigidly bolted to the shaking platform. This experimental study justifies the accuracy of the MO method for maximum responses for sufficiently flexible walls. Moreover, it pointed out that the effect of the progressive build-up of permanent deformation over a number of cycles (no later study has been found on this phenomenon) [11].

Sherif et. al [22] experimentally investigated neutral and active static and dynamic stress and the points of resultant by granular soils against rigid retaining walls. They also critically evaluated the displacement needed to develop an active state for both static and dynamic cases and proposed that it increases with wall height and decreases with backfill soil strength [22]. It lays the foundation for further research on dynamic response for various displacements respectively.

Ishibashi and Fang [10] conducted a series of well known shaking table experiments and numerical analysis on a rigid wall with a dry cohesionless backfill. Their research focused on various displacement modes: rotation about the base, rotation about the top, translation and combined modes. The earth pressure distribution, total thrust, and points of application are produced. These results are widely used as reference results for relevant researches. Moreover, the results pointed out the strong dependence of lateral earth pressure on wall displacement modes and influencing factors for soil arching [10].

Fishman et al. [7] conducted laboratory and computational modeling studies on the seismic free field response of sand. They found the benefit of using a flexible end wall for relevant experimental set-ups [7]. Combined with numerical results, the wall pressure, displacement and shear stress were produced for both rigid and flexible walls. One featured finding is that the wall deforms in the same way as the free field (perfectly flexible wall), and the pressure, displacement, and shear stress on the wall are the same as those on the free field [7]. What's more, the methods used for obtaining both small strain and high-strain shear moduli shed lights on relevant experimental researches [7].

The centrifuge shaking table test is conducted by Atik and Sitar [2] to investigate the dynamic pressure and pressure distribution of seismically induced lateral earth pressures on the cantilever wall. In combination with nonlinear finite element analysis, the results firstly prove that triangular pressure distribution, which is assumed by most studies, is reasonable [2]. Another significant finding that the authors proposed is that dynamic earth pressure and inertia force do not act simultaneously and so is maximum earth pressure and maximum moment, which is assumed by the MO method and Seed and Whiteman's solutions [2]. Based on this, suitable suggestions are made to amend the design approach.

Table 2 provides a summary of reviewed shaking table experiments

.

Table. 2 Lists of Reviewed Experimental Findings on Wall Response

Experiment	*Model Wall*	*Type of Soil*	*Experimental output*
Ortiz [15] centrifuge shaking table test	two aluminum plates dip – brazed together (reinforced concrete cantilever)	fine sand with medium density, varied slopes of backfill	plots of moment, shear, pressure, and displacement over the height of the walls as a function of time
Bolton and Steedman's [11] centrifugal shaking table test	reverse t – section retaining wall made of micro-concrete	dry sand backfill with varying density	base moment due to tip load, wall crest deflection with acceleration
Shaking table test OF Sherif et al. [22] (large shaking table – retaining wall assembly)	rigid retaining wall, movable	granular soils	lateral pressure in active state and at rest, the location of force application
Ishibashi and Fang's [10] shaking table test (large shaking table – retaining wall assembly)	rigid movable retaining wall with configurations allow various displacement modes	dense air – dried Ottawa sand	pressure distribution, dynamic resultant force, incremental dynamic thrust, and points of application under various displacement modes
Atik and Sitar's [2] centrifugal shaking table test	cantilever retaining wall	fine, uniform, angular Nevada sand under medium-dense state	dynamic earth pressure and moment along depth and with time of shaking

III. Numerical Studies

Recently, engineering numerical techniques are developing very fast, which renders numerical methods as a crucial tool in engineering research, design, and analysis. Nowadays, numerical analysis usually accompanies experimental findings for geotechnical research. In this review, no holistic history of numerical studies is provided: instead, some significant recent studies using more advanced modeling techniques are selected. The numerical studies that have been used to assist analytical or experimental studies that have been mentioned above are neglected.

Veletsos and Younan [25] did numerical studies on the influence of wall and it's base flexibility on the response of retaining wall subjects to horizontal ground shaking. Both harmonic base motions and an actual earthquake record are investigated. The results show that a fixed based flexible wall triggers significantly higher wall pressure than walls of realistic base and wall flexibilities [25]. Besides, the dynamic amplification factor is also affected by those flexibilities [25].

Al-Homoud and Whitman [1] developed a two dimensional finite element model for THE seismic response of highway bridge abutment. FLEX is the verified code used in this case, and a viscous cap is the constitutive model [1]. Far–field ground motion is modeled by placing shear beams [1]. The results of this numerical study agree well with relevant experimental results and have shown that outward tilting is a dominant mode of response for this case. This also corresponds well with a real case [1].

Psarropoulos et al. [17] utilized the commercial finite–element package ABAQUS to test some analytical solutions (Veletsos and Younan's elasticity method mainly) and the range of applicabilities of these solutions [17]. The soil model is visco-elastic. The results also verify the MO method and the elasticity method for flexible walls [17]. It also investigated the effects of soil inhomogeneity, flexural wall rigidity and translational flexibility of the base of the wall.

Green et al. [8] conducted a series of non–linear finite difference analyses to investigate cantilever walls using FLAC as the code, and an elasto-plastic constitutive model combined with a failure criterion of Mohr-Coulomb is used to model the soil [8]. Emphasise is on calibrating and validating the soil–wall system model. This study justifies the MO method for low acceleration level, but showed

discrepancies when acceleration is high, which is due to flexibility of the wall [8]. Also, the study found a different critical load case between soil failure and structural design, which corresponds well to Atik and Sitar's [2] experimental findings mentioned above.

For reference of a detailed numerical review, Pathmanathan [16] produced a more detailed account of some of the numerical studies with useful comments.

A list of critical points of reviewed numerical studies is listed in Table 3.

Table 3: Lists of Configurations for Reviewed Numerical Studies Lists of Configurations for Reviewed Numerical Studies

Experiment	***Model Wall***	***Dynamic Excitation***	***Soil Model***	***Constitutive Modes***	***Soil Wall Interaction***	***Numerical Output***
Veletsos and Younan's [25] numerical study	flexible cantilever wall with various flexibilities, the base is elastically constrained against rotation	static excitation, harmonic base motion, actual earthquake record, respectively	linear, uniform, and visco-elastic stratum with semi-infinite boundary	n/a	complete bonding	displacement of the wall, wall pressure, shear, bending moments
Al-Homoud and Whitman's [1] two-dimensional finite element model using finite element code FLEX	rigid structure to model bridge abutment	different sinusoidal and earthquake acceleration input motions	dry sand by 2D element grid	viscous cap constitutive model	interface elements that interpret bonding, de-bonding, and sliding	wall pressure, wall tilt, dynamic resisting moment, etc.
two – dimensional finite element analysis of Psarropoulos et al. [17]	flexible wall elastically restrained at base, rigid gravity wall	effectively static / dynamic harmonic excitation	visco–elastic material, homogeneous and inhomogeneous respectively	n/a	complete bonding	dynamic earth pressure of varied wall structural and base flexibilities
non – linear explicit finite difference analyses using FLAC code of Green et al. [8]	concrete wall consists of five segments with constant parameters, and made by elastic beam elements	excitation generation techniques using other software	compacted soil with medium density and without cohesion	elastic-perfectly plastic , plus Mohr-Coulomb failure criterion	interface elements developed to overcome restrictions	wall pressure, permanent relative displacement, etc.

IV. Conclusion and Comments

Current theories, experimental findings and numerical studies for retaining walls subject to dynamic excitation have been briefly listed in a generally chronological order. Numerical analyses are an accurate way to solve relevant problems, while experiments are good but incur big cost to conduct an accurate one. In spite of these, the MO method is still a current main approach for practical use due to its simplicity. But the MO method becomes impractically complex when more factors like the influence of pseudo–dynamic, logarithmic failure plane etc is being considered, not to mention the widely known assumptions that are inherent with the MO method. It is found that the results from the elasticity method are from 2.5 to over 3 times higher than those from widely used the MO approaches [25]. Also, for the method of Rowland et al.'s [19], the obtained pressure is on the conservative side of the MO results [19]. However, although some people states that the MO method is not safe under seismic excitation (a typical example is active failure of bridge abutment under seismic excitation), it seems that there are more researches found from real earthquake records that show walls designed for a static case are already satisfactory [12], so efforts need to be made to make the retaining systems more economic. In this sense, considering the current sub-grade modulus method is even more conservative than limit equilibrium methods, the practical use of sub-grade modulus method can be accompanied with a reduction factor. On the other hand, the sub-grade modulus method tries to interpret real soil behavior and wall response, so the underlying theories and concepts being used are highly valuable for understanding the real physical behavior of dynamic retaining walls.

The assumption of a rigid wall is one reason for high pressure obtained from non–numerical analysis of sub-grade modulus theories. Besides, it is widely suggested that the MO method should be used for low excitation and flexible walls. Both experimental and numerical results have pointed out the strong dependence of earth pressures on wall flexibility, which is in essence a matter of displacement trigged stress variation [22] [25]. However, although soil displacement in a free–field has been studied by some researched mentioned above, there is a paucity of understanding about soil displacement behind the wall or in the near field for dynamic cases. As a result, dynamic soil displacement and stress–strain behavior would be an area of future interests.

Reference

[1] Al-Homoud, A. S. and R. V. Whitman (1999). "Seismic analysis and design of rigid bridge abutments considering rotation and sliding incorporating non-linear soil behavior." Soil Dynamics and Earthquake Engineering **18**(4): 247-277.

[2] Al Atik, L. and N. Sitar (2010). "Seismic Earth Pressures on Cantilever Retaining Structures." Journal of Geotechnical and Geoenvironmental Engineering **136**(10): 1324-1333.

[3] Anderson, D. G. (2008). Seismic analysis and design of retaining walls, buried structures, slopes, and embankments. Washington, D.C., National Cooperative Highway Research Program National Research Council Transportation Research Board, American Association of State Highway

[4] Anderson, D. G. N. C. H. R. P. N. R. C. T. R. B. A. A. o. S. H. and O. Transportation (2008). Seismic analysis and design of retaining walls, buried structures, slopes, and embankments. Washington, D.C., Transportation Research Board.

[5] Basha, B. and G. Babu (2010). "Seismic Rotational Displacements of Gravity Walls by Pseudodynamic Method with Curved Rupture Surface." International Journal of Geomechanics **10**(3): 93-105.

[6] Bolton, M. D. and W. Powrie (1988) Behaviour of diaphragm walls in clay prior to collapse. Géotechnique **38**, 167-189

[7] Choudhury, D. and S. Nimbalkar (2005) Seismic passive resistance by pseudo-dynamic method. Géotechnique **55**, 699-702

[8] Choudhury, D. and S. Nimbalkar (2007). "Seismic rotational displacement of gravity walls by pseudo-dynamic method: Passive case." Soil Dynamics and Earthquake Engineering **27**(3): 242-249.

[9] Diakoumi, M. and W. Powrie (2013) Mobilisable strength design for flexible embedded retaining walls. Géotechnique **63**, 95-106

[10] Fishman, K. L., et al. (1995). "Laboratory study of seismic free-field response of sand." Soil Dynamics and Earthquake Engineering **14**(1): 33-43.

[11] Green, R. A., et al. (2008). "Response and Modeling of Cantilever Retaining Walls Subjected to Seismic Motions." Comp.-Aided Civil and Infrastruct. Engineering **23**(4): 309-322.

[12] Huang, C. (1996). Plastic analysis for seismic stress and deformation fields. Department of Civil Engineering, SUNY at Buffalo.

[13] Ishibashi, I. and Y.-S. Fang (1987). "Dynamic Earth Pressures With Different Wall Movement Modes." SOILS AND FOUNDATIONS **27**(4): 11-22.

[14] M.D.Bolton and R. S. Steedman (1982). Centrifugal Testing of Microconcrete Retaining Walls Subjected to Base Shaking. Soil Dynamics and Earthquake Engineering Conference.

[15] Mikola, R. G. and N. Sitar (2013). Seismic Earth Pressures on Retaining Structures in Cohesionless Soils, California Department of Transportation.

[16] Mononobe, N. and M. Matsuo (1929). On The Determination of Earth Pressures During Earthquakes. Proc., Proc. World Engrg. Congress.

[17] Nadim, F. and R. Whitman (1983). "Seismically Induced Movement of Retaining Walls." Journal of Geotechnical Engineering **109**(7): 915-931.

[18] Ortiz, L. A., et al. (1983). "Dynamic centrifuge testing of a cantilever retaining wall." Earthquake Engineering & Structural Dynamics **11**(2): 251-268.

[19] Osman, A. S. and M. D. Bolton (2004). "A new design method for retaining walls in clay." Canadian Geotechnical Journal **41**(3): 451-466.

[20] Pathmanathan, R. (2006). Numerical Modelling of Seismic Behaviour of Earth - Retaining Walls. European School for Advanced Studies in Reduction of Seismic Risk. **Master of Earthquake Engineering**.

[21] Psarropoulos, P. N., et al. (2005). "Seismic earth pressures on rigid and flexible retaining walls." Soil Dynamics and Earthquake Engineering **25**(7-10): 795-809.

[22] Rowland Richards, J. and D. G. Elms (1979). "Seismic Behavior of Gravity Retaining Walls." Journal of the Geotechnical Engineering Division **105**(4): 449-464.

[23] Rowland Richards, J., et al. (1999). "Seismic earth Pressure on Retaining Structures." Journal of Geotechnical and Geoenvironmental Engineering **125**(9).

[24] Scott, R. F. (1973). Earthquake-induced pressures on retaining walls. 5th World Conf. on Earthquake Engrg., Tokyo, Int. Assn. of Earthquake Engrg.

[25] Seed, H. B. and R. V. Whitman (1970). Design of Earth Retaining Structures for Dynamic Loads, University of California.

[26] Sherif, M. A., et al. (1982). "Earth Pressures against Rigid Retaining Walls." Journal of the Geotechnical Engineering Division **108**(5): 679-695.

[27] Steedman, R. S. and X. Zeng (1990) The influence of phase on the calculation of pseudo-static earth pressure on a retaining wall. Géotechnique **40**, 103-112

[28] Su Yang, et al. (2013). "Review of Studies on Retaining Wall's Behavior on Dynamic / Seismic Condition." International Journal of Engineering Research and Applications **3**(6): 01-05.

[29] Veletsos, A. and A. Younan (1997). "Dynamic Response of Cantilever Retaining Walls." Journal of Geotechnical and Geoenvironmental Engineering **123**(2): 161-172.

[30] Wong, C. P. (1982). Seismic Analysis and Improved Seismic Design Procedure for Gravity Retaining Walls. Department of Civil Enigneering. Cambridge, Mass., Massachusetts Institute of Technology. **Master of Science**.

[31] Wood, J. H. (1973). Earthquake-induced Soil Pressures on Structures: Thesis. California Institute of Technology. Earthquake Engineering Research Laboratory, California Institute of Technology.

[32] Wood, J. H. (1975). "Earthquake induced pressures on a rigid wall structure." Bull. of New Zealand Nat. Soc. for Earthquake Engrg. **8**(3): 175-186.

[33] Wood, J. H. and C. I. o. T. E. E. R. Laboratory (1973). Earthquake-induced Soil Pressures on Structures: Thesis, California Institute of Technology.

[34] Zarrabi, K. (1979). Sliding of Gravity Retaining Wall During Earthquakes Considering Vetical Acceleration and Changing Inclination of Failure Surface. Department of Civil Engineering, Massachusetts InstiInstitute of Technology. **Master of Science**.

[35] Zeng, X. and R. Steedman (2000). "Rotating Block Method for Seismic Displacement of Gravity Walls." Journal of Geotechnical and Geoenvironmental Engineering **126**(8): 709-717.

[36] Zhang, J., et al. (1998). "EVALUATION OF EARTH PRESSURE UNDER ANY LATERAL DEFORMATION." SOILS AND FOUNDATIONS **38**(1): 15-33.

[37] Zhang, J., et al. (1998). "SEISMIC EARTH PRESSURE THEORY FOR RETAINING WALLS UNDER ANY LATERAL DISPLACEMENT." SOILS AND FOUNDATIONS **38**(2): 143-163.

Appendix B: Paper for publication "Modelling Evaluation of Seismic Retaining Wall Theories Based on the Displacement-Stress Relationship and Free Field Response"

Modelling Evaluation of Seismic Retaining Wall Theories Based on the Displacement-Stress Relationship and Free Field Response

Corresponding First Author: Su Yang*[1]

Co-authors: Amin Chegenizadeh[2], Hamid Nikraz[3]

[1]*Master Candidate, Department of Civil Engineering, Curtin University, Perth, Australia;yang.su2@postgrad.curtin.edu.au*

[2] *Research Fellow, Department of Civil Engineering, Curtin University, Perth, Australia;*

[3]*Professor, Department of Civil Engineering, Curtin University, Perth, Australia*

Contact Email: yang.su2@postgrad.curtin.edu.au

Abstract

Nowadays the effect of seismic forces on any structure is of interest and stress–displacement behaviour is considered to be a crucial factor in the interpretation of the real response between soil and structure. This paper considers different approaches to addressing seismic effects on retaining walls and relevant stress – displacement relationships. A strutted retaining wall was modelled by using finite elements software. In the first step, PLAXIS was used to model the case and in the second step ABAQUS was used to model the same retaining system. Finally, the results from both PLAXIS and ABAQUS were verified against significant existing analytical theories based on the stress-displacement relationship: strain increment ratio lateral earth pressure theory for seismic cases, subgrade modulus theory and free field theory. The results showed, despite some variance in local response, acceptable agreement between PLAXIS results and theoretical results for both lateral earth pressure and free field displacement. And ABAQUS produced somewhat greater lateral earth pressure and also similar free field responses to PLAXIS and theory. Utilizing modelling results, new methods were established to obtain critical wall displacement, elastic and plastic subgrade modulus and other essential theoretical parameters. The performance of numerical softwares under certain conditions was evaluated. Else, it is found that local response of the wall is controlled by the combined displacement between wall and free field ("spring displacement"). This proved the significance of using spring

displacement to establish future stress displacement relationship for seismic response of retaining systems.

1. Introduction

Retaining walls are important structures due to the complexity of behaviour of the geotechnical and structural components. There are already many studies which have considered the seismic effect on retaining walls ([1], [2], [4], [5], [6], [7], [8], [9], [10], [11], and [13]).

However, it is widely accepted current analytical approaches in seismic retaining wall response have limitations. For example, traditional failure wedge equilibrium method (such as in [6] and [8]) is believed to be inaccurate at predicting local pressure especially when the wall has relatively high rigidity. The elastic methods (such as [11]) are found to produce highly conservative results and numerical tools are essential for their use. There are several other limitations for these methods, so it is meaningful to work out a comprehensive solution that considers real wall soil behaviour under various conditions. To realize this, for seismic cases, it is essential to understand the stress strain behaviour or stress displacement behaviour of the soil right behind the wall and the free field displacement.

Considering these, relevant displacement – stress dependent retaining wall theories such as strain increment ratio lateral earth pressure theory for seismic case [12] [13] and subgrade modulus theory using free field [7] have stood out as they are based on stress displacement relationships and capable of predicting wall and soil responses at all states between passive and active states. However, those methods have yet to be critically evaluated for their accuracy on interpreting right stress strain relationship using popular modelling softwares such as PLAXIS and ABAQUS; and reversely, modelling softwares and built models are yet to be critically evaluated for their stress displacement relationship and free field response. Else, the difficulties still exist in terms of obtaining more accurate relevant parameters for the use of the above mentioned theories. Lastly, there is a lack of information regarding stress-displacement relationship of the wall incorporating free field displacement.

As a result, modelling soft wares PLAXIS and ABAQUS are used under different conditions in present study to investigate the stress strain relationship and free field

relevant theories, while the software's performance for different modes and acceleration level could also be mutually evaluated. This study intends to provide useful data base and findings for future research in seismic soil and wall behaviour or the amendment of software modelling. The ultimate goal of this study is to lay a foundation for interpretative and comprehensive seismic solutions for seismic response of retaining walls under various conditions. Ideally it will be a relatively simple and comprehensive approach that is built on the true soil and wall behaviour.

2. Theories

There are two stress–strain or displacement–stress theories studied in this paper including strain increment ratio lateral earth pressure theory [12] [13] and free-field subgrade modulus method [7]. Analytical solutions provided by these two theories are introduced below:

2.1. Strain increment ratio lateral earth pressure theory

Zhang et al. [12] [13] conducted a series of triaxial tests on normally consolidated dry sand and have concluded that there was a relationship between strain increment ratio and stresses, based on which an equation was derived for the coefficient of lateral earth pressure based on a lateral strain parameter R:

$$K=\begin{cases}(1-sin\phi')/(1-sin\phi' R) & (\text{for } -1.0 \le R \le 1.0)\\ 1+sin\phi'(R-1)/(1-sin\phi') & (\text{for } 1.0 \le R \le 3.0)\end{cases} \quad (1)\ [12]$$

in which ϕ' is friction angle and parameter R is determined by lateral displacement of the wall and critical state displacement, plus other two exponential parameters β_a and β_p:

$$R=\begin{cases}-(|\Delta|/\Delta_a)^{\beta_a} & (-\Delta_a \le \Delta \le 0)\\ -1 & (\Delta < -\Delta_a)\end{cases} \quad (2)\ [12]$$

$$R=\begin{cases}3(\Delta/\Delta_p)^{\beta_p} & (0 \le \Delta \le \Delta_p)\\ 3 & (\Delta > \Delta_p)\end{cases} \quad (3)\ [12]$$

Originally introduced by Zhang et al. [12], Δ_a, Δ_p, β_a and β_p could be obtained from empirical estimation and schematic methods, the details of which are listed in relevant papers. These are very rough estimations and can be back-analysed using modelling results for better accuracy.

This equation was originally built for static cases, and, Zhang et al. [13] transferred this theory for seismic retaining wall behaviour using the concept of 'intermediate wedge' theory, which could also be viewed as a combination of strain increment ratio theory and Mononoke Okabe's classical seismic retaining wall solution [6]. This new strain increment ratio dependent method is able to evaluate lateral earth pressure in any state between active and passive states under seismic conditions for various displacement modes. The equations are in a similar form to the MO method but incorporate the strain ratio parameter R as shown below:

$$K=\frac{2COS^2(\phi\prime-\mathrm{i})}{COS^2(\phi\prime-\mathrm{i})(1+R)+\mathrm{COS(i)}*COS(\delta_{mob}+i)(1-R)\left[1+\sqrt{\frac{SIN(\phi\prime+\delta_{mob})SIN(\phi\prime-\mathrm{i})}{COS(\delta_{mob}+\mathrm{i})}}\right]^2},$$

(for -1.0≤R≤1.0)(4) [13]

$$K = 1+\frac{1}{2}(R-1)\left[\frac{cos^2(\phi\prime-i)}{COS(i)*COS(\delta_{mob}+i)\left[1-\sqrt{\frac{SIN(\phi\prime+\delta_{mob})SIN(\phi\prime-i)}{COS(\delta_{mob}+i)}}\right]^2}-1\right],$$

(for 1.0≤R≤3.0) (5) [13]

in which δ_{mob} is the friction angle between soil and wall, i is angle of seismic coefficient. This equation only applies to a vertical wall–soil surface and a horizontal soil surface without surcharge.

Then, neglecting vertical wall acceleration, soil vibro-densification and surcharge, the lateral earth pressure along the wall could be expressed as :

$$Pz = \gamma z\ \mathrm{COS}(i)\ K+\gamma(H-z)(1-\mathrm{COS}i\ )K$$

(6) [13]

2.2.Free-field subgrade modulus method

Free field is a useful concept in earthquake engieering, as it represents the displacement of the soil field without the influence of obstructions such as end walls. In retaining wall systems, a free field appears at a location that is 2.0H from the end wall [3]. Based on free field displacement theories and subgrade modulus method, a simple method has been established by Rowland Richards et al. [7] to evaluate the lateral earth pressure on a wall. This method can be used to obtain the wall pressure in

any states if the displacement is known, since the soil between the wall and free field is modeled as springs with constant, which has elastic and plastic values respectively.

In seismic analysis in geotechnical engineering, free field response represents the soil field where no influence is incurred from the wall. This normally means the response of the soil domain which is around 2.0H from the end wall (Fishman, Mander et al. 1995). Rowland et al. [7] worked out pseudo-static solutions for the calculation of free field displacement based on a shear modulus that varies with depth. In this PLAXIS model, a constant G (shear modulus) is provided throughout the soil cluster as shown in Table 1. Using a constant shear modulus G through the whole soil body, the free field displacement from Rowland et al. [7] is modified as:

$$u_f = k_h r(z^2 - H^2)/(2G) \quad \text{(elastic response)(7)}$$

$$u_f = k_h r(z^2 - H^2)/(2Gsp) \quad \text{(plastic response)(8)}$$

in which u_f is free field displacement, H is the depth of the soil strata, $k_h$is coefficient of horizontal acceleration and $G_{sp}$is secant plastic shear modulus. It should be noticed that these equations (7) and (8) are based on zero ground displacement and u_f is zero when z = H.

For the calculation of earth pressure, a subgrade modulus similar to spring's constant should be identified for the retained soil:

$$\mathbf{K_s} = \mathbf{C_2} G/H \quad (9)\ [7]$$

In which C2 is suggested as 1.35 by Rowland Richards et al. [7]. Normally, for constant shear modulus, G could be changed to G_{sp} for seismic cases.

With equations (7) (8) and (9), the lateral earth pressure could be calculated based on principles similar to Hook's law:

$$\sigma_w = \sigma_{xo} + Ks \times \Delta u = \sigma_{xo} + C_2 G/H \times \Delta u$$

(10) [7]

in which $\sigma_{xo}$is the horizontal earth pressure at rest, Δu the change of distance between wall and free field.

3. Computational modelling

3.1.PLAXIS 2D simulation

A diaphragm retaining wall with two struts was built using commercial geotechnical engineering modelling software PLAXIS.

3.1.1. Wall configurations

An 11 m high wall with 2 m buried and 9 m facing excavation was modelled using plate element without damping (see Table 1). Fixed end anchors were used to model the strut with an EA of 2e6 kN at a spacing of 5 m and equivalent length of 15 m. The struts were located at 1 m and 5 m below the top of the wall respectively.

Table 3: concrete wall properties

Density (kg/m3)	***Elasticity (Pa)***	***Poisson ratio v***	***Strut siffness (kN)***	***Strut Length(m)***	***Strut spacing (m)***	***Interface Rint***
378.774	5366726000	0.15	2e6	15	5	0.67

3.1.2. Soil Model

The soil body was modelled with the following parameters shown in Table 2. The soil body was 60 m long and 13 m high.

Table 4**:** The properties of soil

Soil type	***Material model***	***Effective angle of friction ϕ' (o)***	***γsat (kN/m^3)***	***γunsat (kN/m^3)***	***Cohesion c_{ref} (kPa)***	***Poisson ratio v***	***Initial void ratio e_0***	***Elasticity (kPa)***
Sand	Mohr-Coulomb	30	20	17	0	0.3	0.5	175000

3.1.3. Boundary conditions and interaction

Standard fixity provided by PLAXIS is applied to the model plus absorbent boundaries to eliminate “box effect” of dynamic waves. A dynamic prescribed

displacement was applied to the bottom line for seismic input. The finished model is shown in Figure 1. Interface element was used along contact areas of wall and soil. $\boldsymbol{R_{inter}}$ = 0.67 is set as soil wall friction parameter.

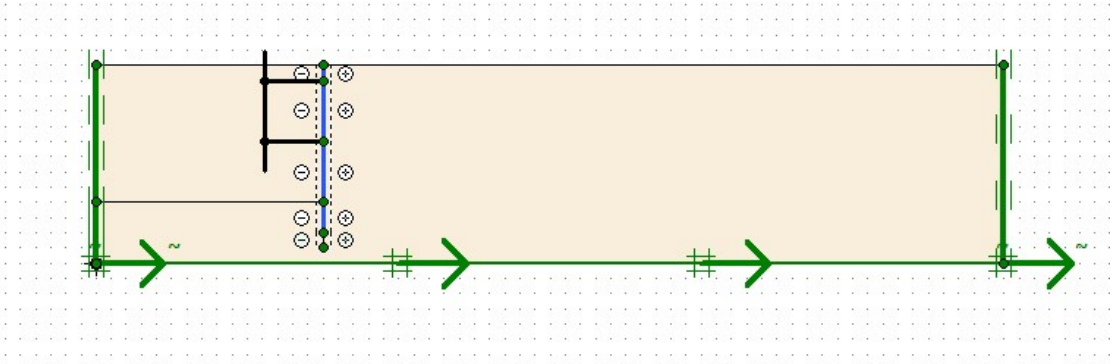

Figure 22: PLAXIS 2D model of strutted diaphragm wall and soil body

3.1.4. Earthquake Excitations

The SMC file recording the ground acceleration of the Offshore Maule Earthquake was applied to the bottom boundary. The accelerograph of this earthquake is shown in Figure 2. The dynamic duration was set at 60 seconds to capture most significant shocks and save computation time.

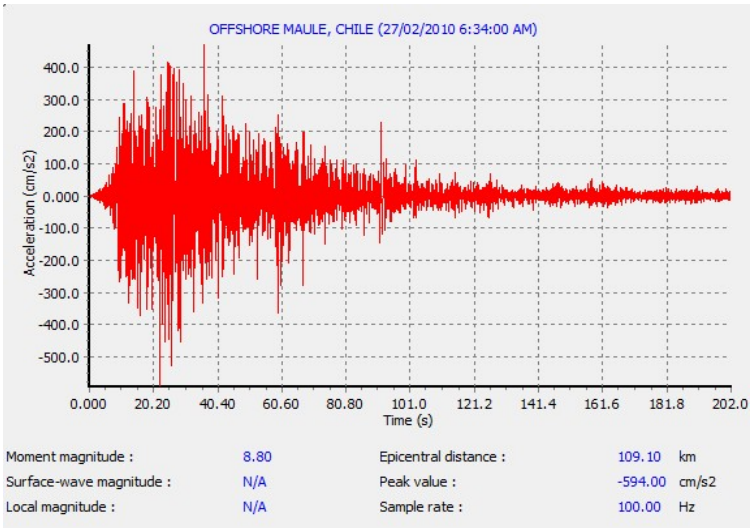

Figure 23: Acceleration versus dynamic time diagram for the Offshore Maule earthquake (courtesy of the U.S. Geological Survey)

3.2. ABAQUS Simulation

Both ABAQUS explicit and ABAQUS implicit simulations were conducted for this study and both methods were also evaluated in terms of competency for relevant research.

3.2.1. Wall and soil model

The wall geometry and engineering parameters (see Table 1) were the same as for the PLAXIS model. However, a 2D shell was used to get around too complex contact areas for the bottom part of the wall soil contact areas. This wall had a width identical to the depth of the plate element used for the PLAXIS wall model. The struts had the same location as for the PLAXIS model, but rather than anchor elements in PLAXIS, connector elements with equivalent EA of 2e6 kPa were used for the ABAQUS model.

An identical soil block was adopted for the ABAQUS model with a soil body of 13 m in height and 60 m in length. The same material properties were adopted as shown in Table 2. To keep the results comparable, the same failure criterion of Mohr-Coulomb was adopted as the plastic response, while soil damping was neglected. Small dilation angle and cohesion values were input to pass the program's numerical requirement with negligible effects on the response of the wall.

Both the wall and soil body were meshed using explicit plain strain linear quadrilateral elements. The wall – soil intersection area was disseminated with finer mesh with coarser mesh used for the far field.

3.2.2. Boundary conditions, interactions and seismic excitations

The bottom of the soil body was constrained from vertical displacement and kept symmetry about Y = constant plane (U2 = UR1 = UR3 = 0). In the seismic stage, harmonic horizontal acceleration was applied to the bottom line to simulate earthquake excitations, and the wall was constrained from horizontal displacement until the soil body was fully settled under the initiation of gravity load. Two connector elements were used to model the struts at the same stiffness parameters and wall location as the fixed end anchors in the PLAXIS model. In the explicit model, connector elements were used for both sides of the soil body to model seismic boundary conditions; while in the Implicit model, springs/dashpot with relevant stiffness and damping parameters were adopted to model seismic conditions and eliminate box effects.

The response between the wall and soil was modelled by a kinematic contact for the seismic stage. A friction coefficient of 0.39 was given (obtained from δ_{mob}=21.2° used in PLAXIS model).

Both representative (2.5m/s2) and peak (5m/s2) acceleration levels were used as seismic input for ABAQUS. They followed a sinusoidal acceleration versus time distribution. The period was 1 second and frequency is 4 circles/second. The acceleration time graph is shown in Figure 4.

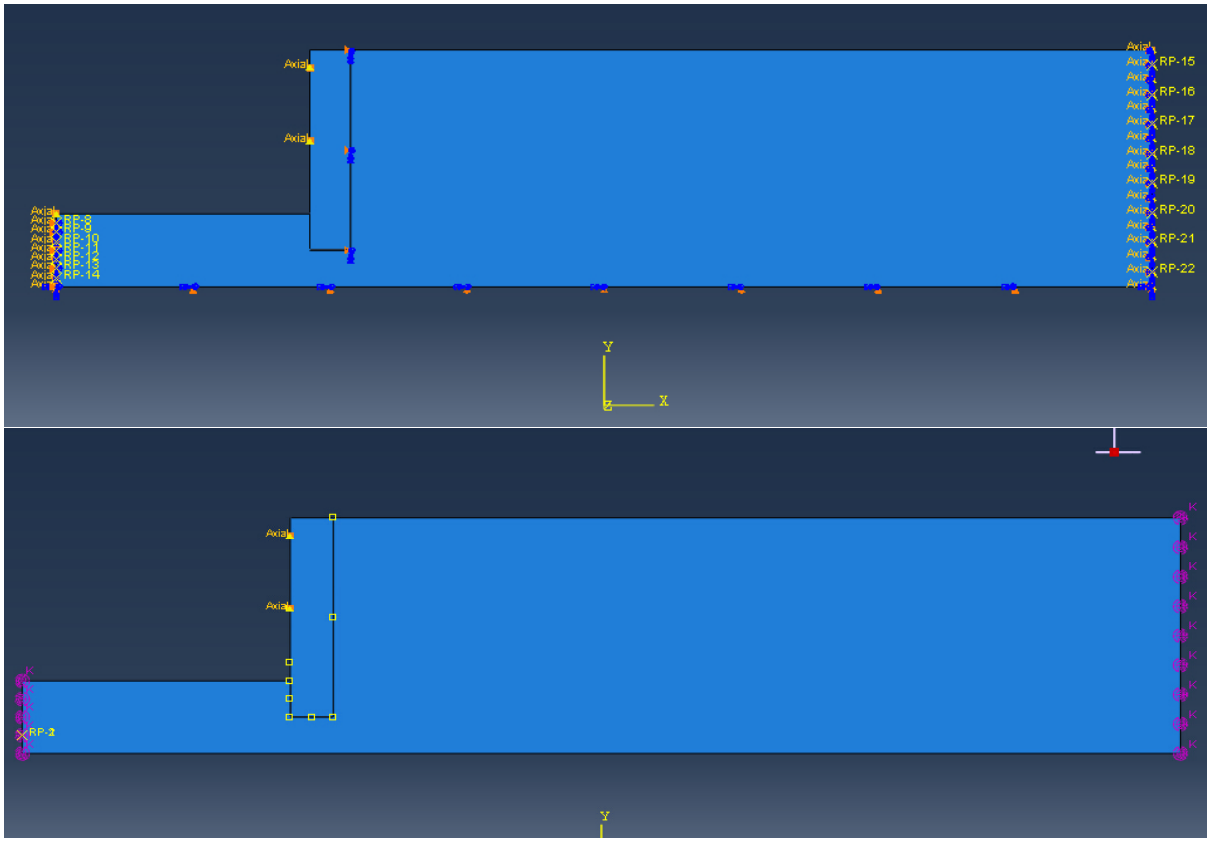

Figure 24: Model view of assembled instances under explicit Analysis (upper) and implicit analysis (lower)

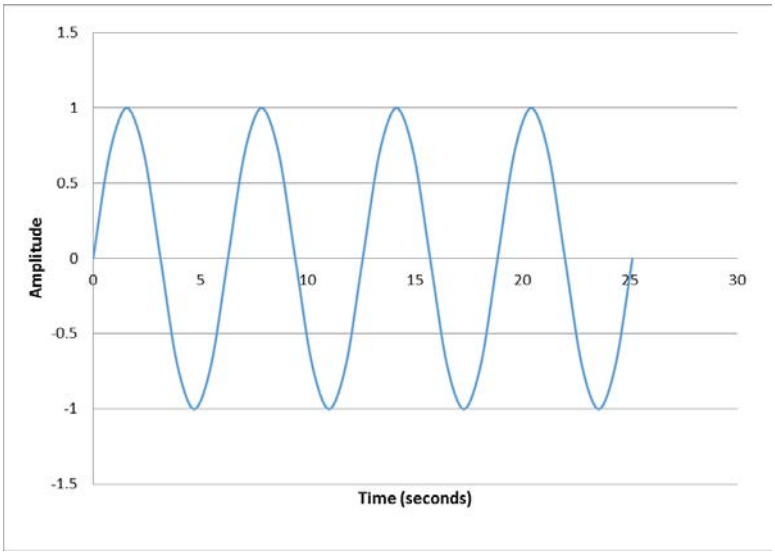

Figure 25: Harmonic ground acceleration amplitude curve (before multiplying acceleration level)

4. Results

PLAXIS lateral wall pressure is shown in Figure 6 together with strain increment ratio method using the parameters in Table 3 and methods described in section 5.1. The wall displacement curves and free field displacement curves for both PLAXIS and ABAQUS are illustrated in Figure 8 and Figure 9 respectively.

ABAQUS results for implicit and explicit, peak and representative acceleration are shown in Figure 7, with PLAXIS and analytical results using set 4 added for comparison.

4.1. Determination of i, Δ, Δ_a,$\Delta_p\beta_a$and $\beta_p$using PLAXIS

With the PLAXIS results for wall displacement and lateral pressure, all of the parameters could be estimated using PLAXIS output or by the original method presented by Rowland Richards et al. [7] and Zhang et al. [12].

Δ could be directly read from the PLAXIS results by showing the horizontal displacement of the wall or interface. PLAXIS also denotes the failure status of each soil element. So from the data of the nodes displacement along the wall, we could read a point of lowest displacement where the soil element starts to fail according to Mohr-Coulomb criteria, which point corresponds to Δ_a . Similarly, a passively displacing wall could be modelled and from that we could obtain Δ_p. However, the

active and passive model we use to acquire Δ_a and $\Delta_p$should use the same soil and wall material with identical wall height. The obtained Δ_a and $\Delta_p$are 19 and 117 mm, which agree well with previous research and empirical results shown in [12].

There are two ways available for the determination of $\beta_a$and $\beta_p$used in equations (2) and (3). Firstly, although being a highly rough estimation, the original pragmatic method is used as provided in Zhang et al. [12]. The roughly estimated $\beta_a$and β_p are 0.4 and 0.51 respectively. Secondly, curve fitting could be carried out to adjust $\beta_a$and β_p values until the generated curve of the analytical solution closely match the PLAXIS results for static cases. The relevant $\beta_a$and β_p could then be used for seismic cases since the expression for R, as shown in equations (2) and (3), is still the same. The $\beta_a$is obtained by curve fitting as 1.1, while $\beta_p$is neglected since equation (3) has very little usage in this case scenario due to that only a small wall section has passive displacement. However, in other cases with more passive displacement, $\beta_p$could be obtained by the same methods.

There are two values of i available according to the accelerograph of the Offshore Maule Earthquake, one of which is calculated from representative acceleration of 2m/s2 as 0.2 and another is from peak acceleration of 5m/s2 as 0.47 based on the accelerograph shown in Figure 2.

Due to the different values used for the parameters there are four sets of input parameters for the analytical solution of lateral earth pressure as shown in Table 3.

Table 5: Parameters used for each set of analytical calculations using the strain increment ratio method [12] [13]

	Set 1	**Set 2**	**Set 3**	**Set 4**
Angle of seismic coefficient i (radian)	0.20 (representative)	0.20 (representative)	0.47 (peak)	0.47 (peak)
$\boldsymbol{\beta_a}$***and*** $\boldsymbol{\beta_p}$	β_a= 0.4 β_p=0.51 (Chart Method)	β_a= 1.1β_p=n/a (curve fitting)	β_a= 0.4 β_p=0.51 (Chart Method)	β_a= 1.1β_p=n/a (curve fitting)

4.2.Determination of the subgrade modulus Ks (spring stiffness)

Since the displacement and distance between wall and free field could be read from the software's output, back analysis of both ABAQUS and PLAXIS results could be used to obtain the subgrade modulus of the soil used mainly for displacement-stress relationships as described in equation (10). The obtained value for plastic Ks is of particular value. Using this method, the Ks values for each depth would vary, but there would still be relatively average value for elastic or plastic responses. One of this back analysis examples was done as shown in Figure 5, the theoretical value based on equation (9) could be calculated as519 kN/m (using H = 13m), which agrees surprisingly well with the estimation made from back analysis shown in right bottom circled area in Figure 5.

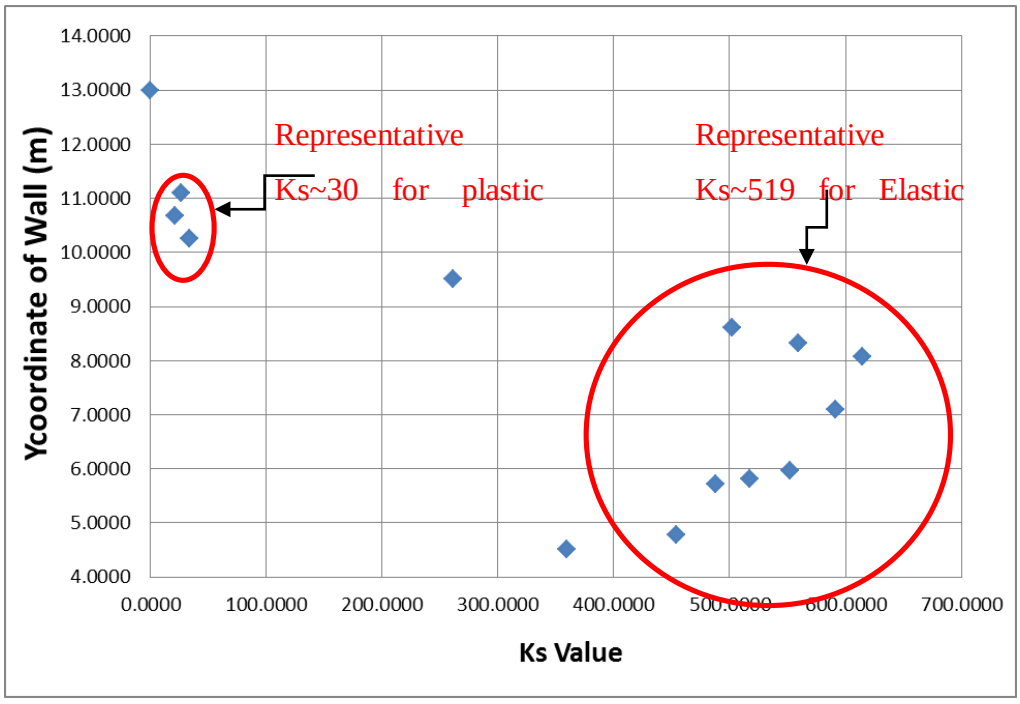

Figure 26: Back analysed Ks values along the wall based on PLAXIS results

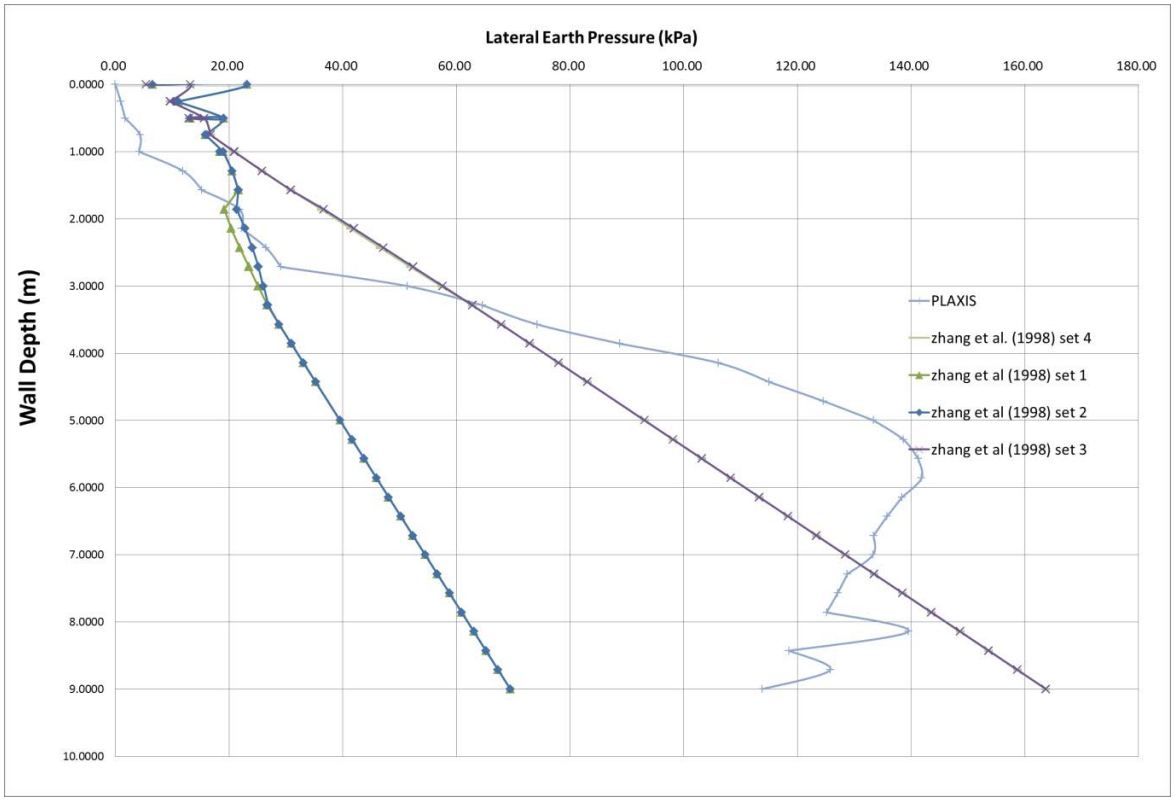

Figure 27: PLAXIS lateral earth pressure along the wall compared to Zhang et al [13]'s strain increment ratio method using data sets listed in Table 3

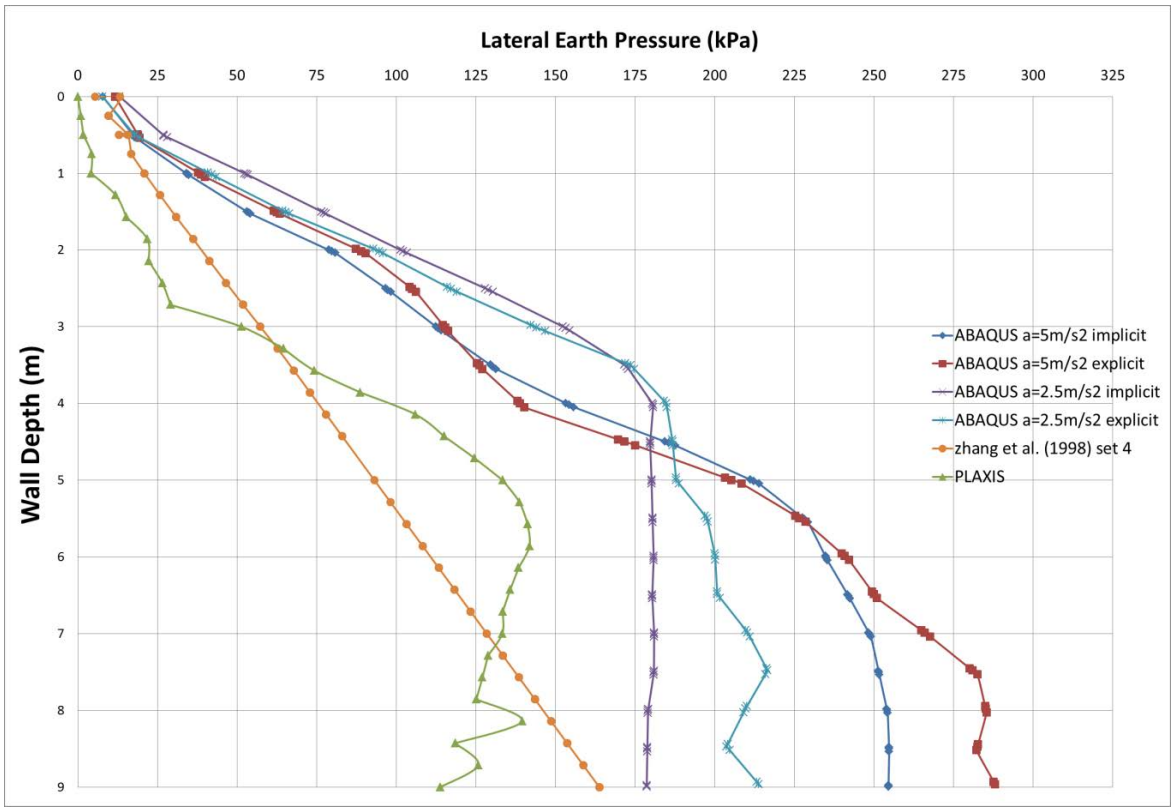

Figure 28: ABAQUS lateral earth pressure

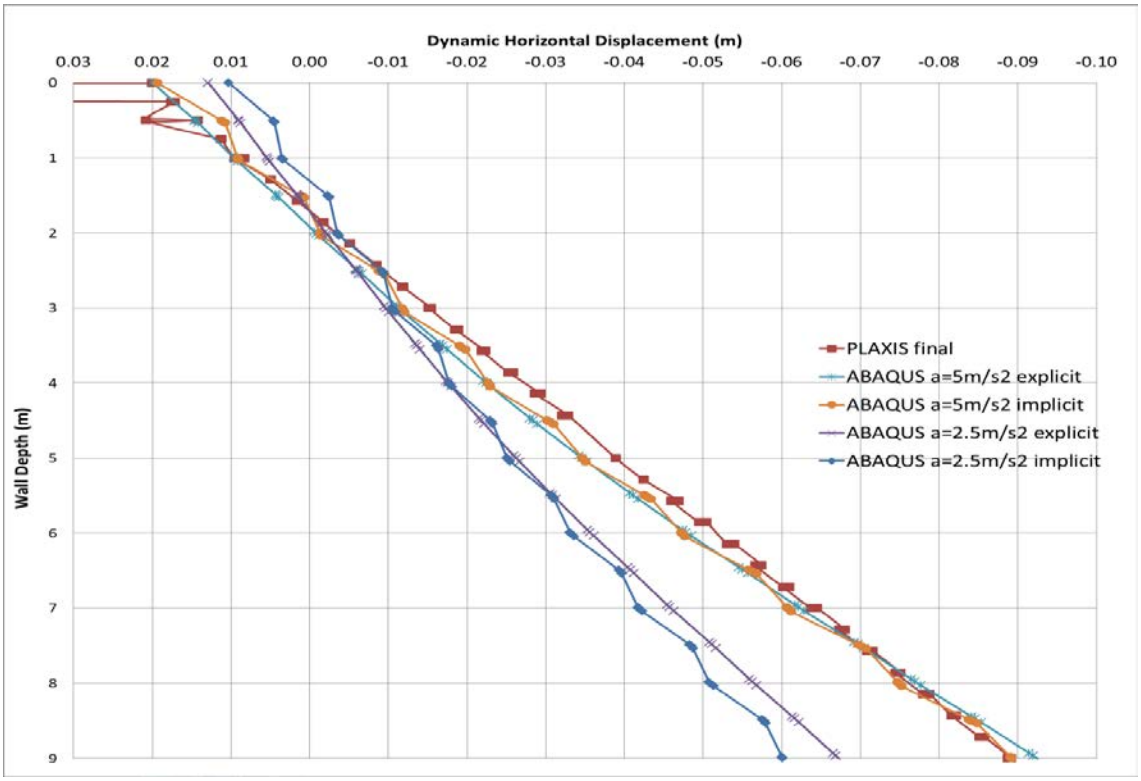

Figure 29: Wall horizontal displacement curve from ABAQUS and PLAXIS

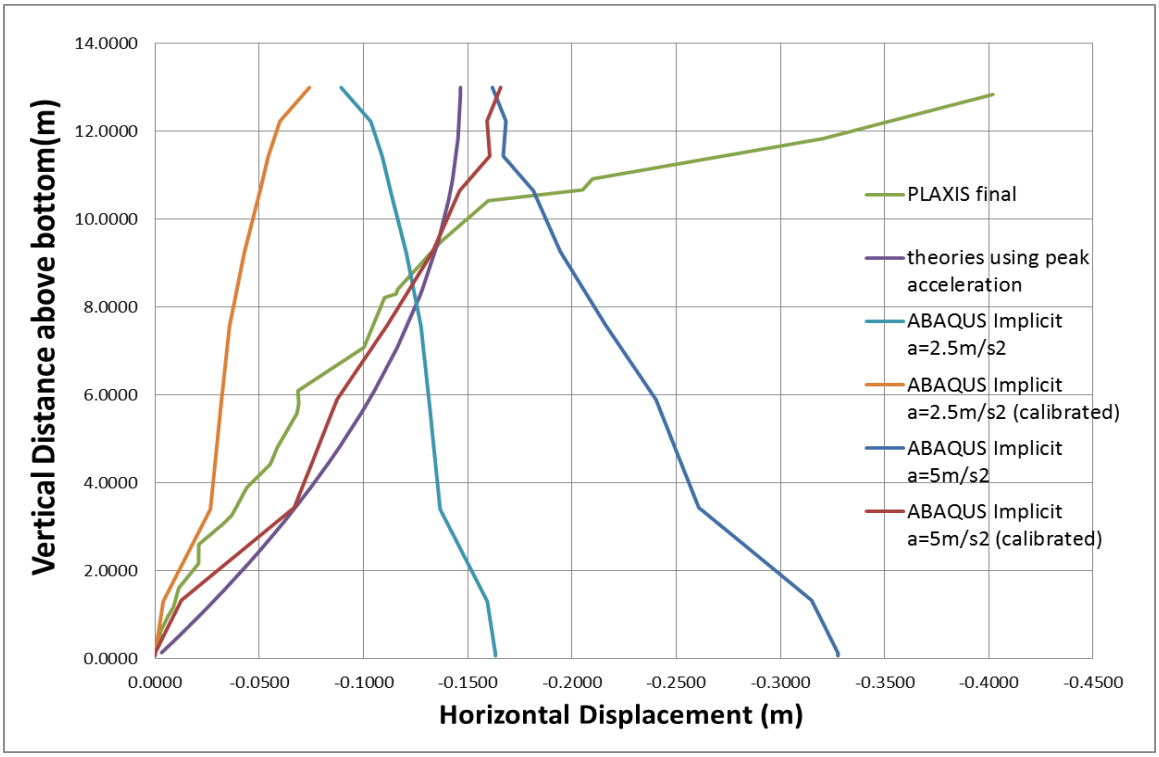

Figure 30: Freefield displacement curves from PLAXIS, ABAQUS implicit and theories

5. Discussion

5.1. Lateral earth pressure

From Figure 6, β_a and β_p produce little difference in terms of lateral earth pressure by curve fitting and pragmatic method, since the curves from different method for these two values almost cover each other. However, as expected, the acceleration level did change the lateral earth pressure significantly, with a representative acceleration level i of 0.2 producing much lower lateral earth pressure compared to that produced by a peak acceleration i of 0.51. PLAXIS produced a pressure distribution that was not linear and even decreases with depth for the lower part the wall (below 6 m depth), although the displacement from PLAXIS increased approximately linearly with the depth of the wall as shown in Figure 8. Once displacement reaches a critical state level or goes beyond it, R will become -1 and equation (4) will change into the MO method. Since the MO method is widely believed to be inaccurate at predicting local pressures, and the lower part of the wall and the soil behind the wall is at failure state due to local displacement and phase effects, the variance between the theoretical curve and the PLAXIS curve is a reflection of this. However, the strain increment ratio method with peak acceleration level produced a lateral earth pressure profile that generally agrees well with the PLAXIS' results. The local pressure between the active and passive states are probably controlled by the distance between wall and freefield, and this will be discussed further in section 5.4. The analytical method has a non zero top earth pressure due to inertia effect when using equation [6].

As shown in Figure 5, both ABAQUS explicit and implicit produced larger lateral earth pressure than PLAXIS and so the theoretical results. According to Figure 7, ABAQUS has similar wall displacement when 5m/s2 peak acceleration is applied, which means if the strain increment ratio method was applied based on ABAQUS' wall displacement, the obtained wall pressure would be similar to that from PLAXIS and lower than software's output. Although this needs to be confirmed by investigating relavant Δ_a , Δ_p, β_a and β_p from ABAQUS, they should keep almost unvaried due to the same soil parameters and wall geometry, which are believed to control the values of these parameters. Under 5m/s2 acceleration, the lateral earth pressure is larger than that from 2.5m/s2, which is around 10 to 100 kpa larger than

the PLAXIS and theoretical results. One possible explanation for this will be discussed further in section 5.4. In general, implicit or explicit does not exert large difference in wall pressure. Implicit analysis using spring/dashpot does reduce the pressure for the lower part, which the increase of pressure against depth slows or stops, compared to explicit analysis using connector element without dashpot. However, for the upper part that shows approximately linear increase of pressure against depth, implicit analysis has nearly equal or slightly lower results compared to explicit analysis.

5.2. Horizontal wall displacement

The horizontal wall displacement (or soil right behind) is drawn in Figure 7 for PLAXIS and ABAQUS implicit and explicit with peak and representative acceleration level. It can be seen that there is no great difference between implicit and explicit wall displacement, and 2.5m/s2 lead to a slightly lower wall displacement compared to the PLAXIS results, very close to the resulting displacement from the 5.0m/s2 acceleration amplitude. This indicates that the ABAQUS model is able to produce similar wall displacement results to PLAXIS, when using the peak acceleration amplitude from the SMC file for its acceleration amplitude (in sinusoidal curve), while a representative acceleration level produces lower displacements.

5.3. Free field displacement

Free field horizontal displacements are produced by reading horizontal displacement values from a line crossing the soil body that is 1.5H-2H (H is the wall height) away from the wall in both ABAQUS and PLAXIS output. Together with theoretical results for constant G and neglecting plastic displacement, the free field displacement curves are shown in Figure 8.

ABAQUS has to use a bottom that is free in a horizontal direction for horizontal earthquake acceleration to be applied, while in PLAXIS, the bottom can be fixed. Also because the displacement values are produced from fixed coordinate systems for both types of software, the generated displacement values from the two programs are not directly comparable. The solution is to calibrate the ABAQUS displacement by subtracting the value with ground displacement. These calibrated curves are further adjusted for directions, since free field response in two directions are symmetric, and are shown in Figure 8.

When peak acceleration values are used in ABAQUS (calibrated), ABAQUS, theoretical (constant G, no plastic) and PLAXIS results on free field displacements agree well with each other for most of the depth, although PLAXIS produces a very large displacement at the top part due to the plastic response there. Representative acceleration levels seem to produce lower free field displacement based on ABAQUS results (calibrated).

5.4. Combined displacement between wall and free field

Since in the ABAQUS model, two struts were simulated as springs connected to a virtual ground which was fixed, this means that the distance between wall and free field should be calculated using original free field displacement. Thus, the output pressure will be larger than that from PLAXIS, which used a horizontally fixed ground. In other words, there is an extra ground movement which changes the distance between wall and free field in ABAQUS, and this was probably the reason for a larger lateral earth pressure from the ABAQUS results as shown in Figure 6. The PLAXIS fixed field anchors should be a better simulation since, in real life, the struts are usually fixed to another structure that will also move in earthquakes.

To investigate the relationship between lateral earth pressure distribution and relevant 'spring displacement' between the wall and free field, the spring displacement from ABAQUS implicit with peak acceleration and representative acceleration and PLAXIS is drawn along the wall in Figure 10. Based on equation (10), the 'spring displacement' Δ controls the magnitude of the lateral earth pressure since the first component of equation (10) is always determined by soil weight which leads to the same magnitude for PLAXIS and ABAQUS due to the same soil weight. As can be seen in Figure 10, ABAQUS peak acceleration produced greater passive spring displacement than that from representative acceleration, and thus a greater lateral earth pressure as shown in Figure 7. PLAXIS has produced negative and thus active displacement in Figure 10, and this agrees well with lowest pressure in Figure 7 compared to that from ABAQUS. There is also a trend towards lower passive 'spring displacement' when the depth goes down for the ABAQUS curve and an increasing of active 'spring displacement' for the PLAXIS curve, which explains the diminished increase ratio with depth for lateral earth pressure for both PLAXIS and ABAQUS results in Figure 6. As a result, although wall displacement and strain increment ratio

method are sufficient for predicting general lateral force and general pressure distribution, 'spring displacement' must have a closer influence on local horizontal pressure along the wall. Thus the original strain increment ratio method for seismic cases (equations 4 and 5) has neglected the influence of free field displacement on local pressure, since R (strain increment ratio) does not take into account free field displacement besides wall displacement.

With regard to limitations of the present study, both ABAQUS and PLAXIS used a simple model: Mohr-Coulomb criterion without considering damping. The soil materials are normally consolidated (necessary for strain increment ratio method) dry sand without cohesion. All theories used were based on pseudo-static method. As mentioned above, the strut elements modelled by connector is not accurate. There are more advanced seismic boundary solutions and this study uses simple ones. Numerical simulation does not represent real behaviour and the analysis made in this paper could be enhanced by experimental investigations.

Figure 31: Distance between wall and free field ("spring displacement") from ABAQUS and PLAXIS

6. Conclusion

ABAQUS and PLAXIS models of strutted diaphragm walls were built. The wall displacement, lateral wall pressure and free field displacement were obtained. These

results were compared and analysed based on two displacement related earth pressure theories: strain increment ratio lateral earth pressure theory [12] [13] and free-field subgrade modulus method [7]. Also, the software's competence and limits in modelling and calculation of such a retaining system were assessed.

The findings of this study are listed as, but not limited to, the following points:

1. Numerical software such as PLAXIS is able to provide a way to determine relevant parameters in strain increment ratio dependent lateral earth pressure theory and the subgrade modulus in the method of Rowland Richards et al [7]'s.

2. Using peak ground acceleration of 5m/s2 as amplitude, ABAQUS obtains close wall displacement to that from PLAXIS and higher lateral earth pressure to that from 2.5 m/s2 amplitude.

3. Using the obtained parameters with peak acceleration, strain increment ratio theory has produced satisfactory lateral earth pressure compared to PLAXIS results, although with variance of maximum 40 kPa in terms of local pressure

4. ABAQUS tends to produce 10 – 150 kPa larger lateral earth pressure along the depth compared to PLAXIS and Zhang et al. [13]'s using peak acceleartion.

5. Both ABAQUS (using peak acceleration) and PLAXIS are sufficient at producing free field displacement that agrees well with theoretical solutions for most part of the wall.

6. ABAQUS produces similar results for implicit and explicit using spring/dashpot and connector as boundary conditions respectively.

7. Strain increment ratio method could be amended using the displacement between wall and free field rather than wall displacement alone. This would lead into a more accurate interpretation of seismic soil wall behaviour and finally a more accurate theoretical prediction of responses.

Future study, both more advanced numerical or experimental, could establish a more accurate and quantitative relationship between lateral earth pressure and wall & free field displacement. Also, more thorough study could be conducted to amend strain increment ratio method for seismic cases. An amended ABAQUS model should be

built to overcome the struts limitations in this paper. Certainly, damping of soil plus other soil types such as clay or soil with water etc. could be studied.

7. References

[1] Bao, X.-H., G.-L. Ye, B. Ye, Y. Sago and F. Zhang (2014). 'Seismic performance of SSPQ retaining wall—Centrifuge model tests and numerical evaluation.' Soil Dynamics and Earthquake Engineering 61–62(0): 63-82.

[2] Conti, R., G. M. B. Viggiani and S. Cavallo (2013). 'A two-rigid block model for sliding gravity retaining walls.' Soil Dynamics and Earthquake Engineering 55(0): 33-43.

[3] Fishman, K. L., J. B. Mander and R. Richards Jr (1995). 'Laboratory study of seismic free-field response of sand.' Soil Dynamics and Earthquake Engineering 14(1): 33-43.

[4] Li, X., Y. Wu and S. He (2010). 'Seismic stability analysis of gravity retaining walls.' Soil Dynamics and Earthquake Engineering 30(10): 875-878.

[5] Liu, Q., Y. Tian and F. Deng (2014). 'Dynamic analysis of flexible cantilever wall retaining elastic soil by a modified Vlasov–Leontiev model.' Soil Dynamics and Earthquake Engineering 63(0): 217-225.

[6] Mononobe, N. and M. Matsuo (1929). On the determination of earth pressures during earthquakes. Proc., Proc. World Engrg. Congress.

[7] Rowland Richards, J., C. Huang and K. L. Fishman (1999). 'Seismic earth pressure on retaining structures.' Journal of Geotechnical and Geoenvironmental Engineering 125(10).

[8] Seed, H. B. and R. V. Whitman (1970). Design of Earth Retaining Structures for Dynamic Loads, University of California.

[9] Theodorakopoulos, D. D., A. P. Chassiakos and D. E. Beskos (2001). 'Dynamic pressures on rigid cantilever walls retaining poroelastic soil media. Part I. First method of solution.' Soil Dynamics and Earthquake Engineering 21(4): 315-338.

[10] Tiznado, J. C. and F. Rodríguez-Roa (2011). 'Seismic lateral movement prediction for gravity retaining walls on granular soils.' Soil Dynamics and Earthquake Engineering 31(3): 391-400.

[11] Wood, J. H. (1975). ‘Earthquake induced pressures on a rigid wall structure.’ Bull. of New Zealand Nat. Soc. for Earthquake Engrg. 8(3): 175-186.

[12] Zhang, J., Y. Shamoto and K. Tokimatsu (1998). ‘Evaluation of earth pressure under any lateral deformation.’ Soils and Foundations 38(1): 15-33.

[13] Zhang, J., Y. Shamoto and K. Tokimatsu (1998). ‘Seismic earth pressure theory for retaining walls under any lateral displacement.’ Soils and Foundations 38(2): 143-163.

Appendix C

The following is the permission from the editor of *International Journal of Engineering Research and Applications* regarding the citation of the author's published paper titled "Review of Studies on Retaining Wall's Behavior on Dynamic / Seismic Condition"

Requesting email:

From: **Su Yang** 苏阳 (suyangyang638@hotmail.com)

Sent: 22 May 2014 14:53:39

To: ijera.editor@gmail.com (ijera.editor@gmail.com)

Dear Editor:

It' s my pleasure to contact you.

I am requesting the permission from your journal for me to cite my published article named **"Review of Studies on Retaining Wall' s Behavior on Dynamic / Seismic Condition"** in the literature review part of my master's thesis. I am the 1st author of this article and it was published in *Vol. 3, Issue 6, Nov-Dec 2013, pp.01-05*

Any suggestions please inform me by this email.

Many thanks,

Yang

Reply email:

From: **ijera.editor** (ijera.editor@gmail.com)

Sent: 27 May 2014 17:29:06

To: Su Yang 苏阳 (suyangyang638@hotmail.com)

Dear Sir,

Yes you can cite this paper

Regards

Editorial Board,

IJERA